Lattice preferred orientation in omphacite: Examples from the Tauern Window, Austria and the Western Gneiss Region, Norway

Dissertation
zur Erlangung des Grades
"Doktor der Naturwissenschaften"

am Fachbereich Chemie, Pharmazie und Geowissenschaften
der Johannes-Gutenberg Universität
in Mainz

Kai Neufeld
geb. in Bremerhaven

Mainz, August 2007

Selbständigkeitserklärung

Ich versichere hiermit, die vorliegende Arbeit selbständig und nur unter Verwendung der angegebenen Quellen und Hilfsmittel verfasst zu haben.

Mainz, August 2007

Abstract

It is lively debated how eclogites find their way from deep to mid-crustal levels during exhumation. Different exhumation models for high-pressure and ultrahigh-pressure rocks were suggested in previous studies, based mainly on field observations and less on microstructural studies on the exhumed rocks. The development and improvement of electron microscopy techniques allows it, to focus interest on direct investigations of microstructures and crystallographic properties in eclogites. In this case, it is of importance to study the applicability of crystallographic measurements on eclogites for exhumation processes and to unravel which processes affect eclogite textures.

Previous studies suggested a strong relationship between deformation and lattice preferred orientation (LPO) in omphacite but it is still unclear if the deformation is related to the exhumation of eclogites.

This study is focused on the questions which processes affect omphacite LPO and if textural investigations of omphacite are applicable for studying eclogite exhumation. Therefore, eclogites from two examples in the Alps and in the Caledonides were collected systematically and investigated with respect to omphacite LPO by using the electron backscattered diffraction (EBSD) technique. Omphacite textures of the Tauern Window (Austria) and the Western Gneiss Region (Norway) were studied to compare lattice preferred orientation with field observations and suggested exhumation models from previous studies. The interpretation of omphacite textures, regarding the deformation regime is mainly based on numerical simulations in previous studies.

Omphacite LPO patterns of the Eclogite Zone are clearly independent from any kind of exhumation process. The textures were generated during omphacite growth on the prograde path of eclogite development until metamorphic peak conditions.

Field observations in the Eclogite Zone show that kinematics in garnet mica schist, surrounding the eclogites, strongly indicate an extrusion wedge geometry. Stretching lineations show top-N thrusting at the base and a top-S normal faulting with a sinistral shear component at the top of the Eclogite Zone. The different shear sense on both sides of the unit does not affect the omphacite textures in any way.

The omphacite lattice preferred orientation patterns of the Western Gneiss Region can not be connected with any exhumation model. The textures were probably generated during the metamorphic peak and reflect the change from subduction to exhumation.

Eclogite Zone and Western Gneiss Region differ significantly in size and especially in metamorphic conditions. While the Eclogite Zone is characterized by constant P-T conditions (600-650°C, 20-25 kbar), the Western Gneiss Region contains a wide P-T range from high- to ultrahigh pressure conditions (400-800°C, 20-35 kbar). In contrast to this, the omphacite textures of both units are very similar. This means that omphacite LPO is independent from P-T conditions and therefore from burial depth.

Further, in both units, omphacite LPO is independent from grain and subgrain size as well as from any shape preferred orientation (SPO) on grain and subgrain scale.

Overall, omphacite lattice preferred orientation are generated on the prograde part of omphacite development. Therefore, textural investigations on omphacite LPO are not applicable to study eclogite exhumation.

Zusammenfassung

Die Exhumierung von Eklogiten ist ein vieldiskutiertes Problem im Bereich der Tektonik und der Strukturgeologie. Zahlreiche Exhumierungsmodelle basieren im Wesentlichen auf Geländebeobachtungen und weniger auf mikrostrukturellen Untersuchungen der exhumierten Gesteine. Die Entwicklung und ständige Verbesserung elektronenmikroskopischer Methoden rückt kristallographische Untersuchungen an Eklogiten verstärkt in den Blickpunkt des Interesses.

Frühere Studien zeigen einen deutlichen Zusammenhang zwischen Deformation von Eklogiten und den kristallographischen Texturen in deren Omphazitmineralen. Allerdings ist unklar ob die Deformation mit der Exhumierung der Gesteine in Zusammenhang steht. In der vorliegenden Arbeit werden die Entwicklung kristallographischer Texturen in Omphaziten sowie sich daraus ergebende mögliche Rückschlüsse zu Exhumierungsprozessen untersucht. Hierfür wurden die Eklogitzone des Tauernfensters in Österreich sowie die Western Gneis Region in Norwegen systematisch beprobt. Die Untersuchungsgebiete umfassen einen weiten Bereich von Hochdruck- und Ultrahochdruckbedingungen, wodurch ein möglicher Zusammenhang zwischen Druck- und Temperaturbedingungen und Omphazittextur untersucht werden kann. Kristallographische Orientierung sowie Orientierungskontraste wurden mittels Elektronenrückstrahlbeugung (Electron Backscatterred Diffraction, EBSD) gemessen und mit Exhumierungsmodellen verglichen. Die Interpretation der Texturen basiert dabei im Wesentlichen auf numerischen Simulationen aus früheren Untersuchungen an Omphazittexturen.

Die kristallographischen Texturen der Eklokitzone des Tauernfensters sind eindeutig nicht durch die Exhumierung beeinflusst. Die Texturen spiegeln Signaturen wieder, die sich dem prograden Pfad der Omphazitentwicklung zuordnen lassen. Die Texturen entwickelten sich während des Omphazitwachstums bis hin zum metamorphen Maximum.

Geländebeobachtungen in der Eklogitzone zeigen, dass kinematische Indikatoren in Granatglimmerschiefern, welche die Eklogite umschliessen, deutlich eine Extrusionskeilgeometrie implizieren. Streckungslineationen verdeutlichen eine nordgerichtete Aufschiebung an der Basis sowie eine südgerichtete Abschiebung mit einer sinistralen Scherungskomponente am hangenden Kontakt der Eklogitzone. Der unterschiedliche Schersinn auf beiden Seiten der Eklogitzone hat keinen Einfluss auf die kristallographischen Texturen der Omphazite.

Die zum Vergleich untersuchten Omphazittexturen der Western Gneis Region können ebenfalls keinem Exhumierungsmodell zugeordnet werden. Die Texturen bildeten sich vermutlich während des metamorphen Maximums und repräsentieren den Wechsel von Subduktion zu Exhumierung.

Eklogitzone und Western Gneis Region unterscheiden sich signifikant in ihrer Größe sowie in den metamorphen Bedingungen. Während die Eklogitzone durch konstante Hochdruckbedingungen (600-650°C, 20-25 kbar) gekennzeichnet ist, umfasst die Western Gneis Region einen wesentlich weiteren Hochdruck- und Ultrahochdruckbereich (400-800°C, 20-35 kbar). Trotz dieser deutlichen Unterschiede sind die Omphazittexturen in beiden Gebieten vergleichbar und demnach unabhängig von den Druck- und Temperaturbedingungen und damit von der Versenkungstiefe.

Außerdem zeigt sich eine Unabhängigkeit der Texturen von Korn- und Subkorngrößen sowie von Korn- und Subkornorientierung in Omphaziten. Diese Beobachtungen gelten sowohl für die Eklogitzone als auch für die Western Gneis Region.

Insgesamt wird deutlich, dass kristallographische Texturen in Omphaziten auf den prograden Pfad der Omphazitentwicklung beschränkt sind und damit keine Rückschlüsse auf mögliche Exhumierungsprozesses zulassen.

Table of contents

1. PROBLEM DEFINITION 2
1.1. Introduction 2
1.2. Aims of the study 4

2. METHODS 5
2.1 Fieldwork 5
2.2. Electron Backscattered Diffraction (EBSD) 5
2.2.1. Introduction 5
2.2.2. Scanning Electron Microscopy (SEM) 6
2.2.3. Sample preparation 6
2.2.4. Formation of electron backscatter patterns 7
2.2.5. Orientation contrast (OC-) imaging 8
2.2.6. Lattice preferred orientation (LPO) in eclogites 11
2.2.7. Analytical procedure 17

3. GEOLOGICAL SETTING (I): ECLOGITE ZONE / TAUERN WINDOW 18
3.1. Introduction 18
3.2. Field data 24
3.2.1. Structural data 24
3.2.2. Mapping 28
3.3. Lattice preferred orientation (LPO) data 29
3.3.1. Sample description 29
3.3.2. LPO patterns in the Eclogite Zone 33
3.4. Discussion & Conclusions (I): Eclogite Zone 46
3.4.1. Discussion 46
3.4.2. Conclusions 48

4. GEOLOGICAL SETTING (II): WESTERN GNEISS REGION 50
4.1. Introduction 50
4.2. Lattice preferred orientation (LPO) data 54
4.2.1. Problem definition 54
4.2.2. Sample description 54
4.2.3. LPO patterns in the Western Gneiss Region 56
4.3. Discussion & Conclusions (II): Western Gneiss Region 64
4.3.1. Discussion 64
4.3.2. Conclusions 67

5. GENERAL DISCUSSION & CONCLUSIONS 68
5.1. General discussion 68
5.2. Conclusions 69

6. LITERATURE 70

Curriculum Vitae 79

1. PROBLEM DEFINITION

1.1. Introduction

High-pressure (HP) and ultrahigh-pressure (UHP) units are exposed in orogenic complexes world wide. The knowledge about the dynamic processes leading to an upward transport of such units is of fundamental interest for understanding processes in the lithosphere during orogenesis. Therefore, it is essential to focus interest on the by far densest crustal rock type, being eclogite, and its journey to the surface.

Eclogite has an extreme density of up to 3600 kg m^{-3} and is thus much denser than any other crustal rock. Furthermore, it is also significantly denser than the lithospheric mantle (e.g. Ring et al., 1999). The question how such extremely dense rocks were exhumed from great depths to mid-crustal levels is a very lively debated problem in tectonics and structural geology. Many previous studies about this topic were carried out on high-pressure and ultra-high-pressure complexes all over the world, leading to a wide range of eclogite exhumation models, which are discussed in highly controversial ways since decades of geoscience research.

While earlier models on eclogite exhumation were mainly based on field observations, it became more familiar over the years to study crystallographic textures on eclogite, especially since the technical capabilities improved rapidly during the last decade. Based on such investigations, it is widely assumed that crystallographic orientation patterns reflect indications for rock deformation.

It is still ambiguous if this means that also the exhumation history of eclogite rocks is displayed in the crystallographic textures. Area-wide crystallographic studies on eclogites, regarding the exhumation of the rocks, are missing. Therefore, this study is focused on the question, if eclogite textures are affected by exhumation or if they are coupled to other processes in any way.

In this case, the exhumation question is addressed by investigating two (ultra-) high-pressure complexes, being the Eclogite Zone of the Tauern Window in the Austrian Alps and the Western Gneiss Region in Norway. These complexes were studied by combining crystallographic orientation measurements with field observations.

The study areas have been chosen with previous investigations in mind. Detailed information about petrologic and geochronologic development of the units were necessary to fit own results into an overall geologic context. According to this, the chosen study areas represent

the best studied HP / UHP complexes world wide. Previous studies indicated detailed information on kinematics and exhumation rates.

Furthermore, a wide range of high-pressure and ultrahigh-pressure conditions are represented by the chosen study areas.

In this case, the study is focused on:

1. The Eclogite Zone (EZ) of the Tauern Window, Eastern Alps (Austria)

This rock unit is a perfect example to address eclogite exhumation studies because of the very well exposure and preservation of its high-pressure rocks. Further, it is a very small unit (see chapter 3), which leads to the possibility for studying it area-wide from bottom to top. Therefore, lattice preferred orientation (LPO) patterns in eclogites were measured in samples, taken over the whole Eclogite Zone to study indications for eclogite deformation. The textures were expected to reflect the deformation of the eclogites during exhumation. The measured LPO patterns were compared with field data, including structural measurements and detailed mapping. This should lead to a better understanding of the overall deformation of the Eclogite Zone and should also help unravelling the exhumation of the eclogites. Finally, previous exhumation models for the Eclogite Zone will be discussed with respect to the results of this study.

2. The Western Gneiss Region (WGR), West Norway

The Western Gneiss Region was chosen for this study to compare LPO data from a large (U)HP rock unit with the textures from the small Eclogite Zone. The latter indicates a superb overview about textural and structural development across an entire unit. In contrast to this, its small size questions the representative character of the Eclogite Zone, regarding general informations about (U)HP exhumation. Therefore, it is advisable to prove indications, given by data from the Eclogite Zone, with data from a study area that might be more representative for general processes because of its larger size.

In this case, lattice preferred orientation patterns in eclogites from the Western Gneiss Region were studied to revise the detailed studies from the Eclogite Zone and to intercalate the results on a general scale.

1.2. Aims of the study

The aims of this study are:

- To verify exhumation suggestions for the Eclogite Zone with own crystallographic and kinematic data, leading to a preferred exhumation model for the Tauern Window eclogites.
- To discuss the exhumation of the Western Gneiss Region by comparing own data with previous exhumation models.
- To compare textures from the large Western Gneiss Region with own data from the Tauern Window to intercalate data from the Eclogite Zone on a general scale.
- To discuss general exhumation models based on data from the Tauern Window and the Western Gneiss Region and therefore based on data, ranging from high-pressure to ultrahigh-pressure conditions.
- To point out the processes that are coupled with the formation of crystallographic textures in eclogites
- To revise the significance of eclogite textures for the deformation and the exhumation of these rocks.
- To test the applicability of lattice preferred orientation patterns for studying the exhumation of eclogites.

2. METHODS

2.1 Fieldwork

The fieldwork for this study was focused mainly on the Eclogite Zone (EZ) of the Tauern Window and in a smaller amount on the Western Gneiss Region (WGR). The first one is a perfect example to study deformation and exhumation on an area-wide scale while the latter was investigated to compare geologic settings under different metamorphic conditions.
In total 28 orientated hand samples of eclogites were collected along 6 profiles across the Eclogite Zone in August and September 2003. The profiles were arranged parallel to the eclogite stretching lineation and therefore orientated in north-south direction. Stretching lineations of eclogites and garnet mica schists in the Eclogite Zone and the surrounding rock units were measured on a wide-area scale in August 2004, together with detailed mapping of selected eclogite blocks to estimate the eclogite / garnet mica schist ratio for the overall unit (for details see chapter 3). Furthermore, shear sense indicators, especially at the contact areas between Eclogite Zone and surrounding units, were studied in detail to define the kinematics of the contact areas on both sides of the Eclogite Zone. The latter was done in September 2005.
Sampling of 9 orientated hand samples along one large profile across the Western Gneiss Region / Norway was done in June 2004. The profile was orientated in an east-west direction parallel to the tectonic transport direction during eclogite exhumation and has a length of ~150 km.

2.2. Electron Backscattered Diffraction (EBSD)

2.2.1. Introduction

The electron backscattered diffraction (EBSD) technique is a part of scanning electron microscopy (see chapter 2.2.2). It was rapidly arising and improving during the last 10 years, exchanging previous universal stage techniques. The EBSD is applied to obtain crystallographic information from analysed minerals of interest, such as grain morphology and orientation, subgrain formation and subgrain orientation as well as crystallographic

preferred orientation. The main advantage of EBSD is its spatial resolution down to ~1 µm with an angular resolution of 1-2° (Venables & Harland, 1973; Dingley et al., 1987).
The following chapter describes the basics and the operation mode of an EBSD system. Further, the applicability of EBSD on eclogites and therefore the use of the technique in this study will be explained.

2.2.2. Scanning Electron Microscopy (SEM)

Scanning electron microscopy (SEM) is widely used to investigate samples of interest under by far greater resolution in comparison to optical microscopy. The SEM resolution reaches down to only a few microns, which allows to study detailed microstructures on a very small scale.
In this study, SEM studies, notably EBSD analysis, were performed on a LEO 1530 scanning electron microscope at Bayerisches Geoinstitut, University of Bayreuth, Germany. This SEM includes dispersive X-ray (EDX) and a detector from HKL technology for electron backscatterred diffraction (EBSD). Further, a LEO 1530 scanning electron microscope at the "Zentrales Rastereletronenmikroskop" of the Faculty of Earth Sciences, University of Bochum, Germany, was used. This microscope includes EDX, cathodoluminescence (CL) and a Nordlys EBSD detector. The electron backscatterred diffraction technique was used for all microstructural and crystallographic investigations in this study. In this case, it is described in detail in the following chapters.

2.2.3. Sample preparation

The samples were cut into small blocks of ~25 by 15 mm with a thickness of ~5 mm. The blocks represent XZ sections of the finite strain ellipsoid (X>Y>Z, i.e. X represents the stretching lineation). For scanning electron microsocopy (SEM) and electron backscattered diffraction (EBSD) investigations, the samples were first mechanically pre-polished for SEM and afterwards chemically polished for EBSD, using a colloidal silica suspension (Syton®). Careful polishing is needed to reduce surface damage. Finally, the samples were lightly carbon coated to a thickness of 3 nm to reduce surface charging effects.

2.2.4. Formation of electron backscatter patterns

An electron beam placed on a specimen in a scanning electron microscope (SEM) produces different scattering events which may be either elastic or inelastic. In a crystalline specimen some of the elastically scattered electrons will be diffracted on crystal planes at angles which satisfy the Bragg equation:

$$n\lambda = 2d \sin\theta$$

in which n is an integer, λ is the wavelength of the electrons, d is the spacing of the diffracting crystal planes and θ is the incidence of the electrons on the diffracting crystal planes (see Fig. 1).

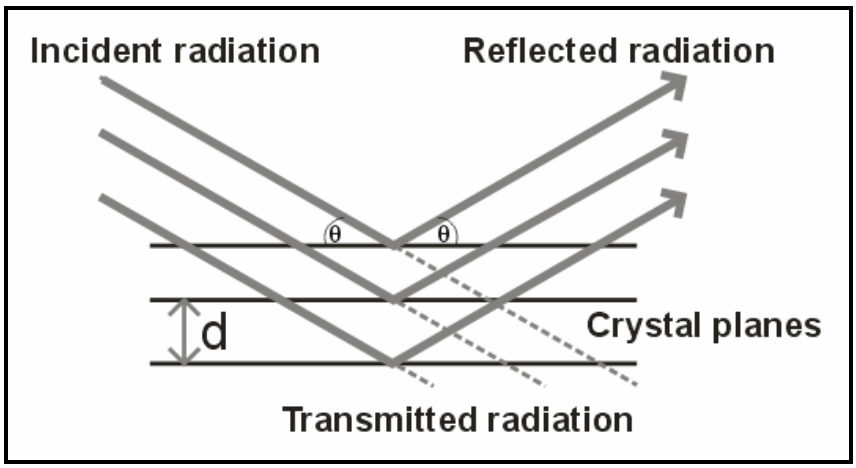

Fig. 1: Principle of Bragg´s law.

EBSD patterns are created by scattering of the entering electrons within the crystal structure on different lattice planes. Such patterns are the backscattered equivalent of so-called Kikuchi patterns (Kikuchi, 1928), observed by using transmission electron microscopy (TEM).
Therefore, the electrons are backscattered to form a pattern on a phosphorous screen strategically placed within the vacuum specimen chamber. The pattern consists of a number of bands. Each of these bands corresponds directly to a specific lattice plane (hkl). The width of the bands and the angles between them are used for the indexing procedure of the diffraction pattern and for the determination of the crystallographic orientation of a crystal lattice in an investigated specimen.
In modern EBSD settings, automatic detection and analysis of EBSD patterns allows the operator to analyse numerous spots in a specimen. Therefore, a representative overview on the lattice preferred orientation of the mineral of interest inside the studied sample is guaranteed.

The indexed patterns are calculated to lattice preferred orientation polefigures and maps of crystal lattice orientation by using the CHANNEL 5 software, developed by HKL technology.

In order to obtain a significant yield of diffracted electrons, the specimen is tilted at a high angle (usually 70°) with respect to the horizontal axes inside the specimen chamber. The calculation of the crystal orientation matrix from the zonal information contained within the pattern necessitates careful consideration of the respective reference axes relating to the beam, specimen and detector.

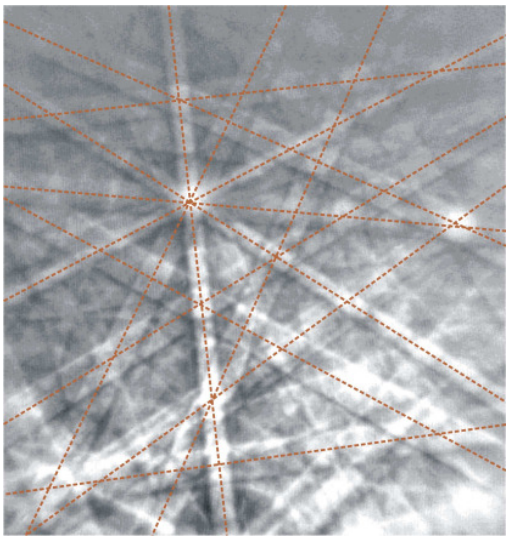

Fig. 2: Omphacite electron backscatter pattern.
The strongest indexing bands are marked by red lines.
Modified after Physics Courses of Daniel Chateigner (homepage),
http://www.ecole.ensicaen.fr/~chateign/enseig/microscopie/.

2.2.5. Orientation contrast (OC-) imaging

Orientation contrast (OC-) imaging was performed to study subgrain formation and orientation as well as shape preferred orientation (SPO) on grain and subgrain scale.
When an electron beam is placed on a specimen, so-called backscatter electrons can be detected with a BSE detector. These electrons differ from SEM standard secondary electrons (SE) by their higher energy. Because the angular deflection is depending on the atomic number, the BSE signal is especially sensitive to chemical differences.
The BSE signal enables the operator to obtain OC-images (Lloyd, 1987). Normally, the atomic number interferes with the orientation contrast signal, but this can be avoided by using a tilted sample (Prior et al., 1996) and by placing a BSE detector at a high angle, related to the electron beam. Such a setting results in a so-called forescatter detector (see Fig. 3).

In an orientation contrast image, areas of different crystallographic orientations are displayed as different grey shades (Lloyd, 1985). This allows the user to study in detail the grain and subgrain structure and development of the investigated specimen (see examples in Fig. 4).

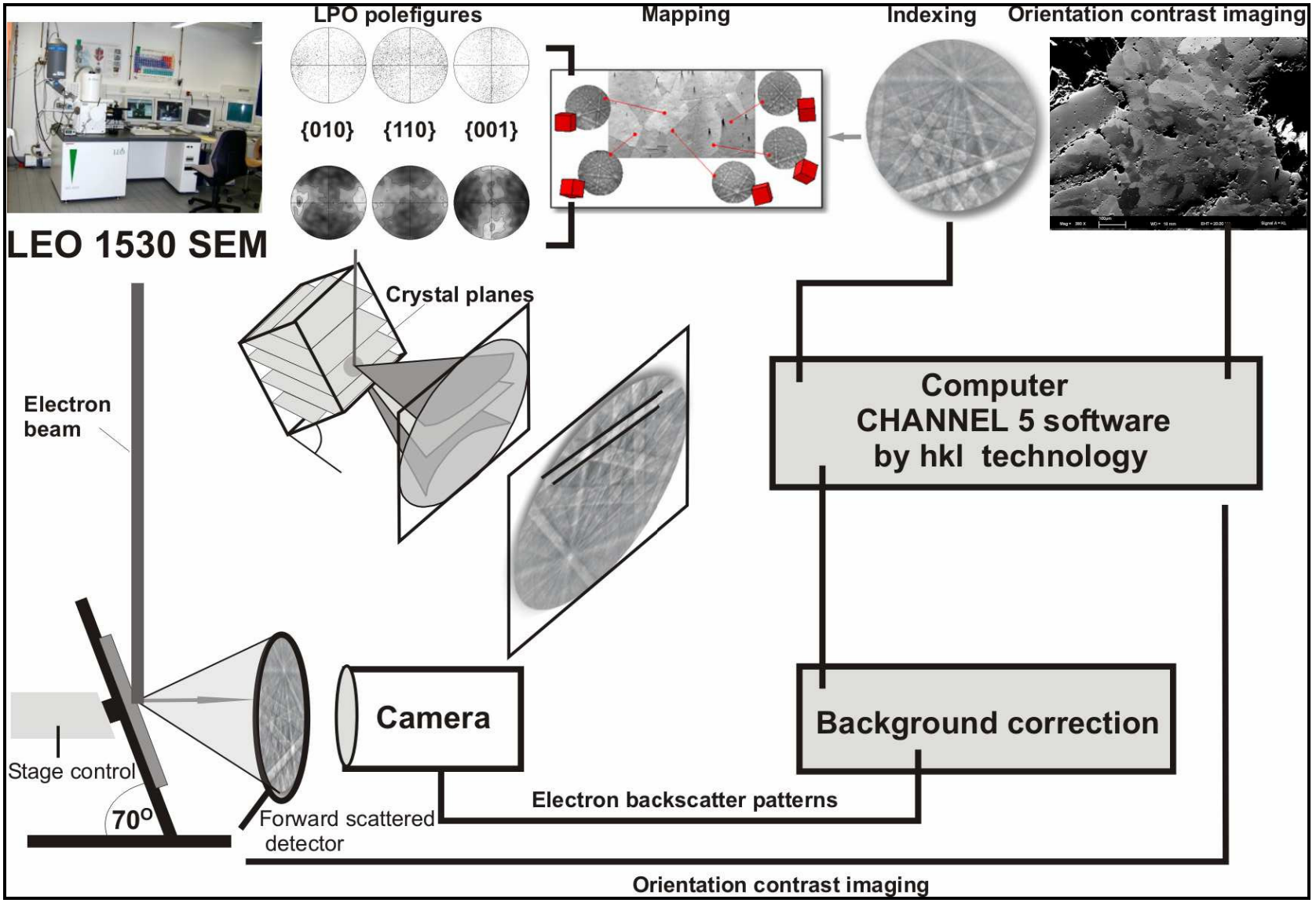

Fig. 3: Principle and setting of the electron backscattered diffraction technique.

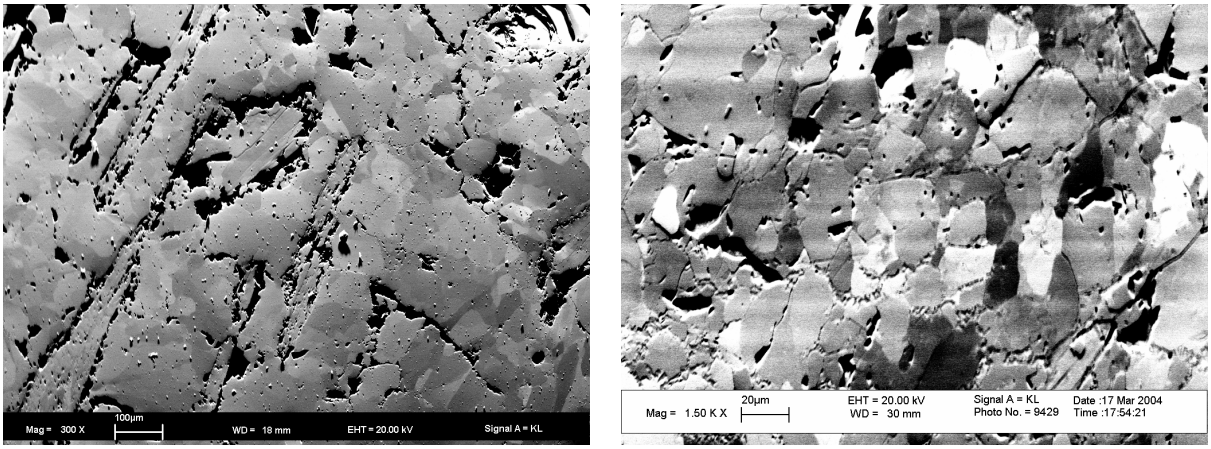

(a) (b)

Fig. 4: OC-images, taken from samples of the Eclogite Zone (a) Subgrains of quartz in a garnet mica schist, magnification: 300 x; (b) Subgrains of omphacite in an eclogite, magnification: 1500 x.

2.2.6. Lattice preferred orientation (LPO) in eclogites

Eclogite textures were investigated intensively in different previous studies (e.g. Godard & Van Roermund, 1995; Abalos, 1997; Mauler, 2000; Mauler et al., 2000; Bascou et al., 2001, 2002). It was documented that of the typically eclogite-forming minerals (omphacite and garnet) only omphacite is suitable as a textural indicator for the development of the rock.

Previous studies on garnet (e.g. Bascou et al., 2001) documented that lattice preferred orientations of garnet show randomly orientated patterns for eclogites, independent from metamorphic conditions or deformation processes. This is in agreement with measurements on garnet during this study. No internal deformation and no preferred LPO was measurable (see Fig. 5). In this case, only omphacite textures are interpreted to be the main carrier of strain.

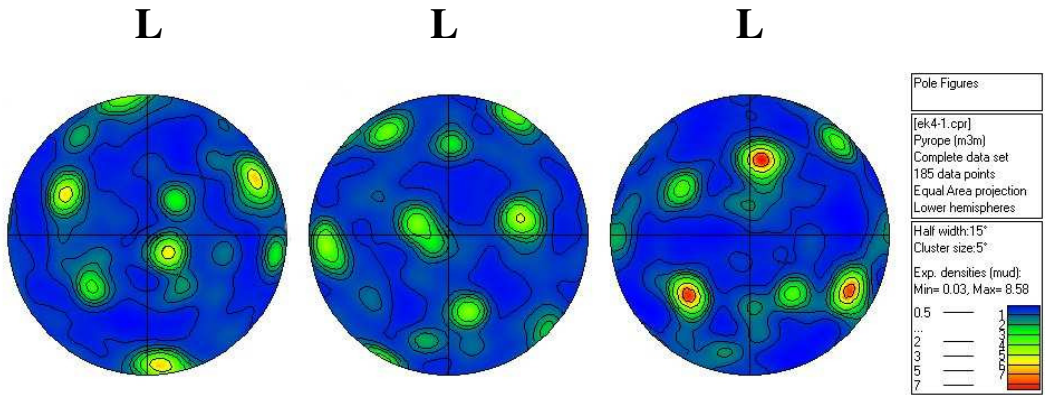

EK-04 mud (max.): 8.58

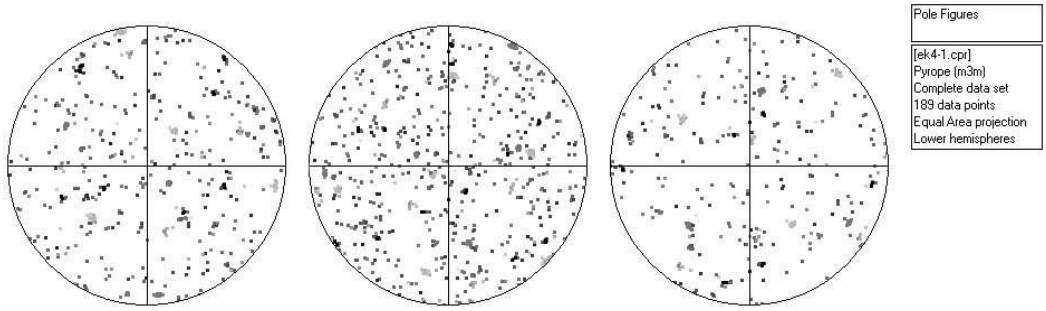

EK-04

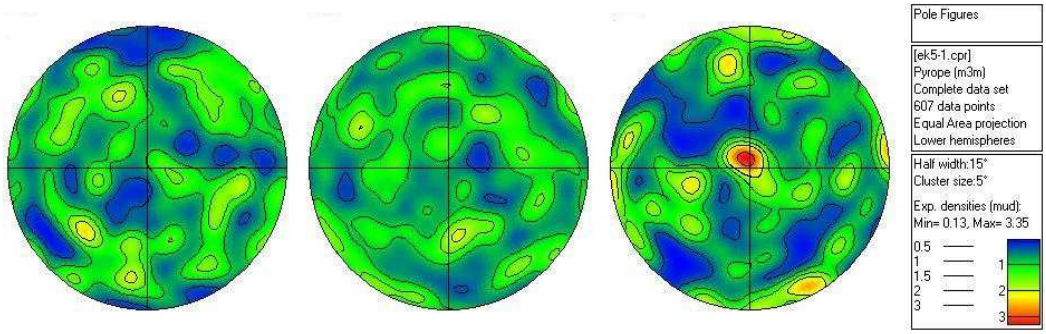

EK-05 mud (max.): 3.35

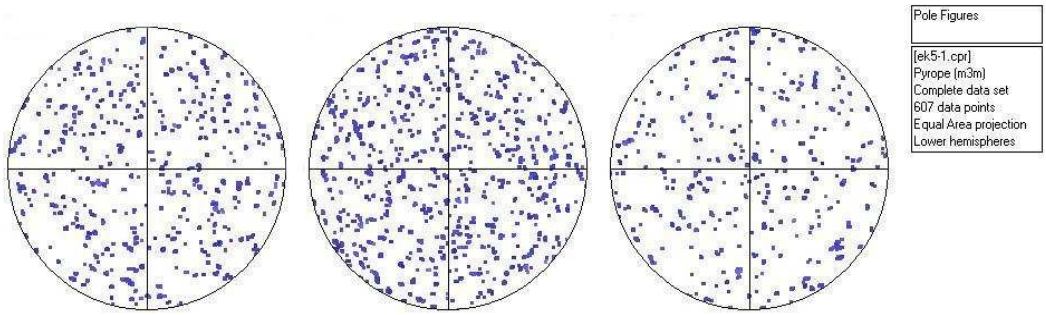

EK-05

{111} {110} {100}

Fig. 5: Garnet lattice preferred orientation in eclogites from the Tauern Window (samples EK-04 and EK-05). Contoured and scattered diagrams are shown. The lineation is marked by L. For sample locations, see Fig. 9. mud (max.) – mean unit deviation maximum.

Basic data on omphacite LPO have been investigated in many previous studies, using universal stage techniques (e.g. Helmstaedt et al., 1972; Boundy et al., 1992; Godard and Van Roermund, 1995; Abalos, 1997) and recently the rapidly improving electron backscatterred diffraction (EBSD) technique (e.g. Mauler, 2000; Mauler et al., 2001; Bascou et al., 2001; Pipenbreier and Stöckhert, 2001). The suitability of EBSD for studying omphacite LPO was demonstrated in detail by Mauler (2000) on natural and synthetic omphacites.

LPO in omphacite was first described by Helmstaedt et al. (1972, Fig. 6), who divided omphacite textures into L-type LPO (linear fabrics) and S-type LPO (planar fabrics). While L-type textures are characterized by a strong point maxima at [001] with the lineation and girdle distribution at [010] perpendicular to the lineation, S-type LPO is defined by the [001] axes lying in the foliation plane and (010) planes parallel to the foliation. Godard & Van Roermund (1995) also recognized those two LPO end member types and also described detailed transition fabrics between the end members.

The processes which control the development of omphacite LPO are still debated but there is a widespread agreement that deformation affects crystallographic orientation in omphacite significantly. Helmstaedt et al. (1972) and Godard & Van Roermund (1995) argued that LPO development is related to the shape preferred orientation (SPO) and that a change in the LPO patterns reflects a changing deformation regime. L-type LPO is interpreted to result from deformation with a constrictional strain type, while S-type LPO results from a flattening strain type (Godard & Van Roermund, 1995, Abalos, 1997). In contrast to this, Brenker et al. (1998, 2002) suggested a temperature dependence for omphacite LPO controlled by the cation ordering in omphacite.

Beside the general omphacite variations in a coaxial deformation regime, LPO asymmetries interpreted as generated by simple shear were described in previous studies (Bouchez et al., 1983; Mainprice & Nicholas, 1989; Boundy et al., 1992; Abalos, 1997). It is suggested that noncoaxial deformation results in an obliquity between LPO and the structural axes X, Y and Z, which should be observable as an asymmetric omphacite LPO pattern.

Bascou et al. (2001, 2002) studied omphacite LPO in eclogites developed under different metamorphic conditions from different orogens and compared their results with numerical LPO simulations of Molinari et al. (1987) and Lebenssohn & Tomé (1993). These models calculated omphacite LPO distribution by simulating different deformation regimes.

The numerical results indicated a clear relationship between deformation mechanisms and omphacite LPO development and approved the previous suggestions about omphacite LPO distribution (e.g. Helmstaedt et al., 1972; Godard & Van Roermund, 1995; Abalos, 1997;

Mauler, 2000). Furthermore, the studies of Bascou et al. (2001, 2002) negated a temperature control of omphacite LPO. The latter was also questioned by Mauler et al. (2001) and Kurz et al. (2004).

Based on numerical simulations, Bascou et al. (2001, 2002) divided omphacite LPO in patterns generated by simple shear, pure shear, axial compression, transpression and transtension, leading to typical patterns for each kind of deformation. The calculations indicated the relationship between deformation and omphacite LPO as follows:

Simulations of pure shear and simple shear deformation produced very similar patterns in which LPO were characterized by transition signatures that closely resemble L-type LPO end members. LPO patterns generated by simple shear depict slightly stronger L-type patterns then pure shear generated textures. Asymmetries, generated by simple shear were depending on the kind of simulation. In comparison to previous suggestions (e.g. Bouchez et al., 1983; Mainprice & Nicholas, 1989; Boundy et al., 1992; Abalos, 1997), the results of Bascou et al. (2001, 2002) indicated only a weak asymmetric signal, generated under simple shear conditions.

Simulations of axial compression and transpression show similar strongly S-type patterns for both deformation regimes. Transpression patterns depict a less clear girdle distribution within the lineation at {001} than textures generated by axial compression. Transpression generated a slight obliquity at {010}, depending on shear plane and direction.

Simulations of transtension generated LPO patterns similar to those resulting from simple and pure shear, but the signatures were strongly asymmetric, depending on the orientation of the shear plane and the shear direction. The main results of the simulations are summarized in Fig. 7, which also includes results of previous studies (Bouchez et al., 1983; Mainprice & Nicholas, 1989; Boundy et al., 1992; Abalos, 1997).

Kurz et al. (2004) argued, by studying combined petrologic and textural data from different (ultra-) high-pressure zones in the Alps, that S-type LPO is related to underplating and L-type LPO is related to exhumation.

Furthermore, Kurz et al. (2004) reported lattice preferred orientation LPO-data on omphacite from the Eclogite Zone of the Tauern Window as obtained by neutron diffraction and argued that there are two different generations of omphacite in the eclogites, defined as omphacite1 and omphacite2. First-generation omphacite has an S-type LPO pattern whereas second-generation omphacite has an L-type LPO pattern. These authors discussed that the S-type fabrics are related to the prograde path while L-type fabrics are related to decompression

following the metamorphic peak. In this case, Kurz et al. (2004) interpreted the two different LPO patterns to reflect a change from subduction to exhumation.

Following these argumentations, one can expect that a systematic omphacite LPO study along the entire study areas should reflect the deformation mechanisms that affected the microstructures in the eclogites.

In this case, high strain areas, especially close to the boundaries between the study areas and the surrounding rock units, should lead to an asymmetric distribution of the LPO patterns on both sides because of the different sense of shear**.**

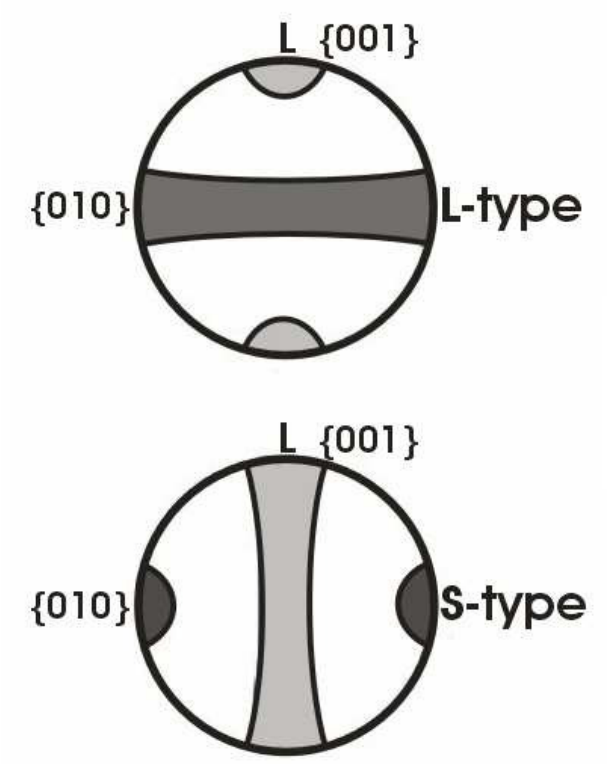

Fig. 6: Schematic view on L-type (linear) and S-type (planar) end members of omphacite LPO, modified after Helmstaedt et al. (1972).

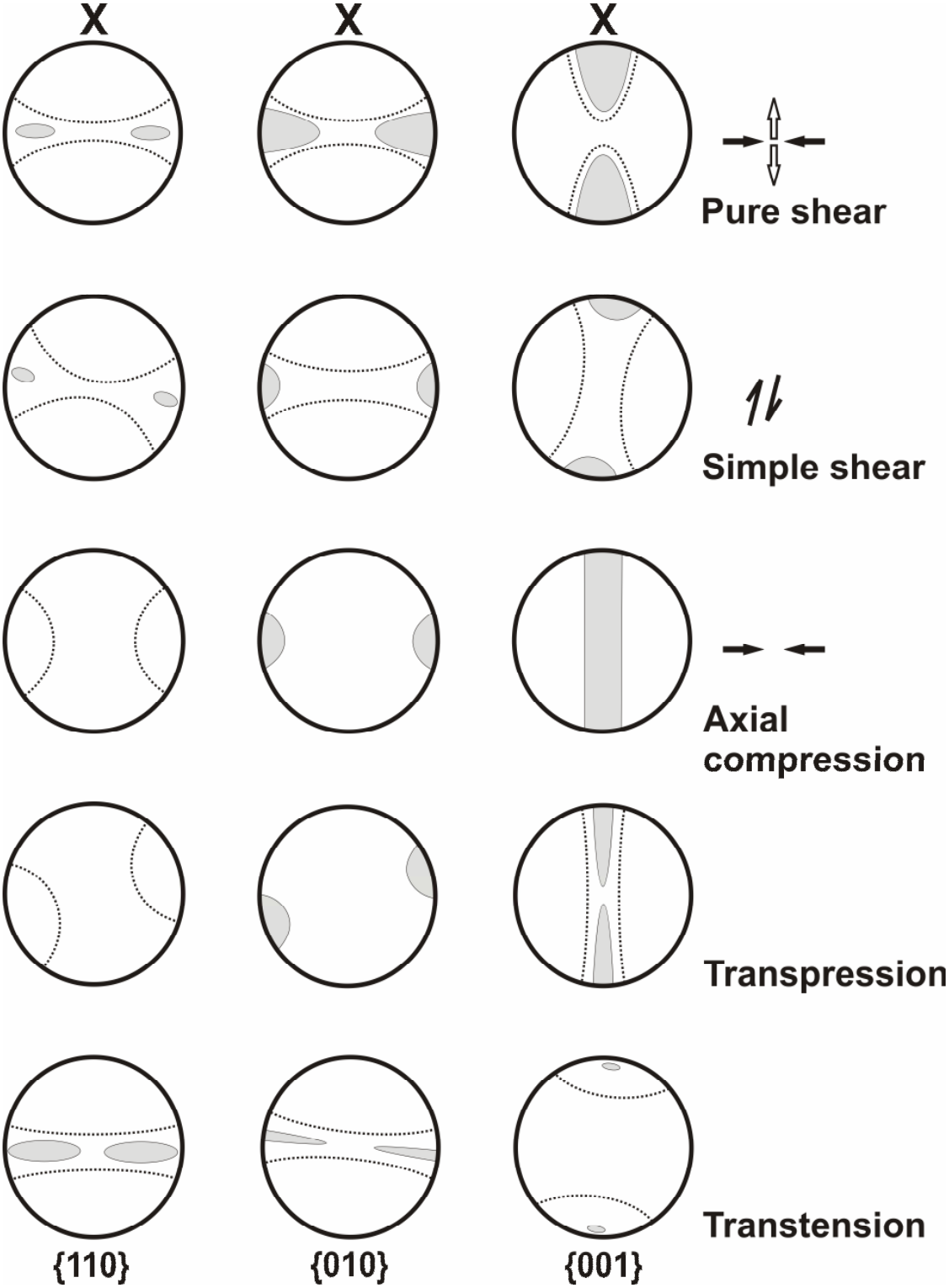

Fig. 7: Omphacite LPO as expected under different deformation regimes. grey colour – strong signal (mean unit deviation maximum), dotted lines – weak signal. The lineation axes is marked by L.

Based on simulations by Bascou et al. (2001, 2002) and universal stage results by Bouchez et al. (1983), Mainprice & Nicholas (1989), Boundy et al. (1992) and Abalos (1997).

2.2.7. Analytical procedure

The samples were placed as small blocks inside the sample chamber of a scanning electron microscope and tilted to an angle of 70°. SEM settings were operated at an accelerated voltage between 20 and 30 kV, depending on the frequency of occurrence and the intensity of indexed patterns. The measurements were carried out automatically, using the stage control of the EBSD setup. This leads to an overall scan across the whole sample surface. The working distance between the specimen and the detector varied between 18 and 25 mm.

The different detectors on both microscopes, used for this study, lead to a strong difference in indexed measure points between samples, measured at University of Bayreuth and samples, measured at University of Bochum. The EBSD setup at the latter produced a much larger data set for each sample. Therefore, some samples were measured on both instruments to check if the results are comparable. Both microscopes produced equal patterns, independent from the number of indexed measure points.

The Tauern Window samples EK-01, EK-08, EK-13, EK-14, EK-15, EK-16, EK-18, EK-20, EK-22, EK-G, EK-H, EK-M, EK-P, EK-R, EK-T and EK-V were measured on a LEO 1530 SEM at University of Bochum. This data set included 16 samples. The Tauern Window samples EK-02, EK-04, EK-05, EK-06, EK-07, EK-09, EK-A, EK-B, EK-C, EK-D, EK-E and EK-F were measured on a LEO 1530 SEM at University of Bayreuth. This data set included 12 samples. The WGR samples WGR-03, WGR-04, WGR-05, WGR-08, WGR-09, WGR-11 and WGR-14 were measured on a LEO 1530 SEM at University of Bochum. This data set included 7 samples. The WGR samples WGR-07 and WGR-10 were measured on a LEO 1530 SEM at University of Bayreuth. This data set included 2 samples.

3. GEOLOGICAL SETTING (I): ECLOGITE ZONE / TAUERN WINDOW

3.1. Introduction

The Alps can be subdivided into the European continental sequences represented by the Helvetic Nappes at the base, overlying oceanic sequences of the Pennine Nappes and continental rocks of the Austroalpine and Southernalpine units at the top (Fig. 8). The Eastern Alps are dominated by the Austroalpine Nappes. In the Tauern and Engadin Windows the underlying rocks of the Pennine and Helvetic nappes crop out.

From top to bottom the Tauern Window consists of the Penninic Glockner Nappe, the Eclogite Zone and the Venediger Nappe.

The Glockner Nappe is made up by rocks of oceanic affinity, which reached blueschist-facies metamorphism (~8 kbar and 500 °C, Se1verstone, 1993). The Venediger Nappe below the Eclogite Zone comprises gneisses and parautochthonous metasediments of the European margin. The rocks of the Venediger Nappe reached metamorphic conditions of ~11 kbar and 540 °C (Selverstone, 1993).

The Eclogite Zone forms a steeply S-dipping thrust sheet and consists of eclogite-facies metasediments with intercalated mafic igneous rocks. The Eclogite Zone is interpreted as a distal succession of the passive European continental margin and tectonically sandwiched between nappes of lower metamorphic grades (e.g. Kurz et al., 2003). The Eclogite Zone crops out along a strike length of 20 km. The north-south extent varies between 1.5 and 3 km. In the Eclogite Zone, the eclogites occur as lenses with a maximum size of 1500 m by 700 m width and a thickness of up to 300 m. Most of the eclogite blocks are significantly smaller with a common size of about 100 m by 20 m. The eclogite blocks are embedded in a matrix of lower density rocks, i.e. garnet mica schist, calc schist, quartzite and marble. Peak metamorphism in the Eclogite Zone was at 20-25 kbar and 600-650 °C and affected the eclogite blocks and the surrounding matrix in a coherent fashion (Holland, 1977; Frank et al., 1987; Stöckhert et al., 1997; Hoschek, 2007). Glodny et al. (2005) dated the peak of eclogite-facies metamorphism at 31 Ma.

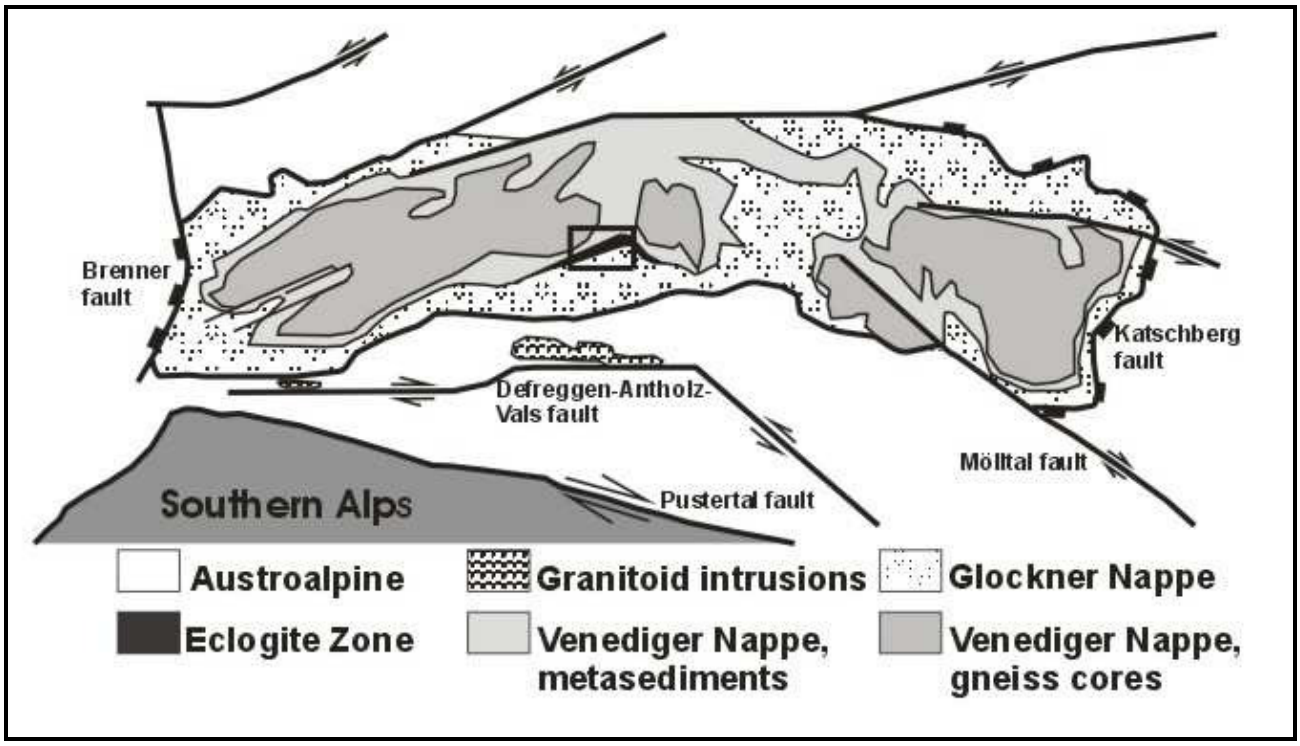

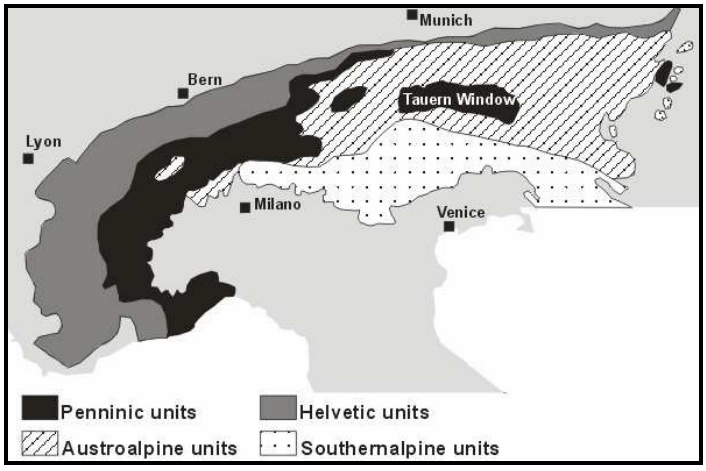

Fig. 8: Position of the Tauern Window inside the Alps (left) and position of the Eclogite Zone in the south-central Tauern Window, Austrian Alps (above). The study area (central part of the Eclogite Zone) is marked by a black box.

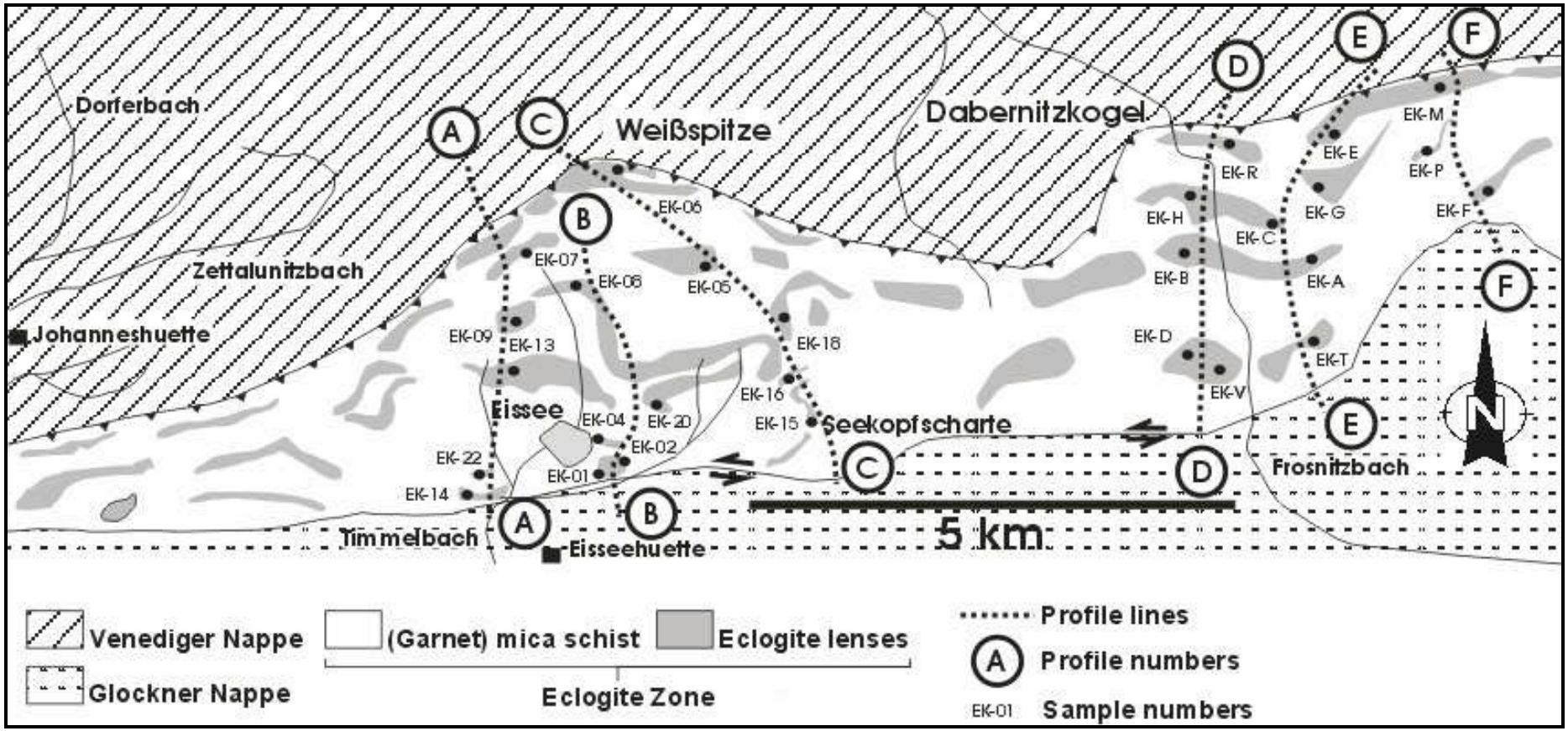

Fig. 9: Distribution of eclogite and surrounding metasediments in the Eclogite Zone and sample locations (black dots, with sample numbers). The profiles for EBSD study are marked by dotted black lines and numbered as A to F.

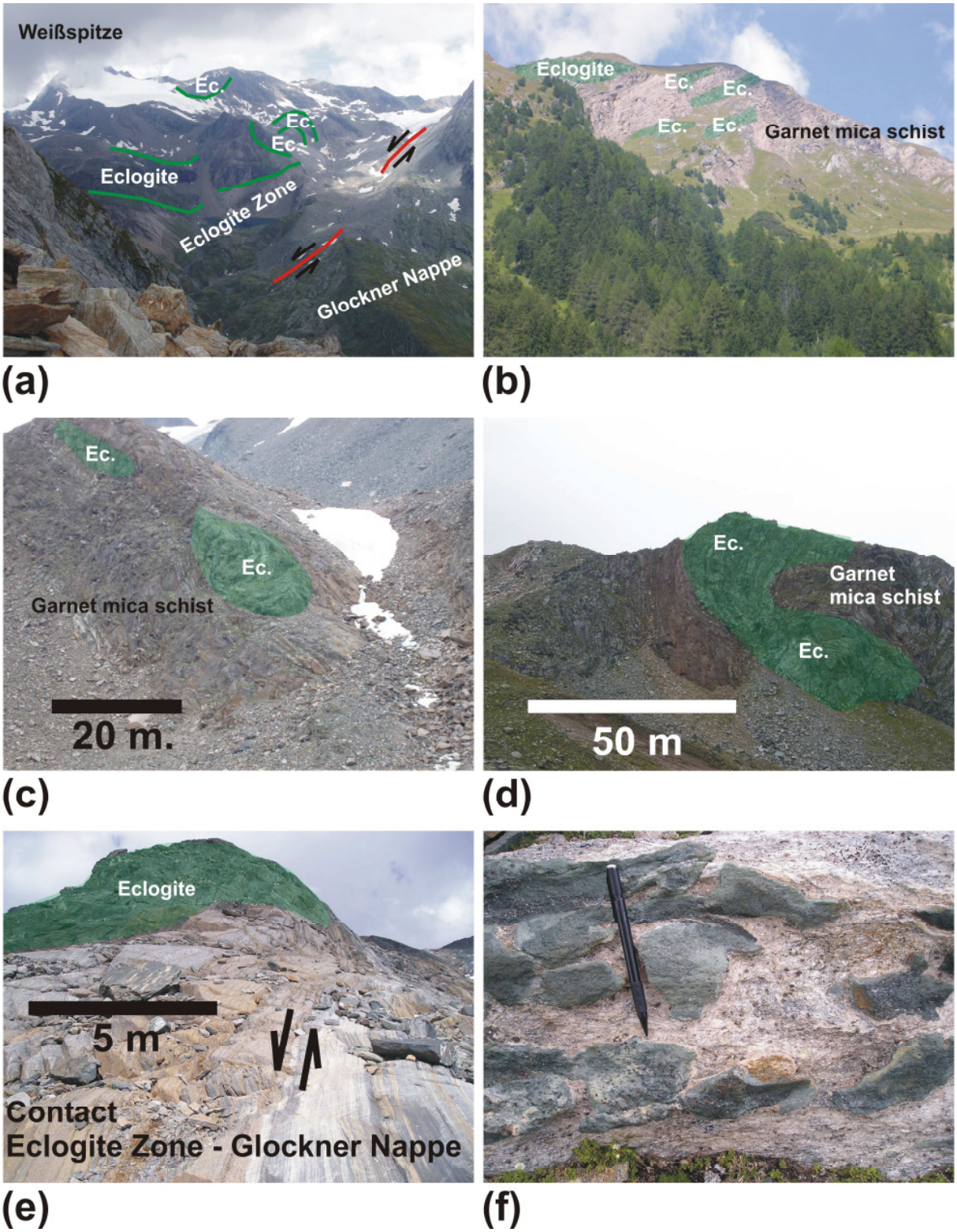

Fig. 10: (a) Overview of the central part of the Eclogite Zone, including marked eclogite lenses; (b, c, d) Pictures of eclogite lenses (marked in green), embedded in garnet mica schist; (e) Eclogite lense (marked in green) close to the contact shear zone at the top the Eclogite Zone; (f) Detailed look on an eclogite lense, including small eclogite lenses (dark colours) embedded in garnet mica schist (light colours).

Kurz et al. (1998, 2004) divided the Tauern Window eclogites into two groups, a coarse grained variation on the one hand and a fine grained to mylonitic variation on the other hand. Further, these authors divided omphacites from the Eclocite Zone in omphacite1 and omphacite2, based on differences in grain size, grain shape and mineral chemistry. Moreover, they showed that omphacite1 has a lower jadeite content (approx. 30 mol%) than omphacite2 (approx. 50 mol%). Kurz et al. (1998, 2004) suggested that the two omphacite generations formed under different metamorphic conditions on the prograde path during the eclogite formation.

While coarse grained eclogites mainly consist of omphacite1, partly surrounded by omphacite2, fine grained to mylonitic eclogites consist mainly of omphacite2. Therefore, fine grained eclogites are interpreted to represent a stage of increased mylonitisation during the prograde metamorphic evolution of the Eclogite Zone (Kurz et al., 1998, 2004). Hoschek (2001), Kurz et al. (2004) and Glodny et al. (2005) showed that there is an increase in the jadeite content of omphacite2 from core to rim. The rims are supposed to have formed at the metamorphic peak (Hoschek, 2007).

Moreover, previous work in the Eclogite Zone resulted in different models for its exhumation. England & Holland (1979) argued that buoyancy might be the main driving force for the exhumation of the Eclogite Zone. They envisaged that lenses of dense eclogite were transported in an uprising lower density matrix and showed that this mechanism can only work when exhumation rates are >40 km Myr^{-1}. Recently, Glodny et al. (2005) calculated that minimum exhumation rates in the Eclogite Zone are 36 km Myr^{-1}. After Behrmann & Ratschbacher (1989), vertical thinning resulting from coaxial ductile flow primarily caused the exhumation. Furthermore, these authors questioned buoyancy as the exhumation driving mechanism for the Eclogite Zone because of a too high eclogite/matrix ratio. This ratio has been estimated by Raith et al. (1980), who suggested that eclogites contain ~50 % of the entire Eclogite Zone.

Kurz & Froitzheim (2002) and Kurz et al. (1998, 2003) assumed wedge extrusion (Fig. 11) in a subduction channel and thereby postulated that the lower contact of the Eclogite Zone is a top-N thrust and the upper contact a top-S normal shear zone.

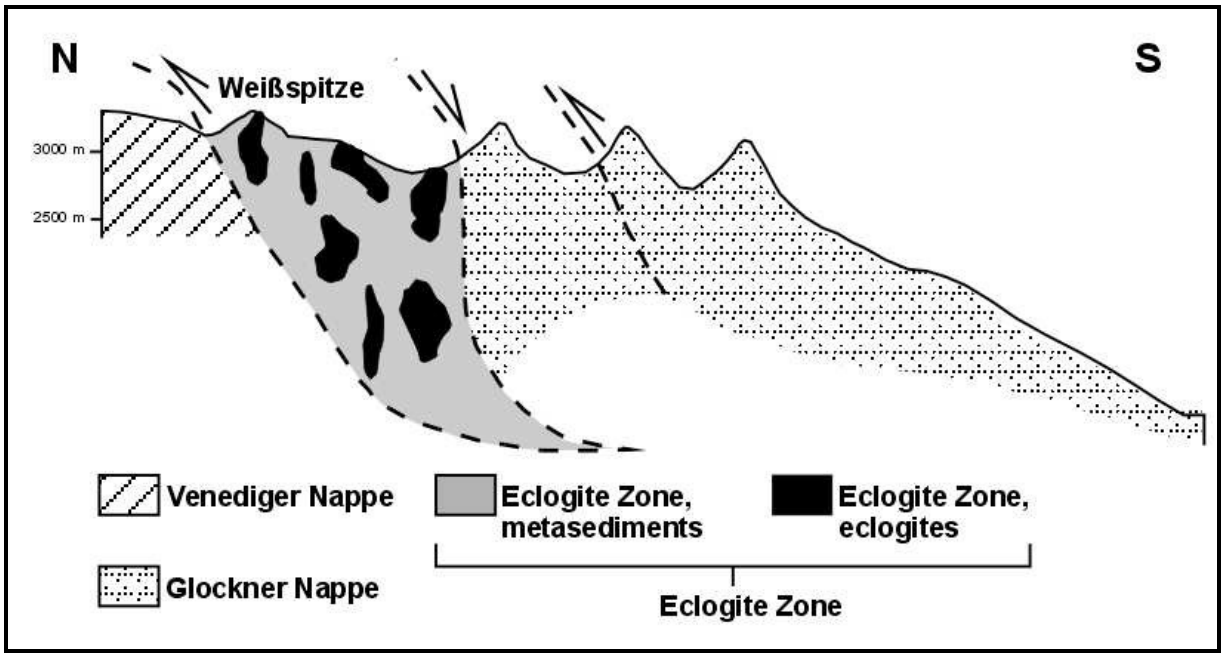

Fig. 11: Schematic cross section across the study area (central part of the Eclogite Zone), modified after Kurz et al. (1998).

3.2. Field data

3.2.1. Structural data

The contact between the Eclogite Zone and the underlying Venediger Nappe is characterized by carbonate-rich and metapelitic mylonites (Fig. 12). The mylonitic foliation dips moderately to steeply to the south and contains a N-S-trending stretching lineation (Figs. 13 and 14). Kinematic indicators yielded a consistent top-N shear sense.

Granitic and pelitic gneisses in the directly underlying Venediger Nappe are commonly strongly deformed and depict also a moderately to steeply south-dipping foliation on which a SW-plunging stretching lineation is developed (Fig. 13). Kinematic indicators yielded a top-NE sense of shear.

Within the Eclogite Zone the deformation is of variable intensity. Carboneous, quartzitic and metapelitic rocks are usually strongly deformed, showing mylonitisation. The mylonitic structures have the same orientations as those at the contact to the Venediger Nappe.

The hanging wall contact of the Eclogite Zone with the overlying Glockner Nappe is characterized by blueschist to greenschist facies carbonate-bearing, metapelitic and quartzitic mylonites. The mylonitic foliation is commonly steeply dipping to the south and contains a WSW-ENE-trending stretching lineation. On average the stretching lineation is plunging at ~15-20º to the WSW. Kinematic indicators in the mylonites record a sinistral shear sense with a top-ENE normal shear component (Figs. 14 and 15). Eclogite lenses close to the boundary are strongly deformed and elongated in the WSW-ENE-oriented shear direction.

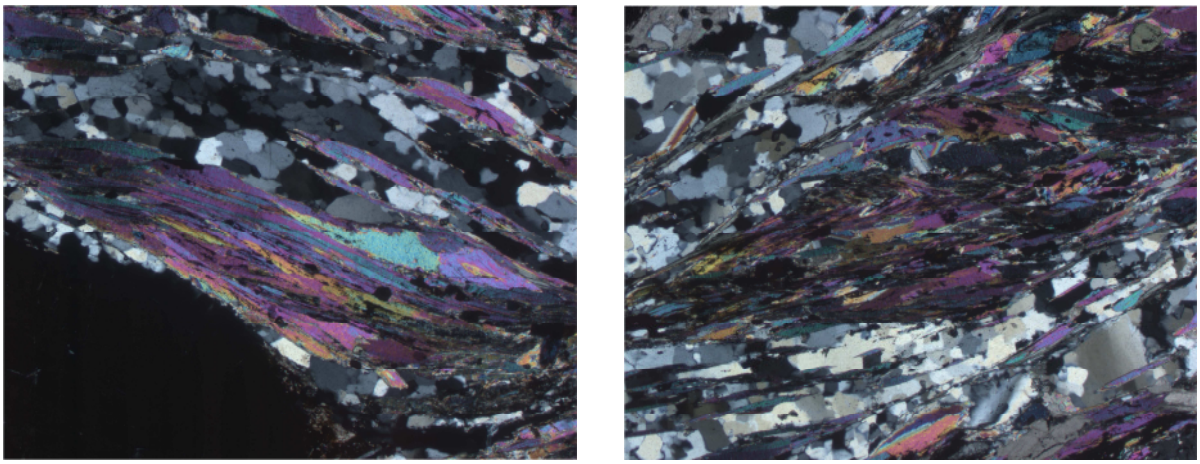

Fig 12: Carbonaceous mylonite (thin sections, crossed nicols) marking the boundary between Eclogite Zone and underlying Venediger Nappe. Magnification: 25x.

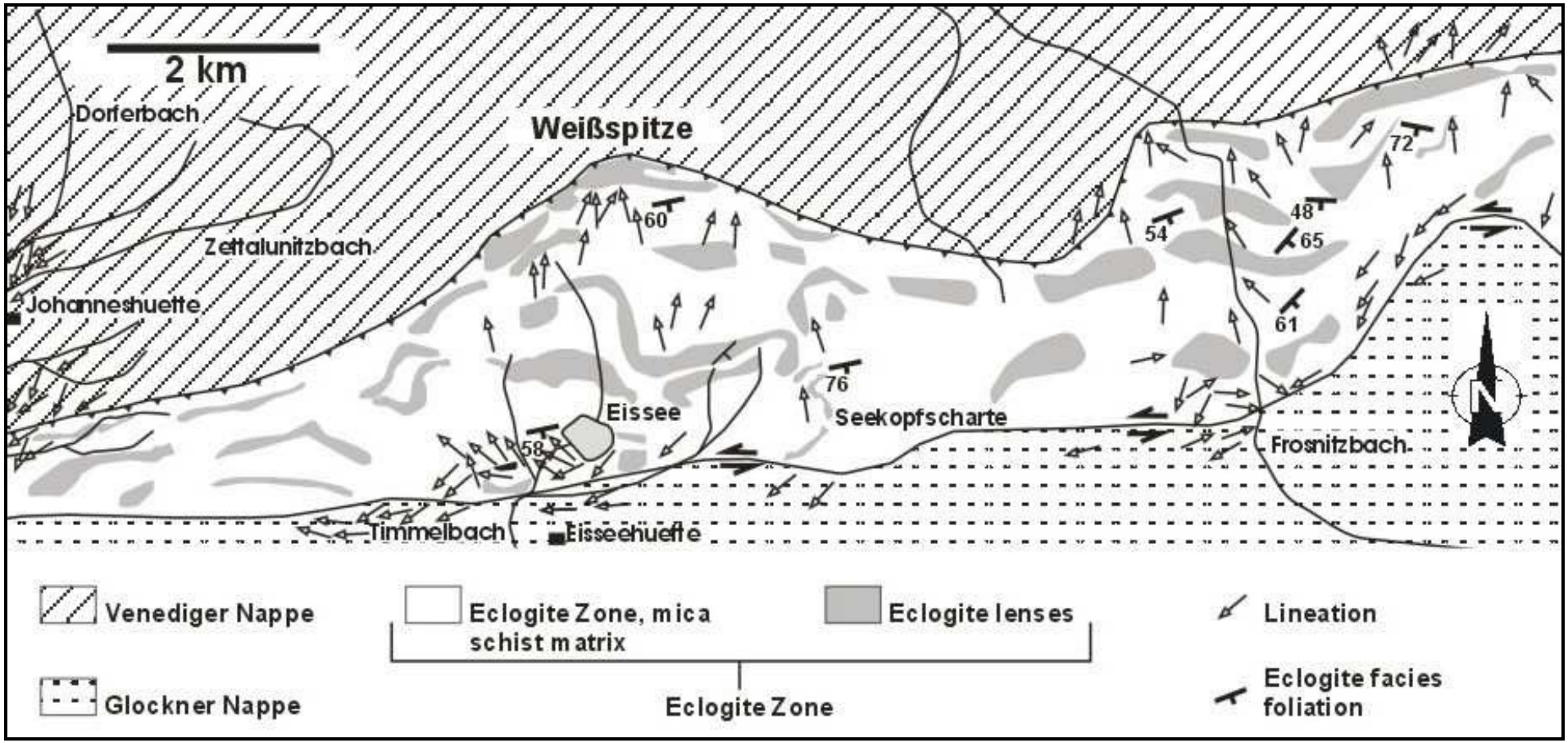

Fig. 13: Structural data of the central part of the Eclogite Zone. Stretching lineations are shown by black arrows with arrow heads pointing down-plunge. The lower boundary and most of the Eclogite Zone are characterized by N-S-trending lineations, whereas the boundary of the Eclogite Zone with the Glockner Nappe is characterized by WSW-ENE-trending stretching lineations.

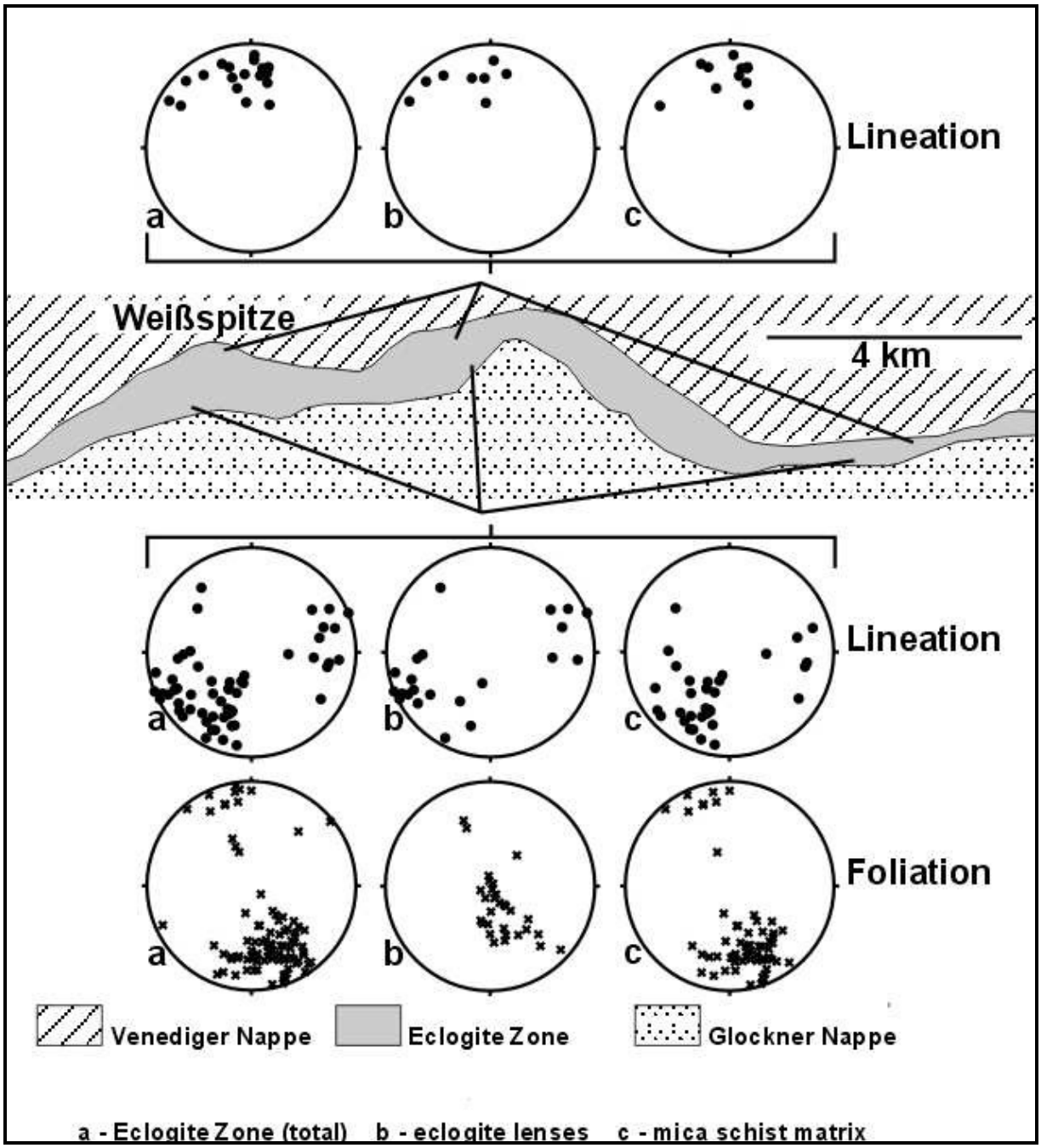

Fig. 14: Orientation of lineation and poles of foliation planes from the boundaries of the Eclogite Zone and from the under- and overlying nappes. Data from Dietrich (2005) and own data.

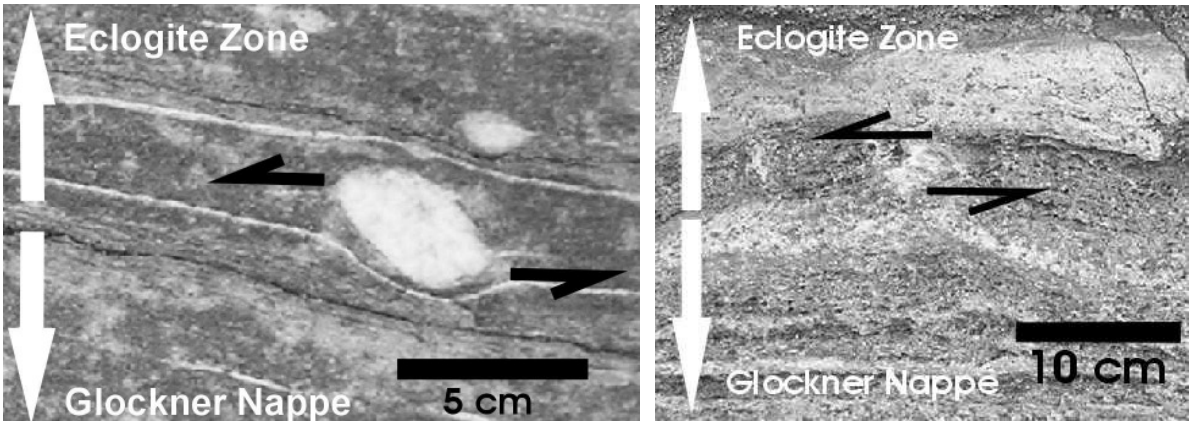

Fig. 15: Marble mylonite at the boundary between the Eclogite Zone and the overlying Glockner Nappe. The asymmetric clasts indicate a sinistral shear sense (in WSW – ENE direction).

3.2.2. Mapping

Detailed field work showed that eclogite lenses make up ~30 % of the Eclogite Zone. The eclogite lenses are not homogeneous but rather composed by an interplay between extremely dense eclogites and less dense mica schist (Fig. 16). The eclogite part contains ~20-25 %. of the overall rock unit.

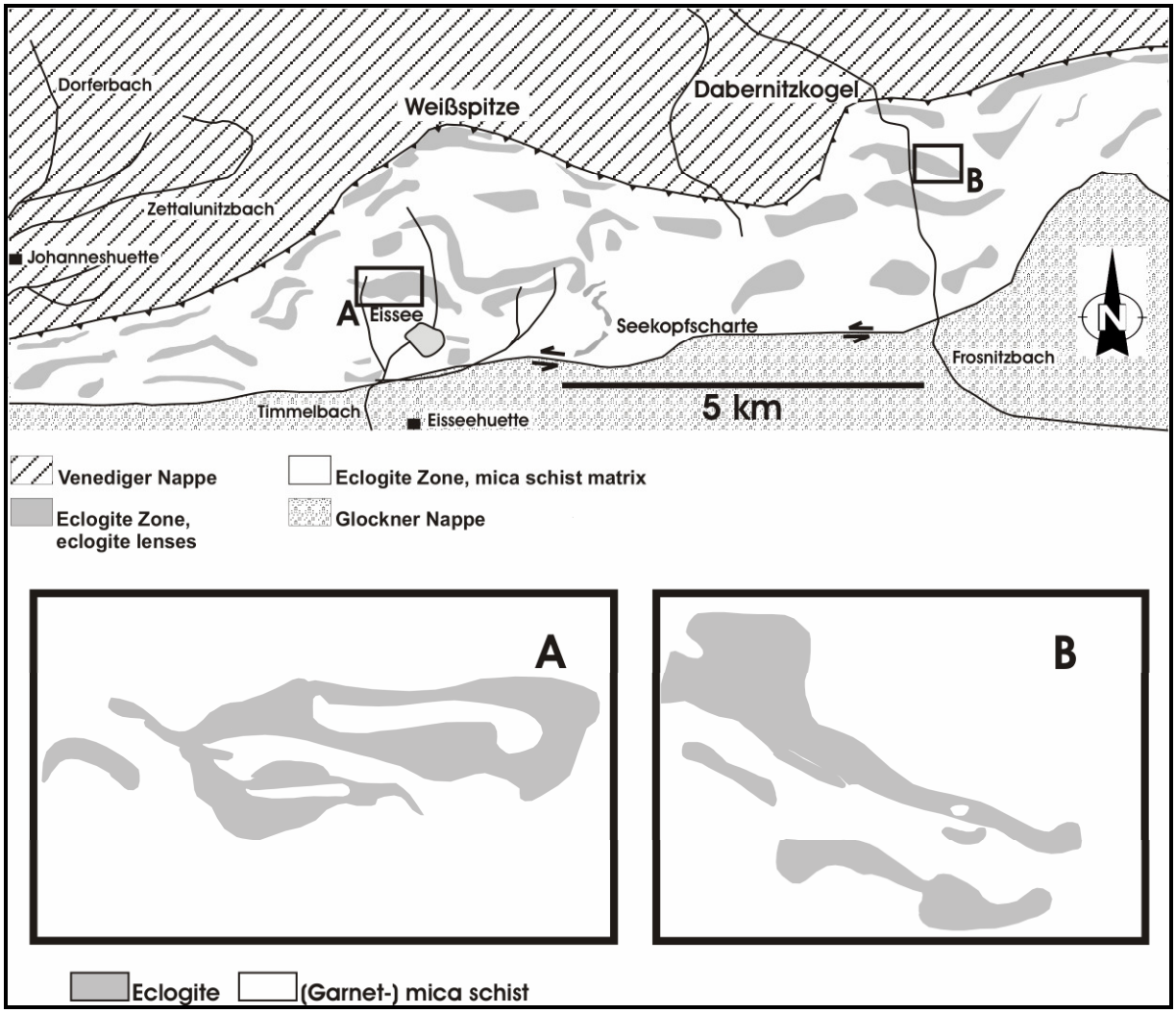

Fig. 16: Detailed geologic maps of eclogite lenses (marked with black boxes).

3.3. Lattice preferred orientation (LPO) data

3.3.1. Sample description

The studied eclogites can be divided into two types (E1 & E2, see Fig. 17). This is in agreement with observations by Kurz et al. (2004). E1-eclogites represent a fine grained to mylonitic eclogite variety that is characterized by fine grained garnet layers embedded in an omphacite groundmass. The E1-eclogites (Figs. 17a to 19d-f) are intensely foliated and commonly show a well-developed stretching lineation. The fine grained eclogites (E1) show differences in garnet grain sizes. The majority of the E1 eclogites are characterized by garnets with a diameter of ~0.5 to 1 mm. Some of these garnets are elongated. In some E1 eclogites, the size of the garnets varies between 3 and 5 mm. Generally the garnets occur in layers.

The omphacite matrix in E1 eclogites is characterized by grain sizes up to 500 µm but often significantly smaller. The grains are strongly lineated (Figs. 18a-c and 19d-f) subparallel to the penetrative foliation. No subgrain formation could be observed. These omphacite minerals can be described as omphacite2, applying the definition of two omphacite generations in the Tauern Window eclogites (e.g. Kurz et al., 2004; Hoschek, 2007). In the overall sample collection, mineral composition and microstructures in E1 eclogites are very homogenous.

E2 eclogite (Figs. 17b and 18d-f) is a coarse grained eclogite variation. It is much less intensely deformed than E1-eclogite and shows a semi-penetrative foliation but usually lacks a stretching lineation. Also in the microstructures, no clear shape preferred orientation is common.

Garnets with a size of mainly up to 5 mm occur in an omphacite groundmass and and do not show any kind of layering. Garnet grain sizes of 3 to 4 mm are most common.

The omphacite groundmass in E2 eclogites is characterized by larger grain sizes in comparison to E1 eclogites. A grain size of 1 to 2 mm is very common, grains up to a size of 5 mm also occur. These omphacites represent the omphacite1 generation in the Tauern Window eclogites. Omphacite1 only occurs in coarse grained eclogites.

The omphacite grains are mainly randomly orientated and show pronounced subgrain formation (Fig. 19a-c) without any shape preferred orientation (SPO). Larger omphacite grains are optically zoned. In some samples, large omphacite1 grains are surrounded by finer grained omphacite2. Omphacite2 occurs in all of the EBSD-measured E2 eclogites, but only in very small amounts.

Beside garnet and omphacite, the mineral assemblages in both eclogite varieties include phengite, paragonite, kyanite, quartz, carbonate and opaque minerals. E1-eclogite is much more common in the Eclogite Zone than E2-eclogite and therefore represents the larger part of the EBSD studied eclogites. Fine grained to mylonitic eclogites represent 85 % of the overall samples, only 15 % of all samples are coarse grained eclogites. The distribution of the coarse grained eclogites inside the study area is not connected to any local parts or structures. All coarse grained E2-eclogites are randomly distributed in the study area.

(a) (b)

Fig. 17: (a) Fine grained eclogite E1; (b) Coarse grained eclogite E2.

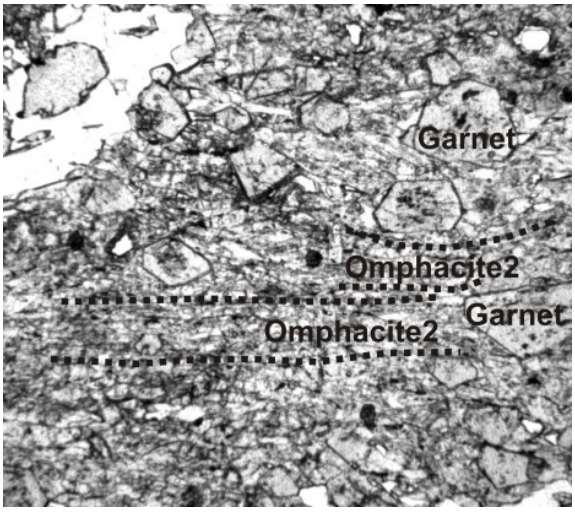

(a) magnification: 25x **EK-02**

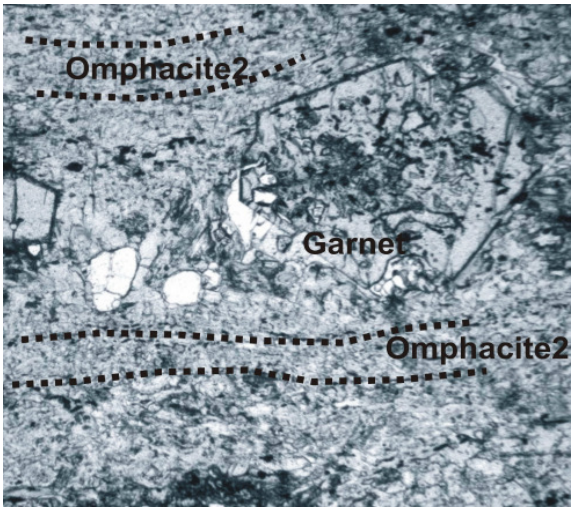

(b) magnification: 25x **EK-06**

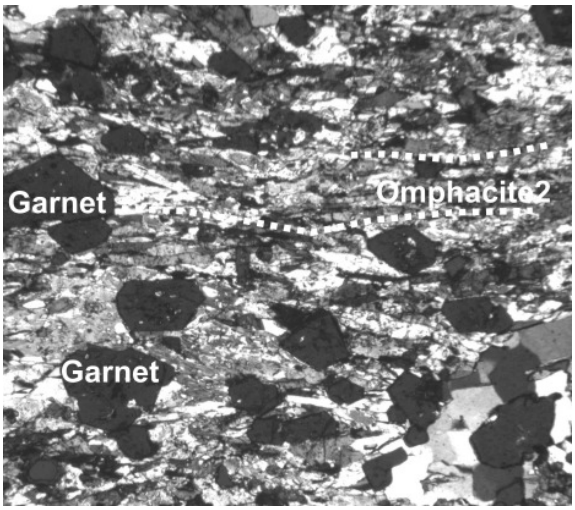

(c) magnification: 25x **EK-P**

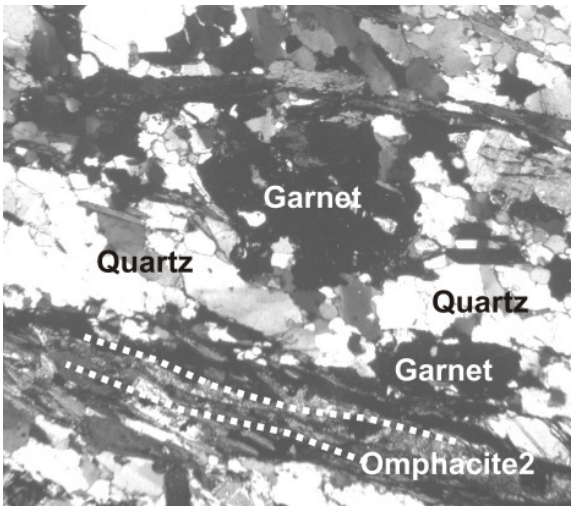

(d) magnification: 25x **EK-08**

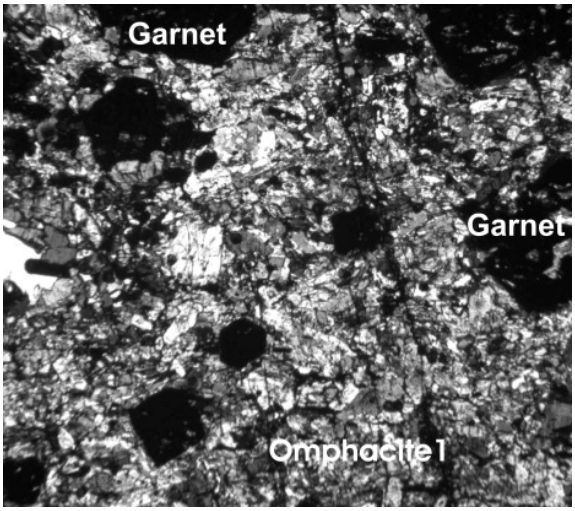

(e) magnification: 10x **EK-A**

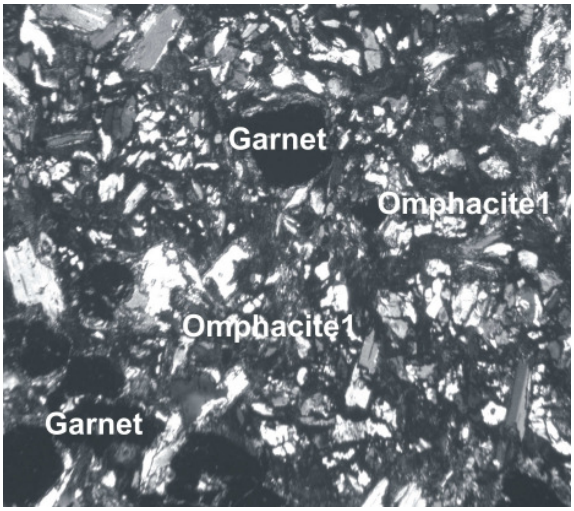

(f) magnification: 10x **EK-G**

Fig. 18: Photographs of Tauern Window eclogite thin sections (XZ-sections). (a) and (b) Fine grained eclogites E1, strongly lineated, the omphacite2 lineation is marked by dotted lines; (c) Fine grained eclogite E1, crossed nicols, the omphacite2 lineation is marked by dotted lines; (d) to (f) Coarse grained eclogites E2, crossed nicols. Note the different magnifications.

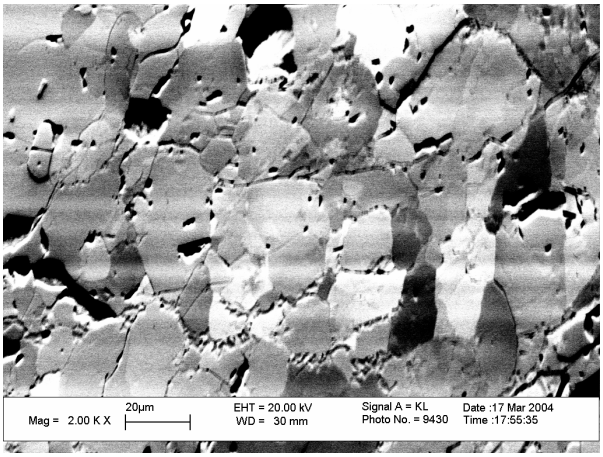

(a) magnification: 2000x **EK-A**

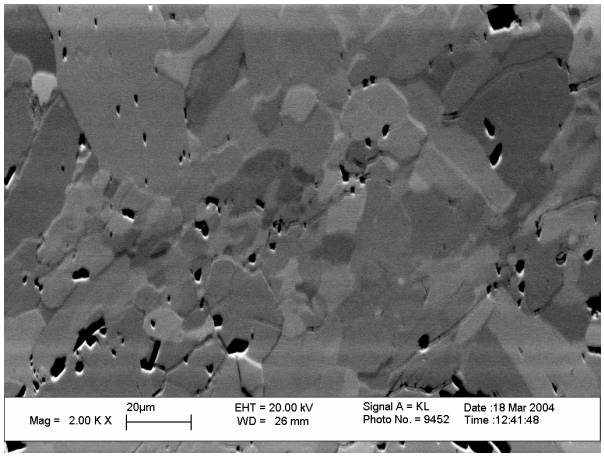

(b) magnification: 2000x **EK-G**

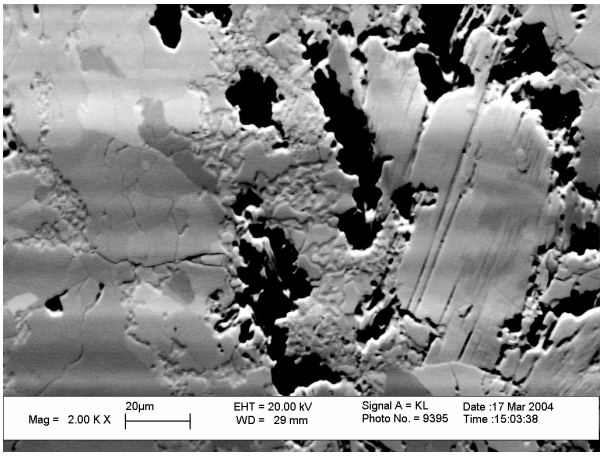

(c) magnification: 2000x **EK-09**

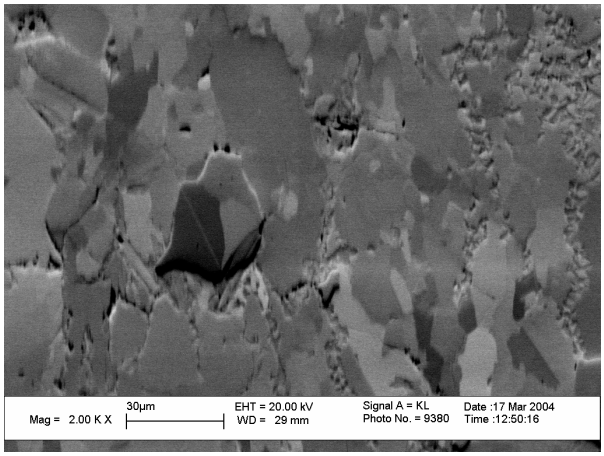

(d) magnification : 2000x **EK-04**

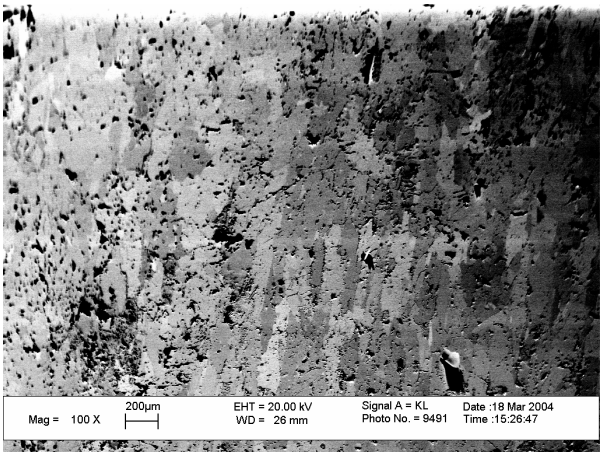

(e) magnification: 100x **EK-06**

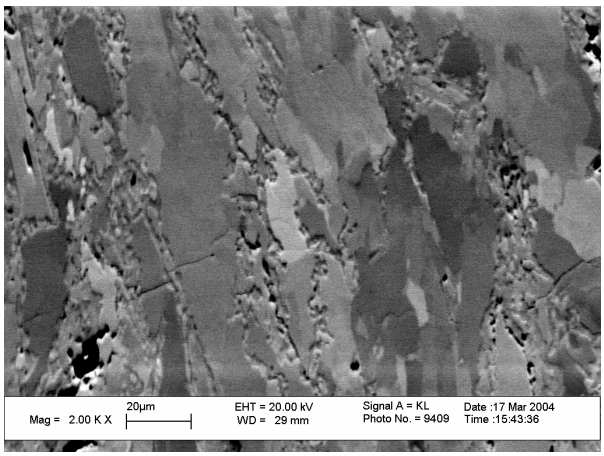

(f) magnification: 2000x **EK-06**

Fig. 19: Orientation contrast pictures of omphacites (XZ-section). (a) to (c) Subgrains of omphacite1, coarse grained eclogite (E2), different samples; (d) Omphacite2, fine grained eclogite (E1); (e) and (f) Omphacite2, fine grained eclogite (E1), one sample. Note the different magnifications.

3.3.2. LPO patterns in the Eclogite Zone

The investigated omphacite LPO patterns from the Eclogite Zone are plotted as contoured polefigures in equal area and lower hemisphere projections (Fig. 20). The samples are presented in north-south profiles (from bottom to top) which are numbered as profiles A to F. The profiles are arranged from west (profile A) to east (profile F). For detailed sample and profile locations, see Fig. 9.

The lattice preferred orientation patterns of omphacite from the Eclogite Zone (Figs. 20a to 20f) mainly show strong point maxima of {001} close to the lineation and are characterized by an alignment of {110} within the foliation plane. In most of the samples across the entire Eclogite Zone, the fabrics are symmetric, even close to the boundaries between Eclogite Zone and surrounding rock units.

The westernmost profile A (Fig. 20a, samples EK-07, EK-09, EK-13, EK-22, EK-14) shows mainly homogeneous patterns with one exception, being EK-22. From bottom to top (north to south), the samples EK-07, EK-09 and EK-13 show very slight asymmetries at {001}. The LPO in these samples displays transition patterns that strongly resemble S-type end members. Sample EK-07 was collected close to the underlying Venediger Nappe. Therefore its LPO was expected to display a significant asymmetry but it is distributed very homogeneous in relation to lineation and foliation. Sample EK-13 reflects a slight {001} asymmetry (~10°) in its girdle distribution in relation to the lineation axes L. Moreover to the top of the profile, sample EK-22 differs remarkably in comparison to most other samples in the Eclogite Zone by strong L-type LPO. It also shows a slight rotation (~20º) in its mean unit deviation maximum perpendicular to the lineation axes L. The uppermost sample EK-14 close to the overlying Glockner Nappe is characterized by a symmetric transition pattern and does not show any asymmetries. No change of asymmetry between upper and lower contact of the Eclogite Zone have been measured.

In profile A, the sample EK-09 represents coarse grained omphacite1 while all other samples represent fine grained omphacite2.

Profile B (Fig. 20b, samples EK-06, EK-08, EK-04, EK-02, EK-01) is characterized by a more irregular LPO distribution than profile A. The lowermost sample EK-06 reflects S-type tending symmetric transition LPO without any expected asymmetries close to the underlying unit. Further to the top, sample EK-08 possesses only a weak mean unit deviation maximum (1.89) but can be described as transition pattern. This sample fits in its symmetry with other samples but its LPO is more randomly distributed than in most of all other samples in the entire study area. The samples EK-04 and EK-02 are very symmetric and show transition

patterns that are similar to the LPO pattern of sample EK-06. The uppermost sample EK-01, close to the top of the Eclogite Zone, depict an S-type-like texture pattern is more randomly orientated that in other samples and the maxima are not very clear. Only in {001} a symmetry corresponding to the lineation axes L is observable, {010} and {110} do not show a clear pattern.

Overall, asymmetries observed in the uppermost part of profile B are not arranged in any systematic way. No clear development in LPO between the bottom and the top boundary of the Eclogite Zone could be measured along this profile. In profile B all samples represent fine grained omphacite2.

Profile C (Fig. 20c, samples EK-05, EK-18, EK-16, EK-20, EK-15) is characterized by a more randomly LPO distribution in comparison to the profiles A and B. Sample EK-05 (lowermost part of profile C) reflects a distinct symmetry in patterns that tend strongly to S-type LPO. No asymmetries have been measured close to the lower boundary of the Eclogite Zone. The remaining samples in profile C display LPO patterns that differ in an outstandingly non-systematic way. LPO in sample EK-18 is strongly rotated in relation to all structural axes and do not express any distinct pattern. Sample EK-16 (central part of profile C) displays a transition pattern that is rotated in relation to the lineation (~25°) at {001} and in relation to the foliation at {010}(~25°). In the uppermost samples EK-20 and EK-15, only weak unit deviation maxima (2.00 and 2.15) are common. The LPO pattern in sample EK-20 is more randomly distributed in comparison with other samples. Furthermore, it is rotated in {010} in its mean unit deviation maximum related to the lineation axes L (~30º). The LPO pattern in the uppermost sample EK-15 is comparable to the one of sample EK-20 but is considerably rotated (~40º) in {010} perpendicular to the lineation axes L.

Overall, in profile C the omphacite LPO distribution is the most non-systematic over the entire study area. All samples in profile C represent fine grained omphacite2.

In profile D (Fig. 20d, samples EK-R, EK-H, EK-B, EK-D, EK-V) the lowermost sample EK-R reflects a strong symmetry in its clear S-type pattern without any measured asymmetries close to the boundary between Eclogite Zone and underlying Venediger Nappe. Sample EK-H shows a transition pattern but is more randomly orientated than all other samples. The LPO distribution in this sample is not very clear. In the central part of profile D, the sample EK-B displays a symmetric LPO pattern that resembles – in contrast to the majority of the samples – L-type LPO. Sample EK-D displays a symmetric transition LPO pattern, characterized by a very strong mean unit deviation maximum (13.36) which is by far the highest in all measured Tauern Window samples. The uppermost sample EK-V is characterized by the clearest S-type

LPO pattern in profile D and is also distinctly symmetric. No asymmetries were measured close to the boundary to the overlying Glockner Nappe.

In profile D, sample EK-D represents coarse grained omphacite1, all other samples represent fine grained omphacite2.

In profile E (Fig. 20e, samples EK-E, EK-G, EK-C, EK-A, EK-T), the lowermost samples EK-E and EK-G are distinguished by transition fabrics that tend remarkably to S-type LPO. No asymmetries close to the boundary to the underlying Venediger Nappe have been measured. In the central part of profile E, the sample EK-C reflects a transition LPO pattern but the maxima in its mean unit deviation are more randomly orientated; the pattern is not very distinct. In the upper part of profile E, the samples are characterized by a very strong S-type signature. The sample EK-A reflects the strongest S-type signature of all samples over the entire study area. It also reflects a very strong symmetry. The uppermost sample EK-T is slightly asymmetric (~8°) in {001} in relation to the lineation axes L. This sample also resembles S-type LPO in a very strong way. No developments in asymmetries from bottom to top of the profile were observed.

Overall, profile E is characterized by the strongest S-type tendency of all investigated profiles inside the study area. In profile E, the samples EK-G (lowermost part of the profile) and EK-A (upper part of the profile) represent coarse grained omphacite1. All other samples represent fine grained omphacite2.

The easternmost profile F (Fig. 20f, samples EK-M, EK-P, EK-F) contains only three samples. The lowermost sample EK-M shows a transition pattern with a rotation of its mean unit deviation maximum (~20º) in {010} and {001} in relation to the lineation axes L. The same rotation can also be observed perpendicular to the lineation.

In the central part of profile F, the sample EK-P depicts a pattern with a clear symmetry that resembles very strongly to S-type LPO and is not rotated in any way. The uppermost sample EK-F also reflects a symmetric S-type like pattern without any asymmetries close to the boundary between Eclogite Zone and overlying Glockner Nappe. In profile F all samples represent fine grained omphacite2.

Based on the model by Helmstaedt et al. (1972, Figs 6 and 21), the 28 samples from the Eclogite Zone presented in this study can be divided into four groups. The largest group contains 15 samples that are interpreted to reflect S-type LPO (EK-02, EK-04, EK-05, EK-06, EK-07, EK-09, EK-13, EK-16, EK-A, EK-E, EK-F, EK-P, EK-R, EK-T, EK-V). Transition signatures are reflected in 8 samples (EK-01, EK-08, EK-14, EK-20, EK-C, EK-D, EK-M, EK-G); two samples (EK-22, EK-B) show L-type LPO patterns. The three samples EK-15,

EK-18 and EK-H do not display a distinct LPO distribution. Therefore, they can be assigned neither to S-type nor to L-type LPO.

Overall, the bulk of the samples vary between strong S-type patterns and predominantly transition fabrics that closely resemble S-type patterns. The majority of the samples reflect highly symmetric LPO patterns. Small asymmetries are present in patterns that show a slight rotation, but no coherence between asymmetry and position of the samples can be observed. Even slightly asymmetric patterns are mainly close to S-type textures.

The distinctness of a symmetric LPO distribution increases slightly to the east, combined with a tendency to S-type LPO end members into eastern direction. The two samples that reflect an L-type texture are placed in the central part of the Eclogite Zone and not related to its footwall of hanging wall contact.

Only a few samples reflect significant asymmetries but without any systematic distribution across the entire Eclogite Zone. These asymmetries are not consistent and differ between each sample. No indications for any preferred noncoaxial deformation have been found.

The distribution of omphacite LPO is not associated with the different eclogite types. Coarse grained eclogites (E2, samples EK-05, EK-09, EK-A, EK-G, see Fig. X) display partly S-type and partly transition patterns that do not differ from LPO distribution in fine grained eclogites (E1). No textural differences in both omphacite generations have been observed. Omphacite1, which is common in coarse grained eclogites displays mainly identical patterns than omphacite2, which is predominantly common in the fine grained samples.

The textures are indicative of intracrystalline glide deformation on the (010) [001] and (110) [001] slip system.

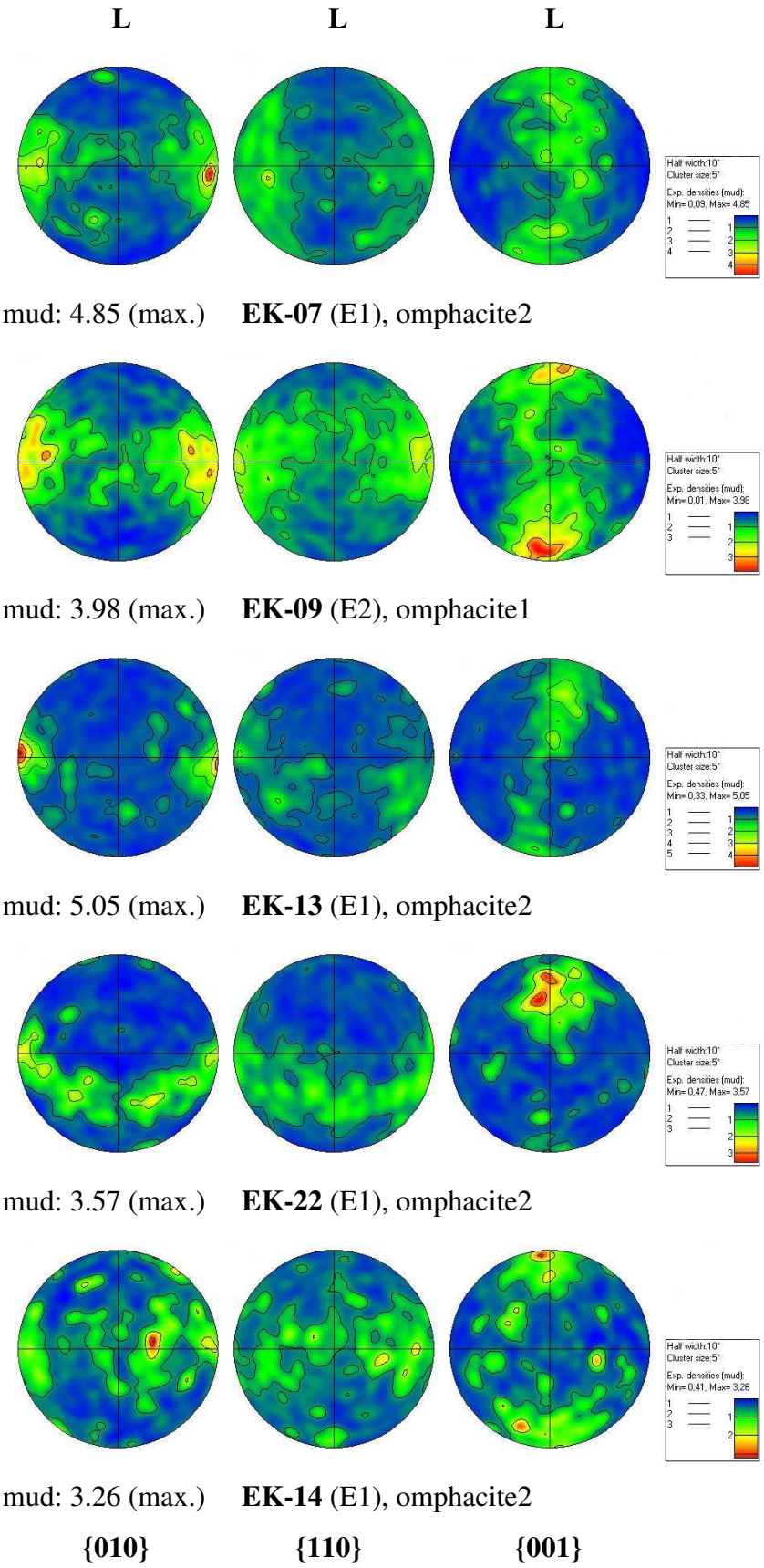

Fig. 20a: Omphacite LPO along **profile A** across the Eclogite Zone. The lineation is marked by L. The profile is north-south directed. Polefigures are plotted in equal area, lower hemisphere projections. For sample and profile locations, see Fig. 9. mud (max.) – mean unit deviation (maximum).

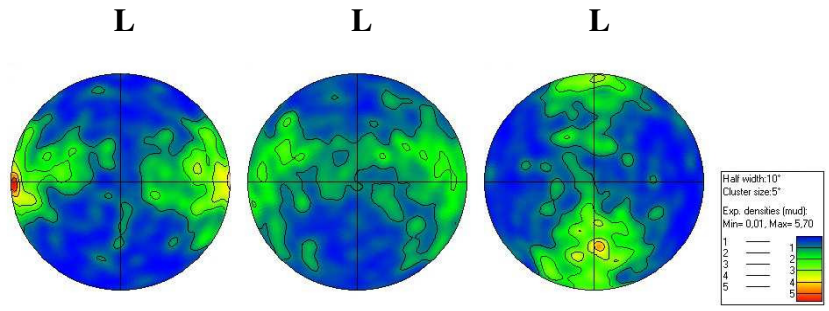

mud: 5.70 (max.) **EK-06** (E1), omphacite2

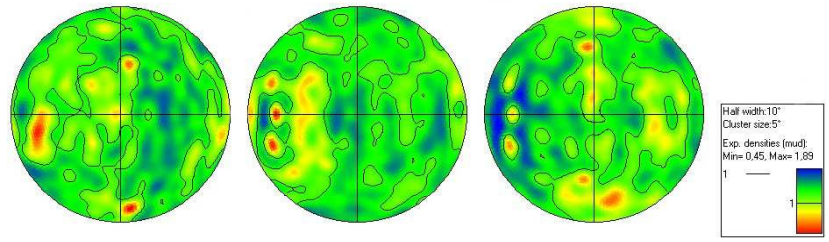

mud: 1.89 (max.) **EK-08** (E1), omphacite2

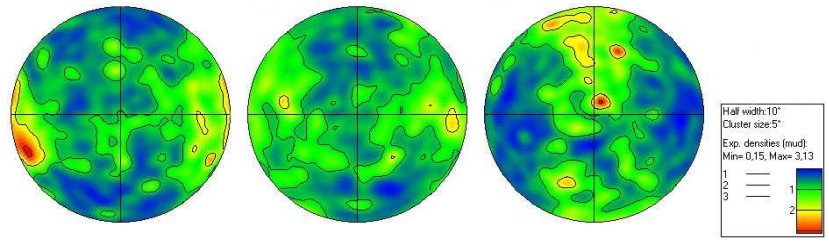

mud: 3.13 (max.) **EK-04** (E1), omphacite2

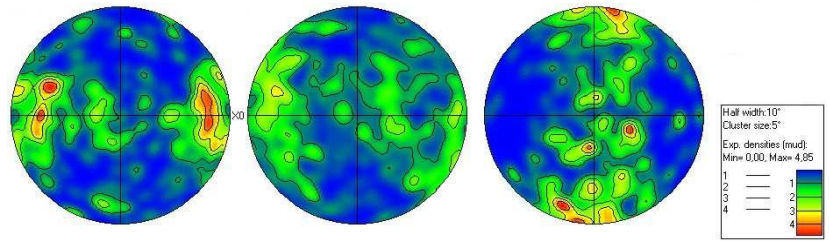

mud: 3.75 (max.) **EK-02** (E1), omphacite2

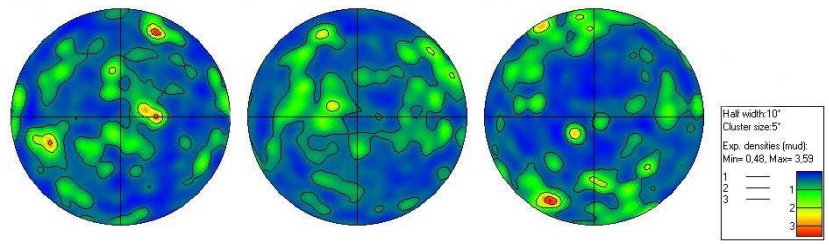

mud: 3.59 (max.) **EK-01** (E1), omphacite2

{010} **{110}** **{001}**

Fig. 20b: Omphacite LPO along **profile B** across the Eclogite Zone. The lineation is marked by L. The profile is north-south directed. Polefigures are plotted in equal area, lower hemisphere projections. For sample and profile locations, see Fig. 9. mud (max.) – mean unit deviation (maximum).

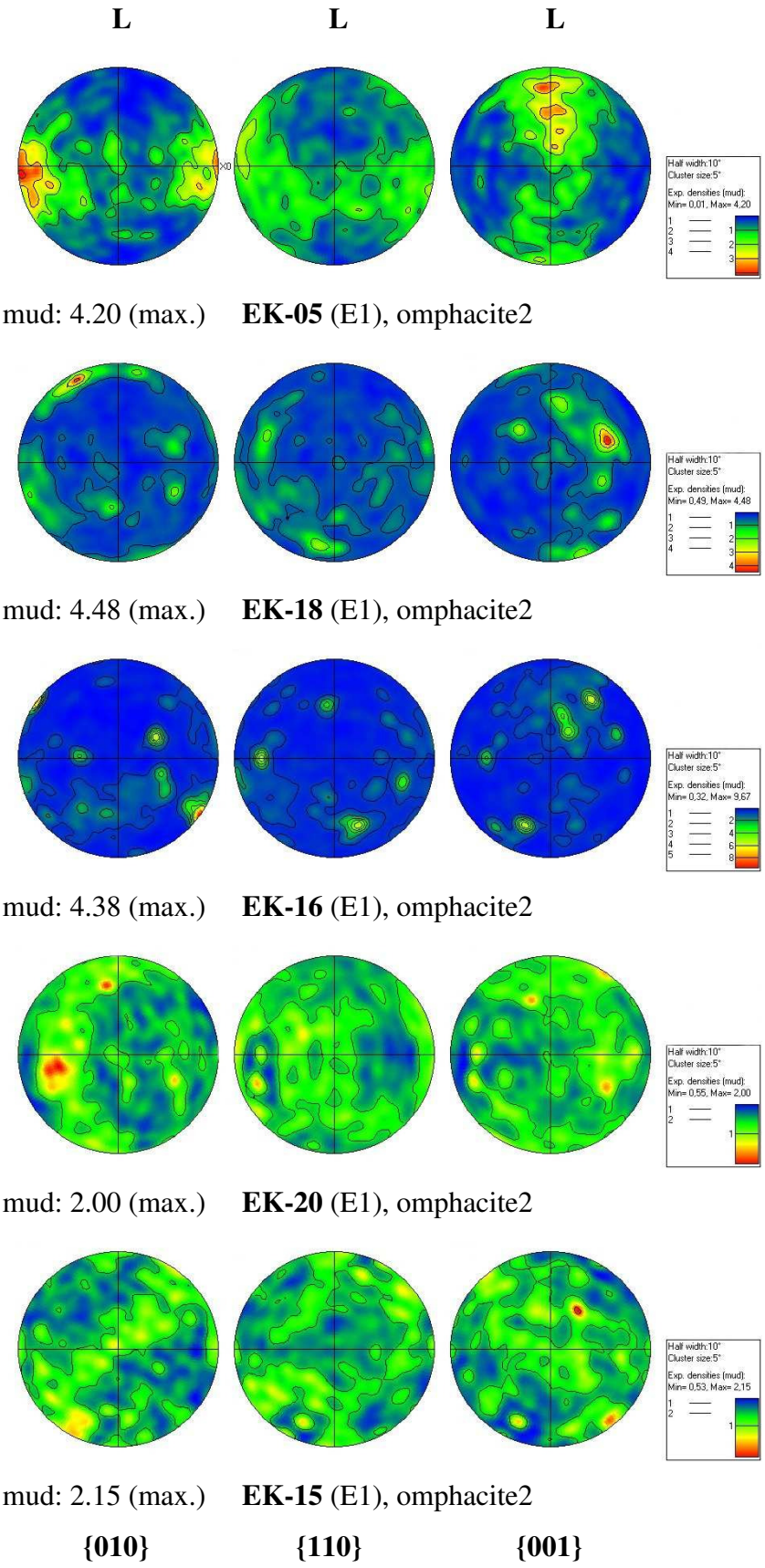

Fig. 20c: Omphacite LPO along **profile C** across the Eclogite Zone. The lineation is marked by L. The profile is north-south directed. Polefigures are plotted in equal area, lower hemisphere projections. For sample and profile locations, see Fig. 9. mud (max.) – mean unit deviation (maximum).

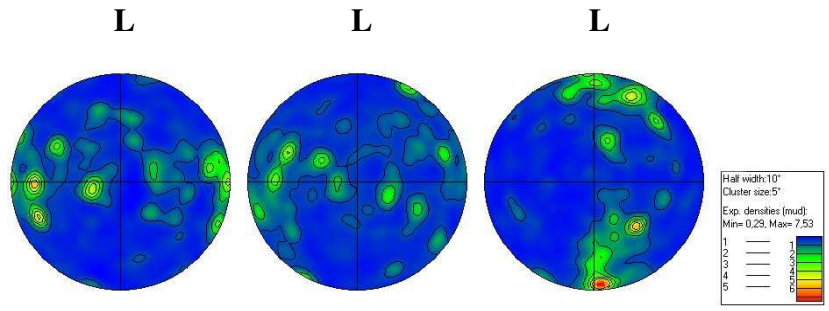

mud: 7.53 (max.) **EK-R** (E1), omphacite2

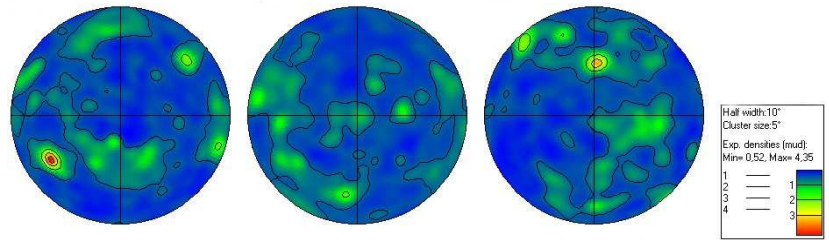

mud: 4.35 (max.) **EK-H** (E1), omphacite2

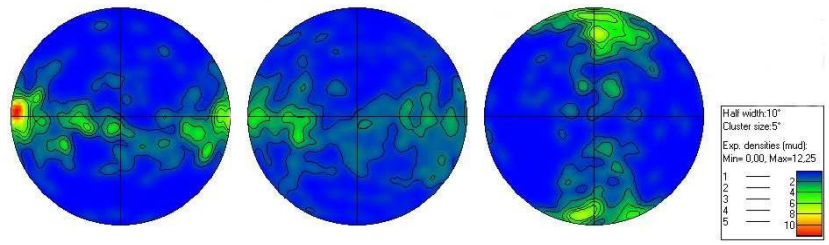

mud: 9.51 (max.) **EK-B** (E1), omphacite2

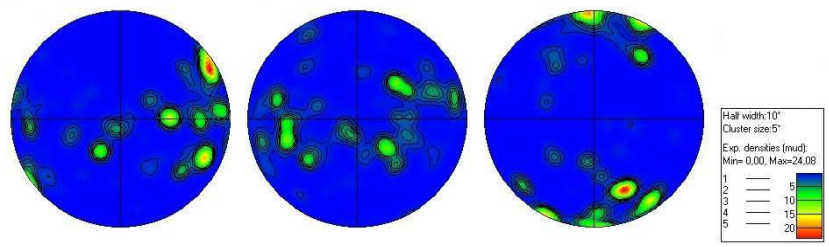

mud: 13.36 (max.) **EK-D** (E2), omphacite1

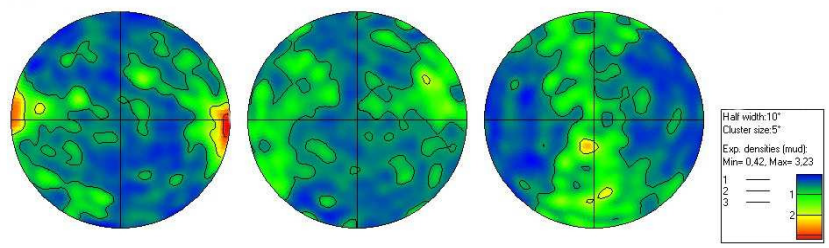

mud: 3.23 (max.) **EK-V** (E1), omphacite2

{010} **{110}** **{001}**

Fig. 20d: Omphacite LPO along **profile D** across the Eclogite Zone. The lineation is marked by L. The profile is north-south directed. Polefigures are plotted in equal area, lower hemisphere projections. For sample and profile locations, see Fig. 9. mud (max.) – mean unit deviation (maximum).

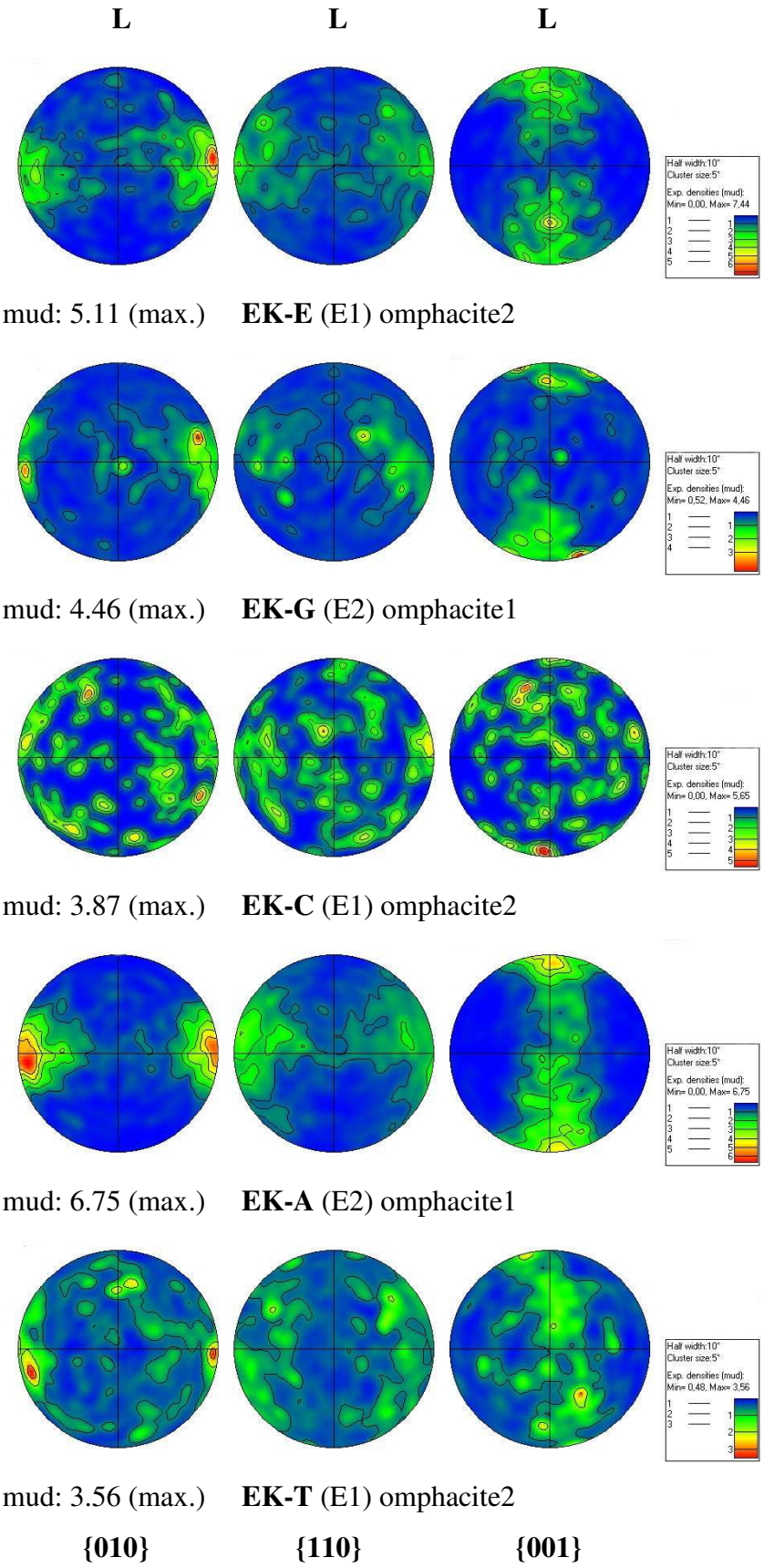

Fig. 20e: Omphacite LPO along **profile E** across the Eclogite Zone. The lineation is marked by L. The profile is north-south directed. Polefigures are plotted in equal area, lower hemisphere projections. For sample and profile locations, see Fig. 9. mud (max.) – mean unit deviation (maximum).

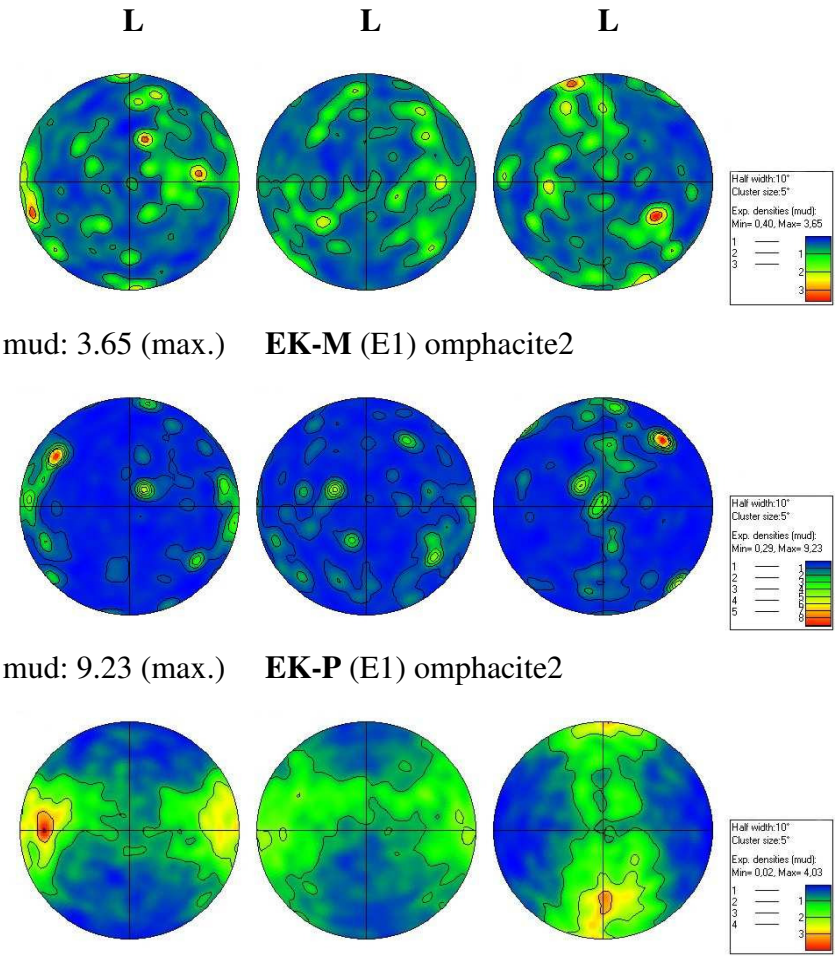

Fig. 20f: Omphacite LPO along **profile F** across the Eclogite Zone. The lineation is marked by L. The profile is north-south directed. Polefigures are plotted in equal area, lower hemisphere projections. For sample and profile locations, see Fig. 9. mud (max.) – mean unit deviation (maximum).

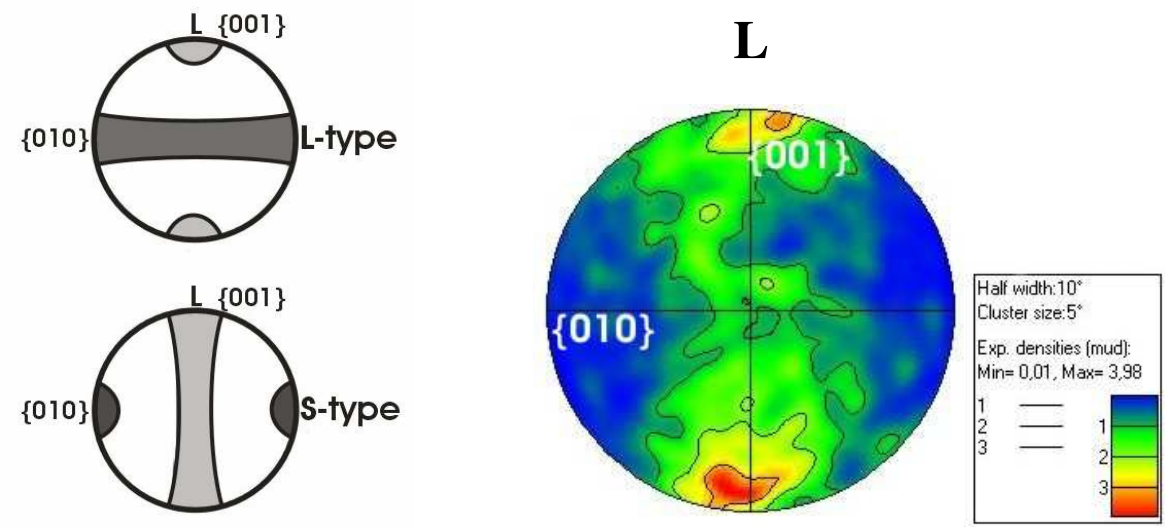

Fig. 21: Comparison between the omphacite LPO endmembers after Helmstaedt et al. (1972) and omphacite LPO of an eclogite from the Tauern Window (sample EK-A, see Fig. 20e). The measured texture is very slightly asymmetric at {001} and close to S-type LPO. The lineation is marked by L; the polefigure is plotted in equal area, lower hemisphere projection.

Beside the lattice preferred orientation measurements, orientation contrast (OC) pictures and mapping (Fig. 22) were carried out to study the relationship between LPO and shape preferred orientation (SPO).

A comparison between LPO and SPO in eclogites from the Tauern Window strongly indicates an independence of the omphacite textures from shape preferred orientation on a subgrain scale. Samples, showing omphacite SPO, display no different patterns than samples, showing no shape preferred orientation. Observed asymmetries in omphacite LPO patterns are not related to SPO.

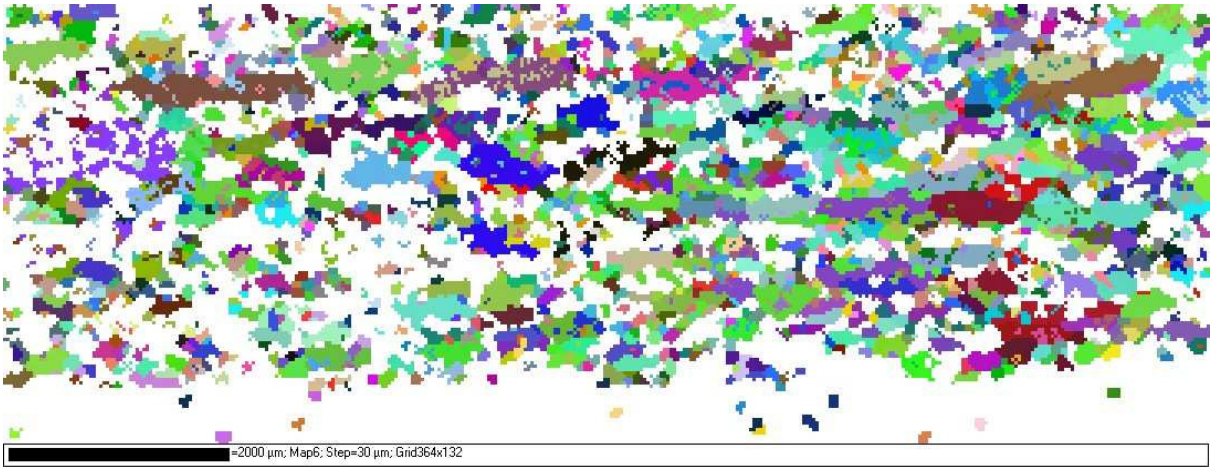

EK- P (E1) omphacite2

(a) magnification: 30x

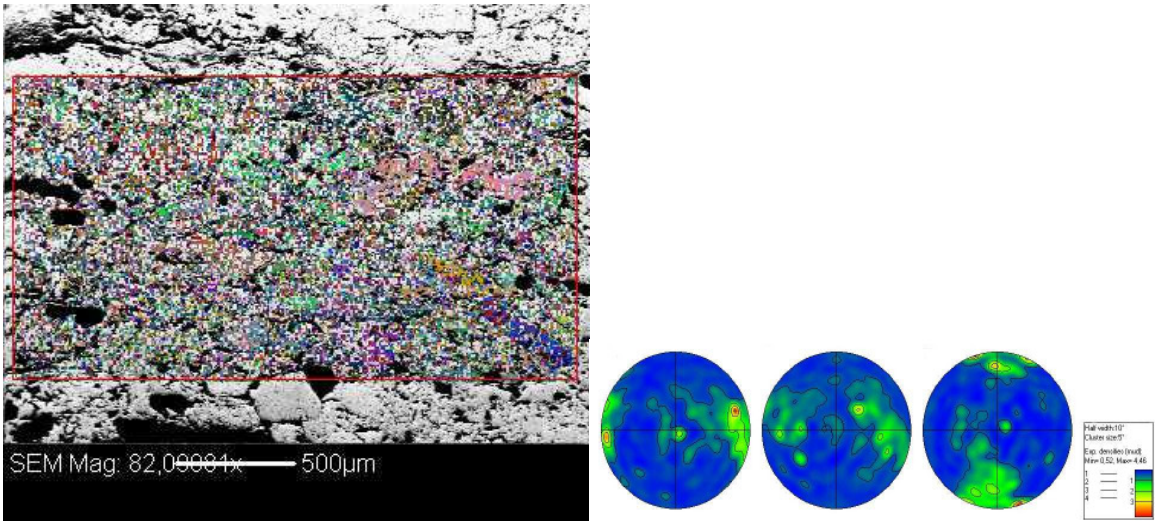

EK-G (E1) omphacite2

(b) magnification: 82x

Fig. 22

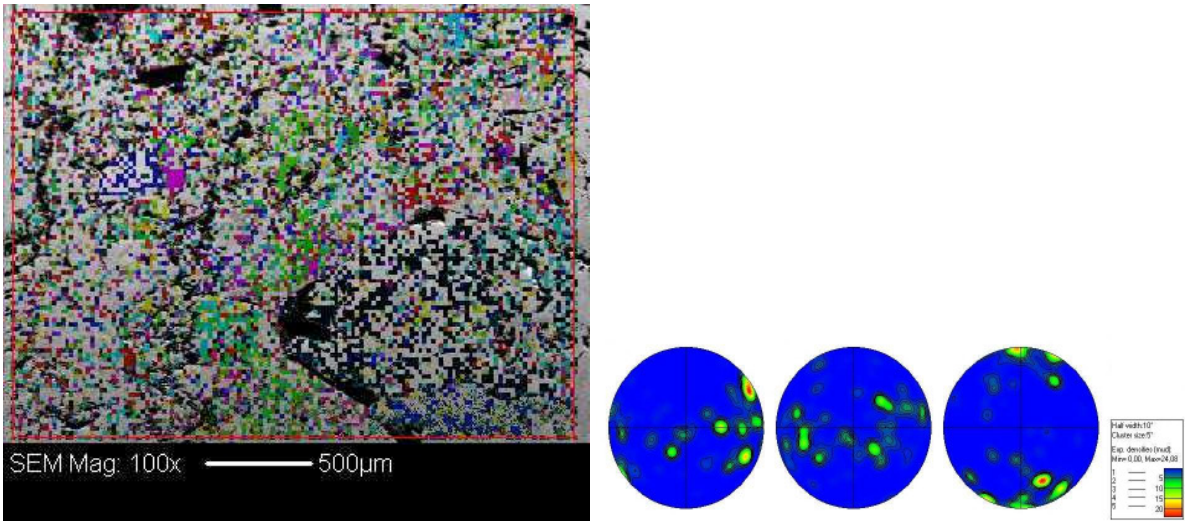

EK-D (E2) omphacite1

(c) magnification: 100x

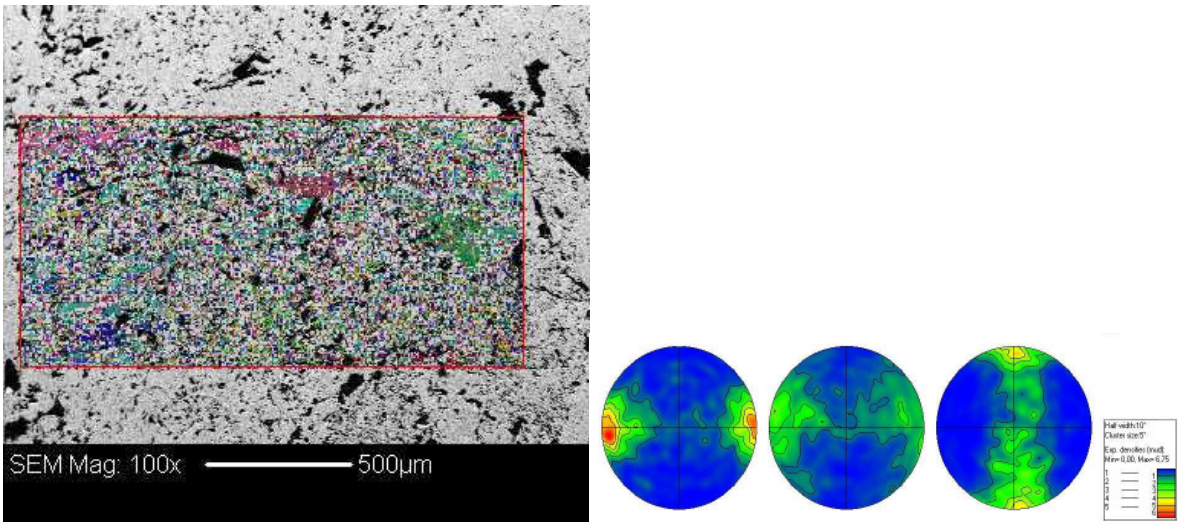

EK-A (E2) omphacite1

(d) magnification: 100x

Fig. 22: Comparison between lattice preferred orientation (LPO) and shape preferred orientation (SPO), subgrain scale; (a) Orientation contrast map and LPO polefigure, sample EK-P; (b) Orientation contrast picture, coloured and LPO polefigure, sample; (c) Orientation contrast picture, coloured and LPO polefigure, sample EK-D; (d) Orientation contrast picture, coloured and LPO polefigure, sample EK-A. Note the different magnifications.

3.4. Discussion & Conclusions (I): Eclogite Zone

3.4.1. Discussion

Previous studies (e.g. Kurz et al., 1998, 2004; Hoschek, 2007) demonstrated that the Tauern Window eclogites represent two different eclogite types that formed under different metamorphic conditions during the prograde evolution up to the metamorphic peak. Based on the studies of Bascou et al. (2001, 2002) and Kurz et al. (2004), a change from contractional to extensional textures should display the change from burial to exhumation as documented for the Eclogite Zone in neutron diffraction patterns by Kurz et al. (2004). These authors described a change from S-type patterns in coarse grained eclogites, which were formed during prograde evolution to L-type patterns in fine grained eclogites, representing the metamorphic peak. This was interpreted by them to indicate the change from subduction to exhumation, reflected in the omphacite LPO of the Eclogite Zone. If this assumption is correct, it can be expected that EBSD generated textures along the entire Eclogite Zone should display the same pattern distribution between coarse grained and fine grained eclogites. The LPO patterns should show a development from S-type LPO in coarse grained samples to L-type LPO in fine grained samples.

In contradiction to the neutron diffraction generated patterns of Kurz et al. (2004), the results of this study predominantly show no differences in the LPO between fine grained and coarse grained eclogites (E1 & E2). The patterns of both groups are close to S-type end members or transition patterns tending to S-type LPO. Only one fine grained eclogite (samples EK-22 and EK-B, see Figs. 20a & 20d) shows strong L-type patterns.

According to Bascou et al. (2001, 2002) and Kurz et al. (2004), the textures are predominantly related to a prograde setting and most of them do not show indications for any kind of extensional processes.

Assuming that coarse grained eclogites were formed on the prograde path and the S-type patterns therefore are indicative for a prograde texture, it can be suggested that comparable S-type patterns in fine grained eclogites also reflect a prograde signature, even if the eclogites were formed during peak metamorphic conditions.

According to experimental studies and modelling by Bascou et al. (2001, 2002), one can assume that the LPO patterns represent a process that induced a contractional or partly transpressional setting on the textures.

Contraction during LPO formation supports the suggestion for LPO development on the prograde path of eclogite formation. Therefore, the patterns can be interpreted to reflect burial signatures that were not affected during the exhumation process.

Even close to the contacts to footwall and hanging wall, no significant LPO asymmetries are observed. This is in contradiction with the kinematic data that indicate varying shear sense on both sides of the Eclogite Zone. Therefore, it can be concluded that the crystallographic textures are not related to the mesoscopic structures recorded in the rocks.

The kinematic data indicate top-N thrust at the base and sinistral strike-slip with a slight signature of top-S normal shearing at the top of the Eclogite Zone. Such a different shear sense at the contact zones of the dense rock unit would fit with extrusion wedge geometry with thrust folding at its base and normal folding at its top (Fig. 11).

The very rapid exhumation rate of minimum 36 mm/yr for the Eclogite Zone, as calculated by Glodny et al. (2005), is fast enough to avoid sinking of the eclogite lenses during the exhumation process. Detailed mapping (Fig. 16) indicates a less eclogite proportion as suggested in a previous study by Raith et al. (1980). The overall eclogite / matrix ratio is significantly smaller than expected. Behrmann and Ratschbacher (1989) questioned bouyancy as exhumation driving mechanism because of too large eclogite lenses based on the previous calculations. Their assumptions are based on the previous calculation by Raith et al. (1980) which is not in agreement with the results of this study.

An obvious model that is suitable with prograde LPO patterns, varying shear sense and a small eclogite/matrix ratio could be extrusion wedge exhumation driven by buoyancy forces (Fig. 23). The textures are not in contradiction with such a model but do also not clearly indicate it. Probably omphacite LPO of the Eclogite Zone is completely independent from the exhumation and instead coupled with the formation of the eclogites. This means that exhumation can not be derived directly by the omphacite textures.

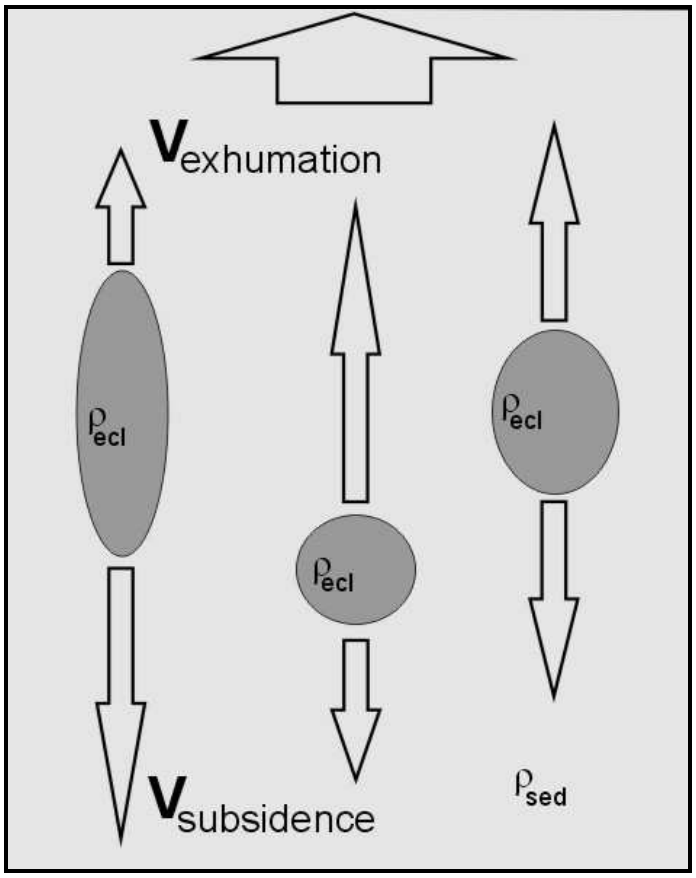

ρ_{ecl} ~ 3.4 g/cm^3

ρ_{sed} ~ 2.8 g/cm^3

Fig. 23: Illustration of buoyancy driven eclogite exhumation. Dense eclogite lenses are embedded and transported upwards inside lower dense rocks. Uplift depends on the density contrast and the size of the dense bodies.

3.4.2. Conclusions

The study of the omphacite textures showed that the LPO patterns for the Eclogite Zone are not coupled with the kinematics and reflect a process which is not connected with the exhumation of the Eclogite Zone.

The LPO patterns are not coupled with any shape preferred orientation (SPO) in the eclogites

The difference between the symmetric omphacite patterns and the kinematic indicators in the garnet mica schist can be interpreted to display strain partitioning during exhumation.

The LPO patterns reflect a prograde, underplating-related texture that was not affected during the exhumation process.

The absence of changes in omphacite LPO patterns is not in contradiction with the kinematic and mapping indicators for an extrusion wedge model.

A possible exhumation model would be buoyancy driven extrusion wedge exhumation for the Eclogite Zone because it is the only model which does not affect the omphacite LPO directly and is in agreement with kinematics and detailed mapping of the eclogite lenses. However, such a model is not clearly indicated by the omphacite textures of the Eclogite Zone.

The eclogite / matrix ratio is smaller than estimated in previous studies.

The very fast exhumation was achieved in a transpressional setting which corresponds with the small size of the Eclogite Zone.

Overall, it is very questionable that omphacite textures of the Eclogite Zone are applicable to indicate exhumation processes in any way.

4. GEOLOGICAL SETTING (II): WESTERN GNEISS REGION

4.1. Introduction

The Scandinavian Calidonides developed over the a timescale of ~150 Ma from ~500 to ~ 350 Ma, formed by a collisional event, in which Baltica and its tectonic cover were subducted beneath the overriding Laurentian plate during the closure of the Iapetus ocean (Harland & Gayer, 1972; Roberts & Sturt, 1980; Gee, 1982). The Norwegian Caledonides are a perfect example to study exhumation processes on high-pressure and ultrahigh-pressure rocks and the large Western Gneiss Region (WGR) serves as a good example.

The Western Gneiss Region is a huge tectonic window, interpreted to represent a region, in which the deepest structural level of the Caledonides is exposed. It is a classic study area for investigations of highly metamorphosed rocks, especially a classic locality for high-pressure and ultrahigh-pressure eclogites. The rock unit is exposed over an area of a length extension (north-south directed) of ~250 km and ~200 km in width (east-west directed).

The Western Gneiss Region is composed mainly of quartz-bearing feldspatic gneisses of granitic or granodioritic composition (e.g. Foreman et al., 2005). It includes further anorthosites, mafic- to ultramafic rocks and metasediments. The rocks were extremely reworked during the Caledonian orogeny, whereby the WGR is dominated now by rocks of amphibolite metamorphic grade, in which the eclogites are embedded. The reworking increases from east to west (Dietler et al., 1985).

Eclogite facies metamorphism was reached during the Scandian orogeny (e.g. Griffin & Brueckner, 1985; Gebauer et al., 1985; Tucker et al., 1992). The eclogites are enclosed in mainly felsic amphibolite rocks. The eclogite rocks reflect a wide range of high-pressure and ultahigh-pressure conditions. Dobrzhinetskaya et al. (1995), Wain (1997), Cuthbert et al. (2000) and Hacker et al. (2003) described in detail coesite-bearing eclogites and diamond-bearing garnet peridotites in parts of the Western Gneiss Region and further described boundaries, dividing high-pressure and ultrahigh-pressure units. Coesite-bearing eclogites were further described in small local places inside the Western Gneiss Region (Smith, 1984, 1988, 1995), indicating pressure conditions of >28 kbar and therefore a burial depth of more than 100 km. The bulk of the eclogites represent a P-T-range from ~20 kbar and 400ºC to 35 kbar and 800ºC (Cuthbert et al., 2000; Terry et al., 2000; Hacker et al., 2003; Labrousse et al., 2004; Ravna & Terry, 2004; Walsh & Hacker, 2004).

The pressure conditions within the Western Gneiss Region tend to increase from the SE to the NW. While in the southern- and easternmost parts, no eclogites occur, the ultrahigh-pressure rocks are dominantly concentrated in the northern and western part of the overall unit (see Fig. 24). Eclogite metamorphic peak conditions were dated mainly by Sm–Nd and U–Pb geochronology, resulting in ages of 400-408 Ma for the metamorphic peak of most of the eclogites (Mearns, 1986; Carswell et al., 2003; Root et al., 2004, Young et al., 2007). In the northernmost part of the Western Gneiss Region, the UHP peak metamorphism occurred around 410-415 Ma (Terry et al., 2000; Krogh et al., 2004).

The question how the Western Gneiss Region was exhumed is still lively debated. Previous studies (Krabbendam & Dewey, 1998; Walsh & Hacker., 2004; Foreman et al., 2005; Wheeler et al., 2005; Walsh et al., 2007) lead to favoured exhumation models, based on transtensional or extensional settings

Krabbendam & Dewey (1998) presented a model, in which exhumation is controlled largely by sinistral transtension, driven by sinistral oblique plate divergence of the Laurentian and Baltic plates. This included the high-pressure rocks as well as the ultrahigh-pressure rocks. This model involves bulk noncoaxial deformation. Foreman et al. (2005) studied a large HP-eclogite body in the southern part of the Western Gneiss Region (Drøsdal eclogite) and showed that a transtensional setting began at eclogite facies conditions. Wheeler et al. (2005) supported the model by Krabbendam & Dewey (1998) and assumed oblique plate divergence, leading to transtension.Walsh & Hacker. (2004) & Walsh et al. (2007) presented petrologic and geochronologic data that lead to an exhumation model in which the UHP and HP eclogites were driven by underplating and extension.

The exhumation rates of the Western Gneiss Region are significantly slower in comparison to the Eclogite Zone. Terry et al. (2000) calculated much faster exhumation rates for UHP exhumation (10.9 mm yr^{-1} on average) than for exhumation under high-pressure conditions (3.8 mm yr^{-1} on average). Labrousse et al. (2004) supported a stepwise exhumation, calculating exhumation rates that decrease with decreasing pressure, starting with 8.1 mm yr^{-1} and decreasing to 4.1 and 1.4 mm yr^{-1}. These data are calculated for the Moldefjord area in the northernmost part of the Western Gneiss Region. For the Nordfjord area, which is mainly the investigated area in this study, exhumation rates from 2.3 to 4.6 mm yr^{-1} were calculated (Labrousse et al, 2004), including high-pressure and ultrahigh-pressure exhumation.

It was lively debated if the Western Gneiss Region represents one coherent unit or if it is divided in different high-pressure and ultrahigh-pressure blocks. Krabbdendam & Wain

(1997) discussed that a connection between HP and UHP units in the Western Gneiss Region is unclear because of contact overprinting by later amphibolite-facies metamorphism. A connection between units of different pressure conditions was also questioned by Wain et al. (2001). Based on detailed mapping and petrologic data, Root et al. (2005) and Young et al. (2007) recently argued that the high-pressure rocks unit overlie the ultrahigh-pressure areas and that HP and UHP eclogites form a consistent unit. Young et al. (2007) argued that the boundary between high-pressure and ultrahigh-pressure units represent a gradational transition into UHP conditions, which indicates a wide range of pressure conditions during a common exhumation process. Therefore, it is widely assumed that the Western Gneiss Region is one huge coherent unit.

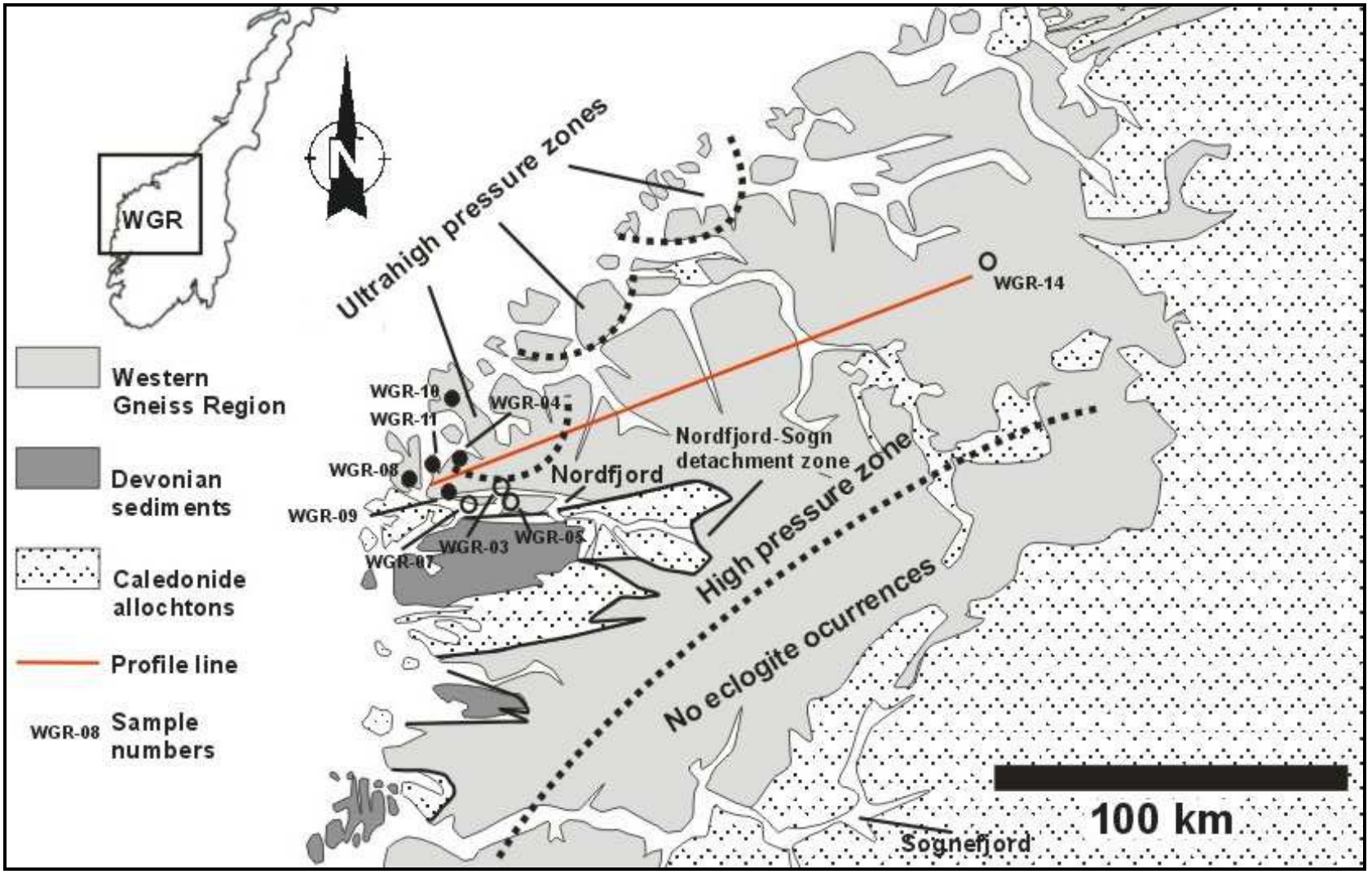

Fig. 24: Geologic overview of the Western Gneiss Region (WGR), western Norway, including profile (red line) and sample locations for EBSD study. Samples of profile part A are marked with black dots, samples of profile part B are marked with circles.

4.2. Lattice preferred orientation (LPO) data

4.2.1. Problem definition

The lattice preferred orientation patterns of the Western Gneiss Region were studied to compare them with the textural data of the Eclogite Zone. Based on the results from the Tauern Window (see chapter 3), an investigation of Western Gneiss Region LPO is focused on the following questions:

- Are the omphacite textures of the Western Gneiss Region similar to the textures of the Eclogite Zone?
- If so, does this indicate that the textures are also independent from the exhumation as assumed for the Tauern Window eclogites?
- If the textures are independent from exhumation, how were they generated and affected?
- Do the textures of the Western Gneiss Region differ from the textures of the Eclogite Zone?
- If so, does this indicate that the Western Gneiss Region textures are connected with the exhumation of the WGR eclogites?

4.2.2. Sample description

The investigated eclogites from the Western Gneiss Region are very homogeneous in their mineralogy but vary significantly in grain size and shape as well as in grain orientation.
The eclogites are composed of ~60 % omphacite and ~40 % garnet. The omphacite / garnet proportion of the eclogites is very homogeneous in the entire sample collection. The omphacite grains vary in size from ~100 µm to 1 cm. Defined by the omphacite grain size, the studied eclogite samples can be devided into two groups. On the one hand, in some samples omphacite shows a wide range of different grain sizes. Fine grained omphacite with grain sizes down to 500 µm occurs as an omphacite matrix. Only in few cases, significantly smaller omphacite grains occur. A grain size between 0.5 and 1 mm is very common. The fine grained omphacite grains are mainly randomly orientated and surround larger omphacite grains that reach sizes of up to 1 cm. The large omphacite grains are optically zoned. Coarse grained garnets with sizes between 0.5 and 1 cm are randomly orientated in the fine grained omphacite matrix.

On the other hand, some samples are characterized by alternating layers of omphacite and garnet. In these samples, the grain sizes of the major mineral components are more homogeneous. Omphacite grains occur in sizes between ~100 µm and 2 mm. The orientation of the alternating layers corresponds with a shape preferred orientation in the omphacites. Garnet minerals are characterized by varying grain sizes between ~200 µm and 2 mm. As accessory components in both eclogite groups, the mineral assemblages include phengite, paragonite, kyanite, quartz, rutile and opaque minerals.

Some samples were collected in areas that were described in previous studies as ultrahigh-pressure eclogite defined by coesite as mineral component in the eclogites. In these samples, no coesite could be identified on thin section scale, only the occurrence of quartz could be verified.

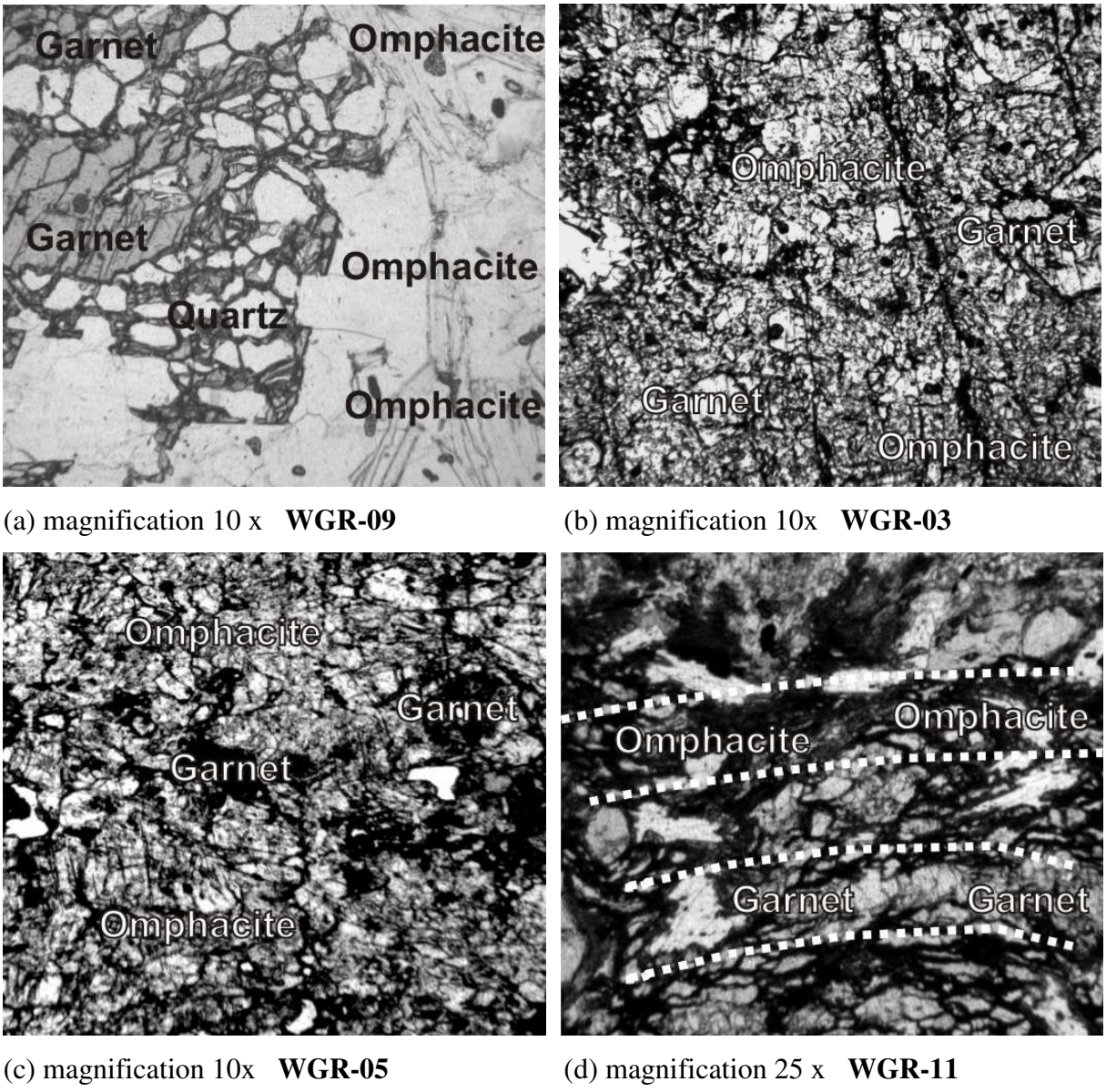

(a) magnification 10 x **WGR-09** (b) magnification 10x **WGR-03**

(c) magnification 10x **WGR-05** (d) magnification 25 x **WGR-11**

Fig. 25: Photographs of Western Gneiss Region eclogite thin sections (XZ-sections). (a) Coarse grained eclogite; (b) Fine grained eclogite; (c) Fine grained eclogites, crossed nicols; (d) Fine grained eclogite with garnet and omphacite layers (marked by dotted lines), crossed nicols. Note the different magifications.

4.2.3. LPO patterns in the Western Gneiss Region

The lattice preferred orientation data from omphacites of the Western Gneiss Region are plotted as contoured polefigures in equal area and lower hemisphere projections. The samples were collected along one SW-NE profile (Fig. 24). Most of the samples were collected close to the boundary between high-pressure and ultrahigh-pressure rocks, which is in the Nordfjord area in the western part of the WGR. Only one sample (WGR-14) was collected in the easternmost part of the Western Gneiss Region. The non-uniform distribution of measured samples along the profile is caused by increasing retrogression of eclogites in eastern

direction inside the Western Gneiss Region. Therefore, some of the collected eclogite samples from the eastern parts of the WGR were unsuitable for EBSD work.

The polefigures are divided in samples from the western part of the profile, marked as part A (see Fig. 26a) and samples from the eastern part of the profile, marked as part B (see Fig. 26b). The western part of the overall profile (part A) contains five samples (WGR-08, WGR-11, WGR-09, WGR-10, WGR-04 from west to east, Fig. 26a). This part is characterized by a nonsystematic mixture of S-type and L-type trending transition LPO patterns. The westernmost sample WGR-08 shows a highly symmetric transition pattern with strong point maxima in its mean unit deviation in {010} and {001}. The pattern can be assigned neither to S-type nor to L-type LPO. No clear asymmetries have been measured in this sample. It is also characterized by a very strong mean unit deviation maximum (27.68), which is one of the highest values in all samples from the Western Gneiss Region. Sample WGR-11 display a marginally asymmetric pattern that tends slightly to L-type-like LPO.

In comparison to the westernmost samples, the sample WGR-09 shows only a weak mean unit deviation maximum (4.00). Further it is characterized by a transition LPO pattern that tends into S-type direction. This sample also displays a clear symmetry. Further east, WGR-10 also reflects symmetric LPO patterns. This sample depicts transition LPO patterns that tend into L-type direction. It does not reflect any asymmetries. The mean unit deviation maxima (10.11) is of average value for the measured Western Gneiss Region eclogites. The easternmost sample in part A of the overall profile, sample WGR-04, is also characterized by a symmetric pattern without any measured asymmetries. The pattern is strongly S-type with an average mean unit deviation maximum of 9.57.

The eastern part of the overall profile (part B) contains four samples (WGR-07, WGR-03, WGR-05, WGR-14 from west to east, Fig. 26b). This part is characterized by very homogeneous LPO patterns, exluding sample WGR-03. The latter is the only sample that shows a distinctly asymmetric LPO pattern. It is slightly rotated (~10º) in its mean unit deviation maximum in relation to the lineation axes L in {001} and extensively rotated (~ 45º) related to the lineation axes L in {010}. The pattern reflects transition fabrics that tend towards an L-type like signature.

The eastern samples of the overall profile, the samples WGR-07, WGR-05, and WGR-14, are very similar in the LPO pattern distributions. All samples show symmetric transition patterns that tend marginally into S-type (WGR-05) or L-type (WGR-14) direction.

The by far easternmost sample WGR-14 is characterized by the highest value of the mean unit deviation maximum (28.72) of all Western Gneiss Region eclogites. Otherwise this sample

does not show any differences in its pattern in comparison to all other samples, even it was collected far away from them.

Overall, the omphacite LPO profile across the Western Gneiss Region is characterized by an overall homogeneous symmetric pattern of the LPO polefigures of its omphacite samples. Only sample WGR-03, which is placed in the central part of the Western Gneiss Region, reflects a significantly asymmetry. All other samples are strongly symmetric and therefore do not represent any kind of noncoaxial deformation. The patterns mainly do not display signatures that are close to S- or L- type endmembers. Most of the patterns are close to transition signature but there is a nonsystematic mixture of transition patterns that tend partly to S- type and partly to L-type LPO. S-type and L-type tending patterns are distributed randomly across the entire study area.

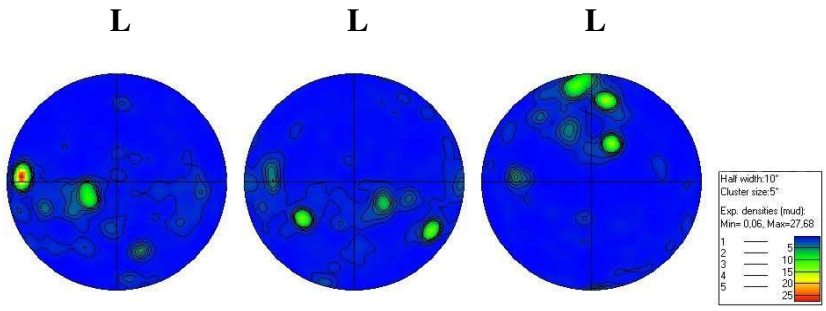

mud (max.): 27.68 **WGR-08**

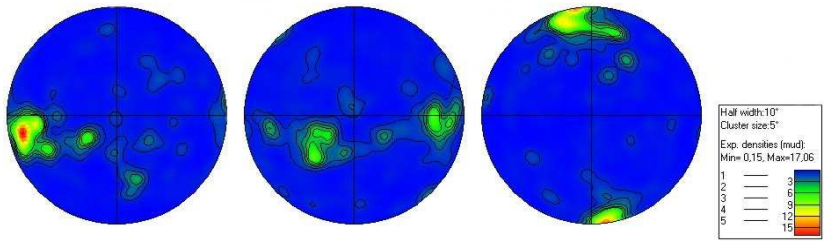

mud (max.): 17.06 **WGR-11**

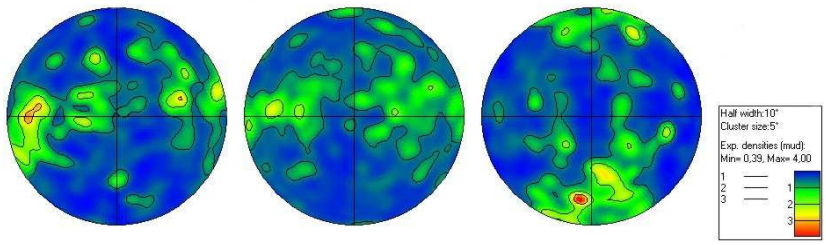

mud (max.): 4.00 **WGR-09**

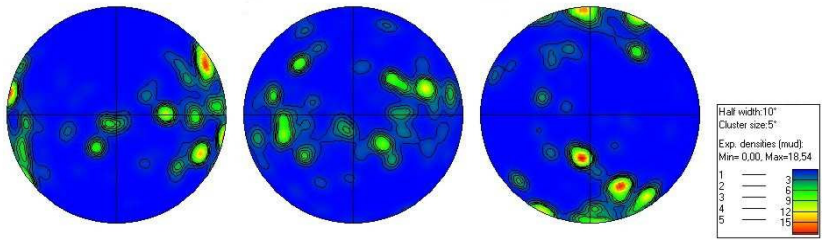

mud: (max.): 10.11 **WGR-10**

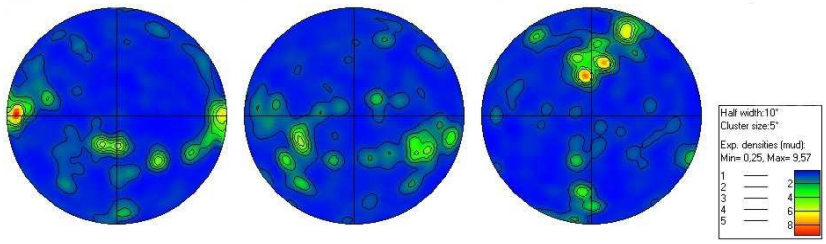

mud (max.): 9.57 **WGR-04**

{010} **{110}** **{001}**

Fig. 26a: Omphacite LPO along **part A** (western part) of a profile across the Western Gneiss Region. The lineation is marked by L. The profile is west-east directed. Polefigures are plotted in equal area, lower hemisphere projections. For sample and profile locations, see Fig. 24. mud (max.) – mean unit deviation (maximum).

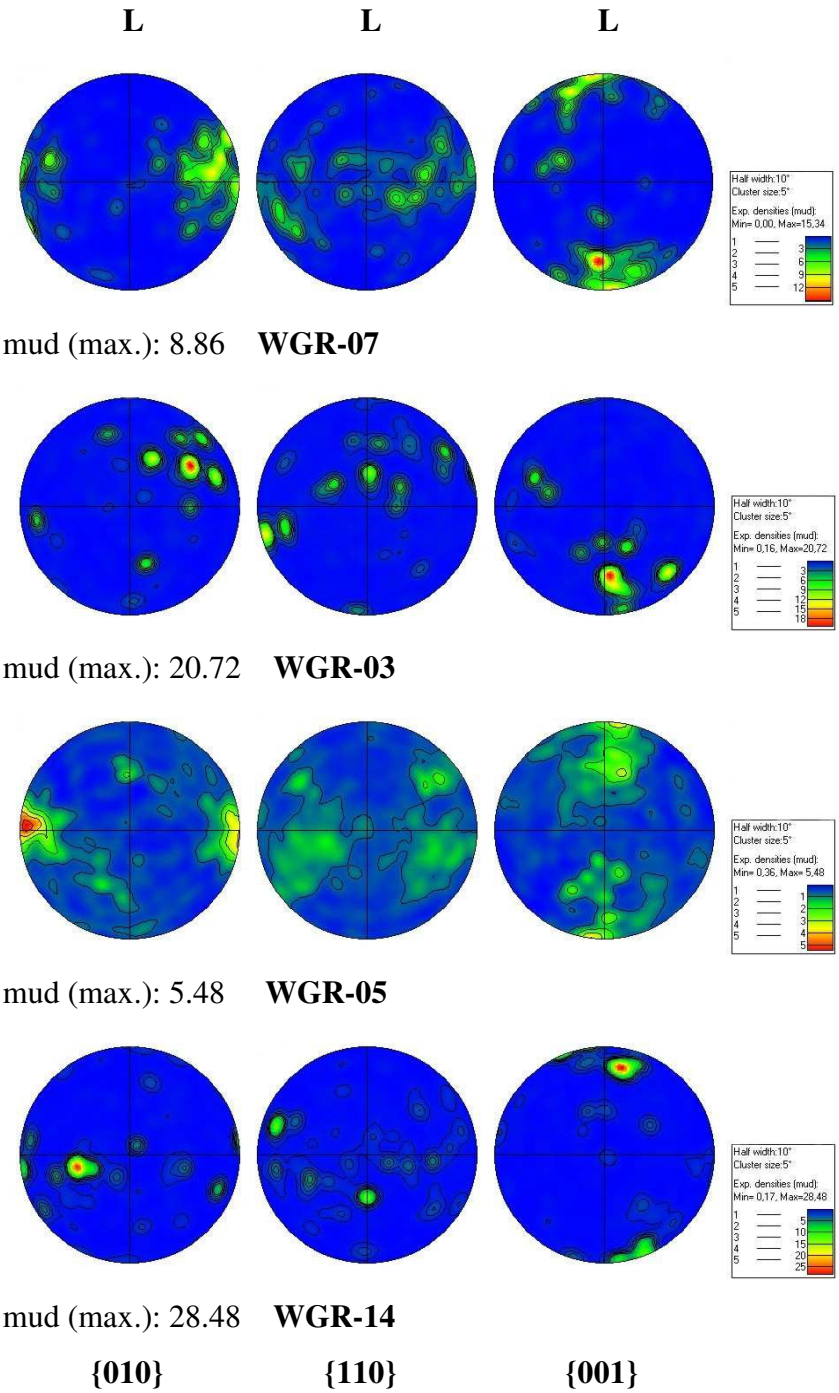

Fig. 26b: Omphacite LPO along **part B** (eastern part) of a profile across the Western Gneiss Region. The lineation is marked by L. The profile is west-east directed. Polefigures are plotted in equal area, lower hemisphere projections. For sample and profile locations, see Fig. 24. mud (max.) – mean unit deviation (maximum).

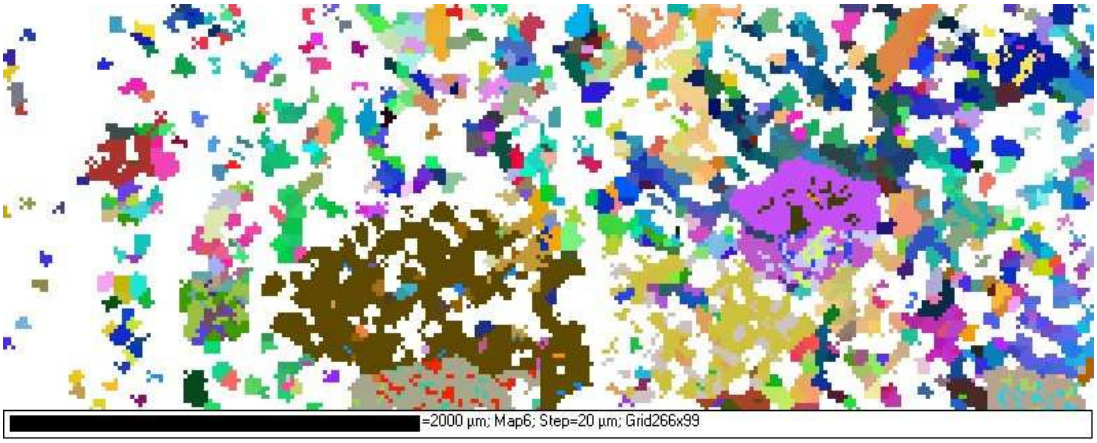

WGR-05 magnification: 30x

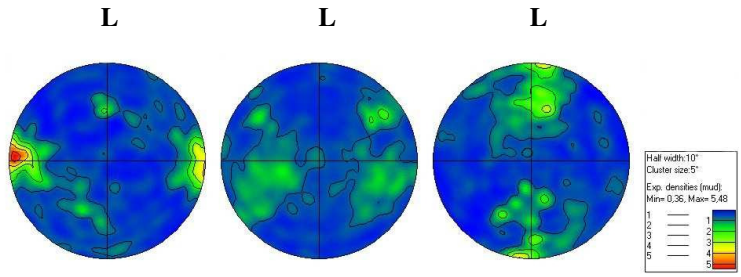

WGR-05

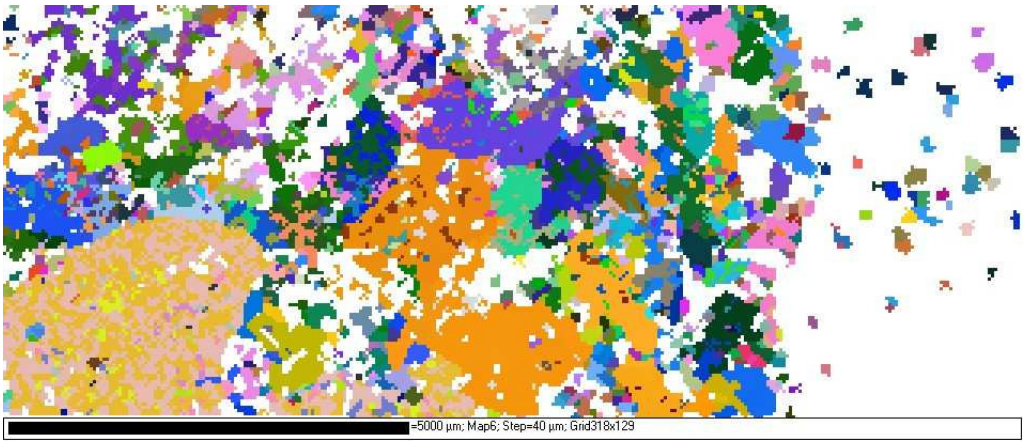

WGR-07 magnification: 12x

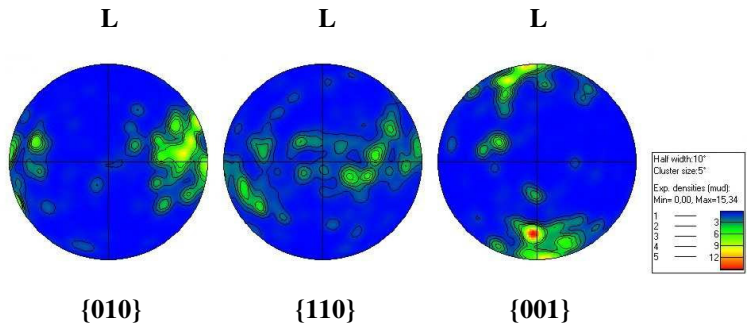

WGR-07

Fig. 27: Orientation contrast mapping of eclogites from the Western Gneiss Region, compared with lattice preferred orientation patterns. Note the different magnifications.

Orientation contrast mapping and orientation contrast imaging of Western Gneiss Region eclogites show no shape preferred orientation on a subgrain scale. Only in a few cases, an omphacite subgrain lineation is observable (see examples in Figs. 27 to 29).

A comparison between orientation contrast images and lattice preferred orientation patterns of the Western Gneiss Region shows that the textures are not related in any way to shape preferred orientation in omphacite. Such a relationship could be observed neither on grain nor on subgrain scale. Samples that show a clear omphacite lineation or a shape preferred subgrain orientation display comparable patterns as samples that show no preferred orientation on grain or subgrain scale.

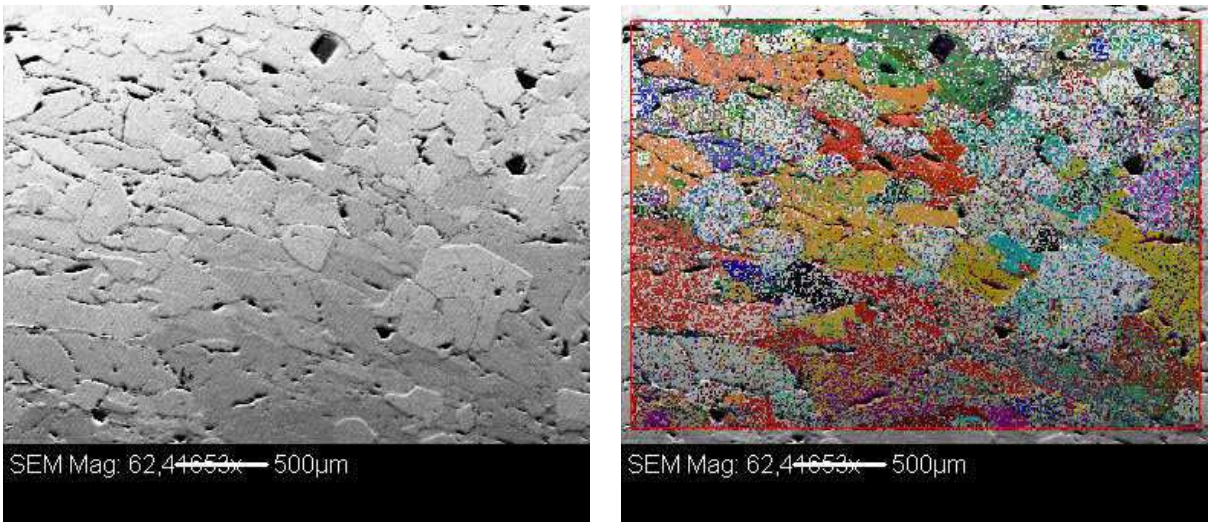

(a) magnification: 62x (b) magnification: 62x **WGR-11**

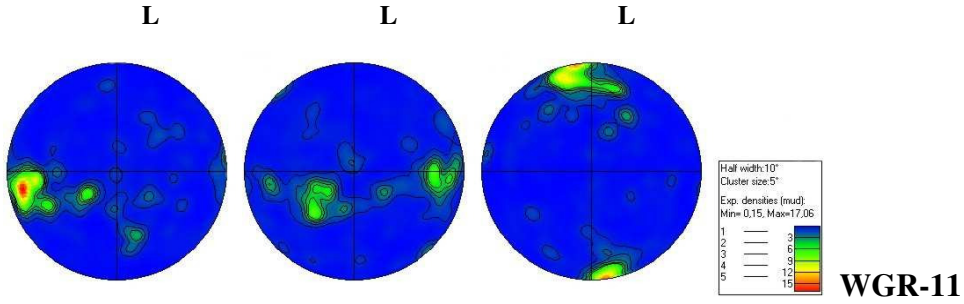

WGR-11

{010} **{110}** **{001}**

Fig. 28

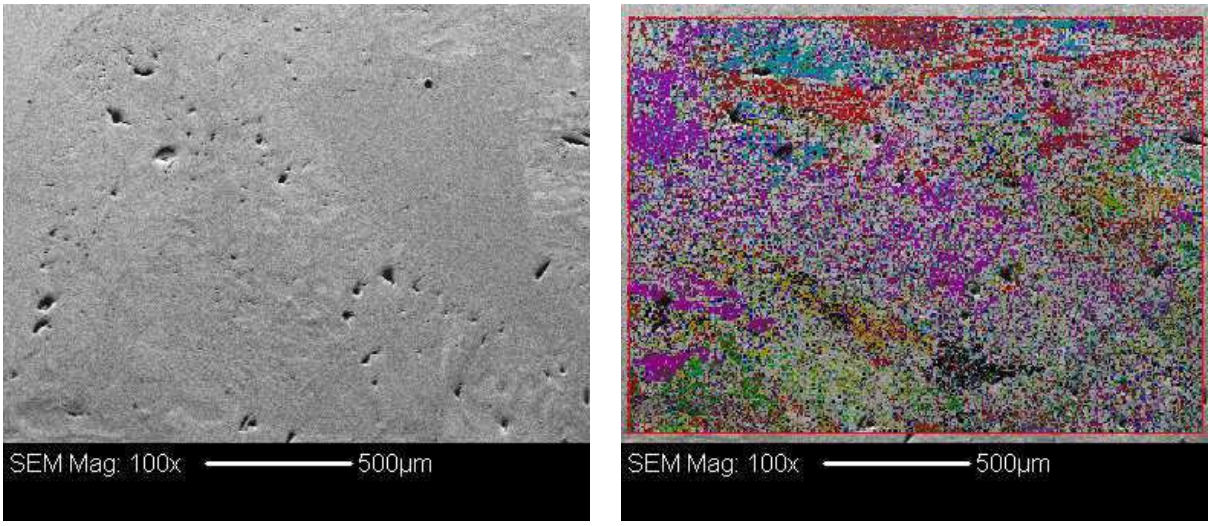

(c) magnification: 100x (d) magnification : 100x **WGR-14**

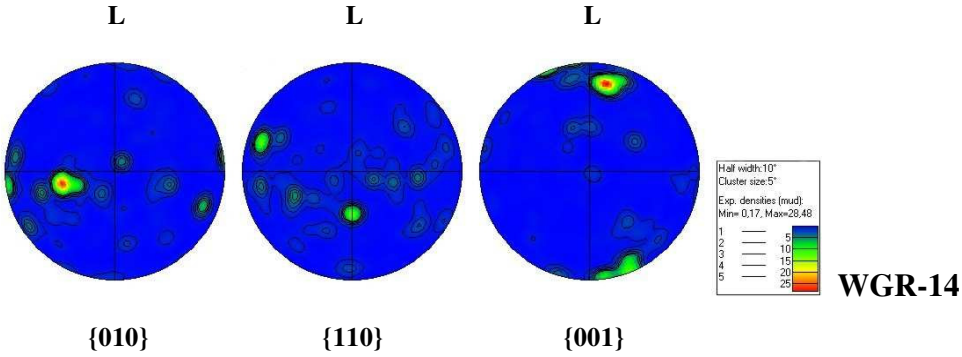

Fig. 28: Orientation contrast images of eclogites from the Western Gneiss Region, compared with lattice preferred orientation patterns. (a) & (b) Subgrain lineation, sample WGR-11, same picture; (c) & (d) Sample WGR-14, showing no subgrain SPO, same picture. Every colour change represents an orientation change on subgrain scale. Note the different magnifications.

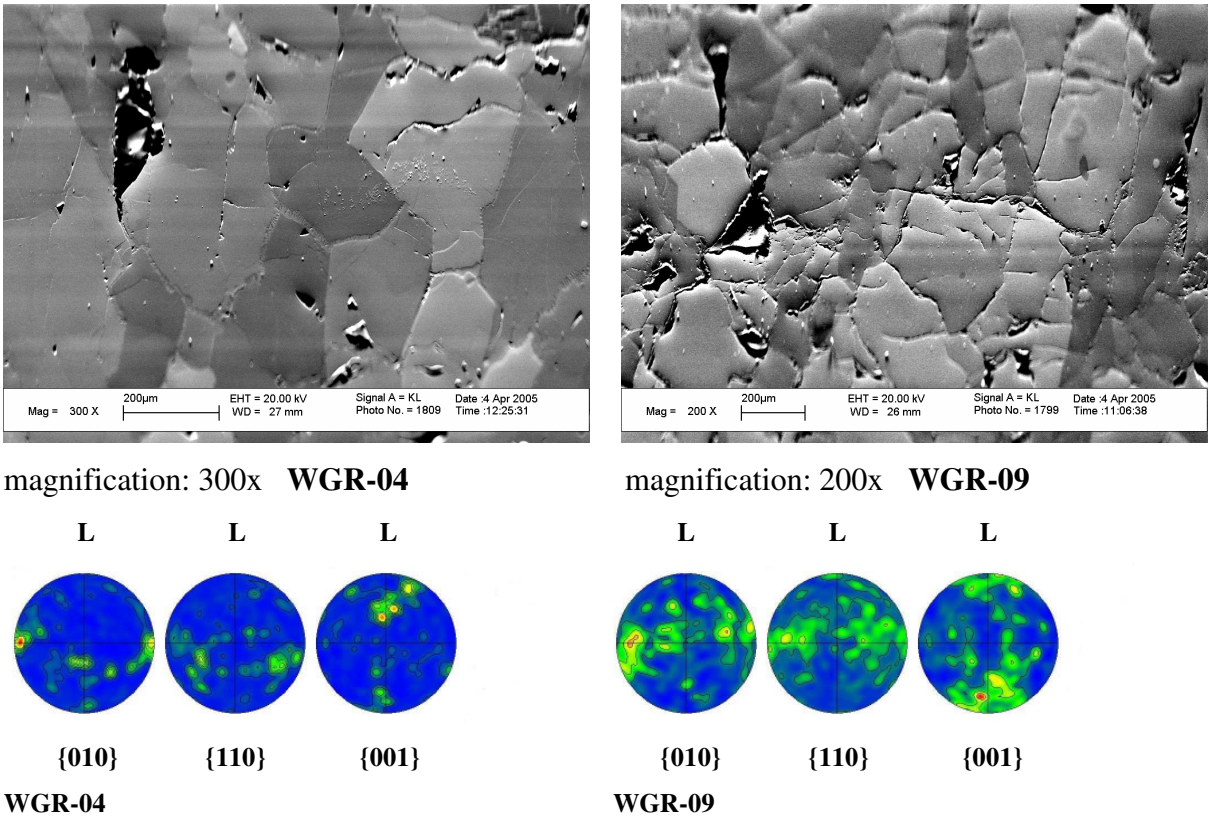

Fig. 29: Orientation contrast images of omphacite subgrains and LPO polefigures of eclogites from the Western Gneiss Region / Norway. (a) Eclogite, showing no omphacite subgrain lineation; (b) Eclogite, showing omphacite subgrain lineation. Note the different magnifications.

4.3. Discussion & Conclusions (II): Western Gneiss Region

4.3.1. Discussion

The lattice preferred orientation patterns of the Western Gneiss Region (Fig. 26) display similar patterns, compared with the textures of the Eclogite Zone (Fig. 20). The textures reflect transition signatures, tending slightly into S-type or L-type direction. Furthermore, the patterns are very symmetric and therefore indicative for coaxial deformation during LPO formation. The symmetry in the Western Gneiss Region LPO patterns is even stronger than in the textures of the Tauern Window eclogites.

The similarity between LPO patterns of Eclogite Zone and Western Gneiss Region leads to two major assumptions:

1. As well as LPO of the Eclogite Zone, the textures of the Western Gneiss Region are independent from exhumation and indicative of prograde pattern formation.

Previous studies suggested coaxial deformation that affected the eclogites before the onset of exhumation. Andersen et al. (1994) have studied tectonic fabrics in eclogites and suggested that eclogites of the Western Gneiss Region were affected by coaxial constrictional deformation at maximum pressure conditions, related to plate convergence.
The hypothesis by Andersen et al. (1994) is the best fitting observation with respect to the measured omphacite LPO patterns of the Western Gneiss Region. In this case, the patterns do not reflect any deformation, that affected the eclogites on the way to the surface and the crystallographic orientation in the samples can not be connected in any way with deformation processes during the exhumation of the eclogites. LPO was formed and affected during omphacite formation.
Presuming that the omphacite textures of the Western Gneiss Region reflect metamorphic peak conditions, then the texture formation corresponds with the accretionary process of the eclogites (e.g. Jolivet et al., 2005). In this case, the omphacite textures would represent the onset of exhumation without being affected during the following way to the surface.

2. In contrast to LPO of the Eclogite Zone, the textures of the Western Gneiss Region are connected to exhumation, because EZ and WGR were exhumed in different ways.

If the omphacite lattice preferred orientation patterns of the Western Gneiss Region are indicative for the exhumation, then the exhumation suggestions for the WGR, as introduced in chapter 4.1., have to be displayed in the omphacite textures.
A transtensional setting is widely assumed for a consistent exhumation of the Western Gneiss Region (Krabbendam & Dewey, 1998; Foreman et al., 2005; Wheeler & Foreman, 2005). In this case, an oblique but homogeneous LPO distribution should be observable along the profile, based on the basic studies of Bascou et al. (2001, 2002). The measured textures do not display any significant asymmetries, and they are therefore not indicative for any kind of noncoaxial deformation that is expected in a transtensional setting. This observation is in agreement with Foreman et al. (2005), who argued that strong noncoaxial deformation, as expected under transtensional conditions, has to be displayed in strongly asymmetric LPO patterns. Foreman et al. (2005) interpreted the absence of asymmetries as indicative for coaxial deformation which is not connected with a transtensional setting and probably also not

with the exhumation process. The investigated patterns in this study also clearly indicate a coaxial deformation setting during LPO formation.
Walsh & Hacker (2004) and Walsh et al. (2007) assumed an exhumation process based on underplating and extension for the whole rock unit, independent from high-pressure or ultrahigh-pressure conditions. Based on the simulations of Bascou et al. (2001, 2002), this should lead to L-type-like LPO patterns along the whole study area. This is not reflected in the omphacite textures of the studied eclogites, which do not show a clear LPO pattern distribution along the entire profile. Therefore the LPO patterns are in contradiction with such an exhumation model.

Overall, I conclude that either the WGR was not exhumed by extensional or transtensional conditions or the omphacite textures do not display the exhumation process. It is not possible to verify any exhumation models by studying the omphacite crystallographic orientation patterns of the Western Gneiss Region. Omphacite LPO is probably not connected with any structural and tectonic processes on the exhumation path of eclogite development.

This assumption can be supported by comparing omphacite oriention contrast images of different eclogites within the Western Gneiss Region. OC-images and OC-mappings (see Figs. 27 to 29) document that some samples reflect a shape preferred orientation (SPO) on the subgrain scale, while other samples do not show any subgrain lineation. This observation is independent from high-pressure or ultrahigh-pressure conditions and from the position of the eclogites along the investigated profile.
In contrast to this, the lattice preferred orientaion patterns are homogeneous in the whole study area and do not reflect any differences in omphacite SPO. Deformation, leading to shape preferred orientation, is therefore not displayed in omphacite lattice preferred orientation patterns of the Western Gneiss Region.

4.3.2. Conclusions

The textures show strongly systematic patterns that indicate coaxial deformation during LPO pattern formation.

The omphacite LPO patterns of the Western Gneiss Region are independent from any observed shape preferred orientation (SPO) on grain or subgrain scale

The omphacite lattice preferred orientation patterns of the Western Gneiss Region do not fit with extension or transtension based exhumation, as postulated in previous studies.

Based on basic studies on omphacite LPO (Bascou et al., 2001, 2002), the patterns display a prograde signature and are not coupled in any way with the exhumation of the Western Gneiss Region.

Overall, it is highly questionable that omphacite lattice preferred orientation patterns contain any exhumation indications for the Western Gneiss Region.

The omphacite textures are probably independent from the exhumation of the eclogites.

5. GENERAL DISCUSSION & CONCLUSIONS

5.1. General discussion

As shown in the chapters 3 & 4, the LPO polefigures of the Eclogite Zone and the Western Gneiss Region display similar textures. In both study areas, the lattice preferred orientation patterns are symmetric. Only in a few cases, significant asymmetries are displayed. These asymmetries are randomly distributed in the study areas and not coupled with any tectonic contacts.

For the Tauern Window eclogites, it is very clear that textures and kinematics are not coupled. The lattice preferred orientation patterns display the prograde path and the metamorphic peak of the eclogite formation. The exhumation-related structures of the Eclogite Zone are recorded in the garnet mica schist, surrounding the eclogite lenses. The similar textures of the Western Gneiss Region are therefore possibly also indicative for a prograde LPO formation. The textures probably formed during eclogite accretion to the overriding plate.

Exhumation processes do probably not affect omphacite LPO patterns in any way. Neither the textures of the Eclogite Zone nor the textures of the Western Gneiss Region can be directly connected with any postulated exhumation model for one of the study areas. The exhumation models, postulated for both units are very different but the textures are very similar. Therefore, it can be assumed that omphacite LPO is coupled with the growth of omphacite on the prograde path and the metamorphic peak of eclogite formation.

The omphacite lattice preferred orientation patterns in both study areas are comparable even the units are characterized by the following differences in their geological settings: While the Eclogite Zone underwent consistent P-T conditions (600-650°C; 20-25 kbar), the Western Gneiss Region is characterized by a wide P-T-range (400-800°C, 20-35 kbar) and ultrahigh-pressure conditions. The WGR underwent a much deeper burial than the Tauern Window eclogites. The exhumation rate, calculated for the Eclogite Zone is much faster than the exhumation of the Western Gneiss Region. The eclogite bodies in the Western Gneiss Region are by far larger than the eclogite lenses inside the Eclogite Zone. This means that the crystallographic preferred orientation in omphacite is obviously independent from such differences in the geological settings.

5.2. Conclusions

Concerning the aims of this study (see chapter 1.2.), the results lead to the following conclusions:

- Structural and mapping observations in the field suggest an extrusion wedge geometry for the Eclogite Zone of the Tauern Window.
- The eclogite / matrix ratio of the Eclogite Zone is significantly smaller than estimated in previous studies.
- Omphacite lattice preferred orientation of the Eclogite Zone formed during prograde omphacite formation and during metamorphic peak conditions and was not affected during exhumation.
- The omphacite textures of the Western Gneiss Region confirm the Tauern Window LPO data by probably showing prograde and metamorphic peak signatures and an independence from exhumation processes.
- The WGR textures probably formed during eclogite accretion to the overriding plate.
- Omphacite lattice preferred orientation patterns are similar under high-pressure and ultrahigh-pressure conditions and therefore independent from burial dep

The applicability of omphacite lattice preferred orientation patterns for eclogite exhumation is highly questionable because:

- The omphacite textures of the Eclogite Zone are not coupled to the exhumation structures in garnet-mica schist.
- LPO of the Eclogite Zone as well as LPO of the Western Gneiss Region probably formed before exhumation.
- Neither the textures of the Eclogite Zone nor the textures of the Western Gneiss Region demonstrably fit with any suggested exhumation models.
- Presuming the correctness of previous exhumation studies for both different units, then LPO patterns are similar even though the units underwent different kinds of exhumation.
- Neither in the Eclogite Zone nor in the Western Gneiss Region, the textures are coupled with observed shape preferred orientation (SPO) on omphacite grains and subgrains.

6. LITERATURE

Abalos, B., 1997. Omphacite fabric variation in the Cabo Ortegal eclogite (NW Spain): relationship with strain symmetry during high-pressure deformation. Journal of Structural Geology 19, 621-637.

Andersen, T.B., Osmundsen, P.T. & Jolivet, L., 1994. Deep crustal fabrics and a model for extensional collapse of the southwest Norwegian Caledonides. Journal of Structural Geology 16, 1191-1203.

Bascou, J., Guilhem, B., Vaucez, A., Mainprice, D. & Egydio-Silva, M., 2001. EBSD-measured lattice preferred orientations and seismic properties of eclogites. Tectonophysics 342, 61-80.

Bascou, J., Tommasi, A. & Mainprice, D., 2002. Plastic deformation and development of clinopyroxene lattice preferred orientations in eclogites. Journal of Structural Geology 24, 1357-1368.

Behrmann, J.H. & Ratschbacher, L., 1989. Archimedes revisited. A structural test of eclogite emplacement models in the Austrian Alps. Terra Nova 1, 242-252.

Boundy, T.M., Fountain, D.M. & Austrheim, H., 1992. Structural development and petrofabrics of eclogite facies shear zones, Bergen Arcs, western Norway: implications for deep crustal deformational processes. Journal of Metamorphic Geology 10, 127-146.

Brenker, F.E., 1998. Mikrogefügethermochronometrie für Eklogite. Ph.D. Thesis, J.W. Goethe Universität, Frankfurt.

Brenker, F.E., Prior, D.J. & Müller, W.F., 2002. Cation ordering in omphacite and effect on deformation mechanism and lattice preferred orientation . Journal of Structural Geology 24, 1991-2005.

Carswell, D.A:; Brueckner; H.K., Cuthbert, S.J., Mehta, K. & O`Brien, P.J., 2003. The timing of stabilisation and the exhumation rate for ultra-high-pressure rocks in the Western Gneiss Region of Norway. Journal of Metamorphic Geology 21, 601-612.

Chateigner, D. Physics Course of Daniel Chateigner, homepage, http://www.ecole.ensicaen.fr/~chateign/enseig/microscopie/.

Cuthbert, S.J., Carswell, D.A., Krogh-Ravna, E.J. & Wain, A., 2000. Eclogites and eclogites in the Western Gneiss Region, Norwegian Caledonites. Lithos 52, 165-195.

Dietler, T.N., Koestler, A.G. & Milnes, A.G., 1985. A preliminary structural profile through the Western Gneiss Complex, Sognefjord, southwestern Norway. Norsk Geologisk Tidsskrift 65, 233-235.

Dietrich, S., 2005. Kartierbericht zur Geologie des Timmeltals, Hohe Tauern. Diploma mapping report, Johannes Gutenberg Universität Mainz.

Dingley, D.J., Longden, M., Weibren, J. & Aldermen, J., 1987. On-line analysis of electron backscatter diffraction patterns. I. Texture analysis of zone refined polysilicon. Scanning Microscopy 1, 451-456.

Dobrzhinetskaya, L.F., Eide, E.A., Larsen, R.B., Sturt, B.A., Trønnes, R.G., Smith, D.C., Taylor, W.R. & Posukhova, T.V., 1995. Microdiamond in high-grade metamorphic rocks of the Western Gneiss Region, Norway. Geology 25, 597-600.

England, P.C. & Holland, T.J.B., 1979. Archimedes and the Tauern eclogites: the role of buoyancy in the preservation of exotic eclogite blocks. Earth and Planetary Science Letters 44, 287-294.

Foreman, R., Andersen, T.B. & Wheeler, J., 2005. Eclogite-facies polyphase deformation of the Drøsdal eclogite, Western Gneiss Complex, Norway, and implications for exhumation. Tectonophysics 398, 1-32.

Frank,W., Höck, V. & Miller, Ch., 1987. Metamorphic and tectonic history of the central Tauern Window. In: Geodynamics of the Eastern Alps (ed. By H.W. Flügel and P. Faupl), 34-54.

Froitzheim, N., 2001. Origin of the Monte Rosa nappe in the Pennine Alps – a new working hypothesis. Geological Society of America Bulletin 113, 604-614.

Froitzheim, N., Schmid, S.M. & Frey , M., 1996. Mesozoic paleogeography and the timing of eclogite facies metamorphism in the Alps: a working hypothesis. Eclogae geologicae Helvetiae 89, 81-110.

Gebauer, D., Lappin, M.A., Grünenfelder, M. & Wyttenbach, A., 1985. The age and origin of some Norwegian eclogites: A U-Pb zircon and REE study. Chemical Geology 52, 227-247.

Gee, D.G., 1982. The Scandinavian Caledonides. Terra Cognita 2, 89-96.

Glodny, J., Ring, U., Kühn, A., Gleissner, P. & Franz, G., 2005. Crystallization and very rapid exhumation of the youngest Alpine eclogites (Tauern Window, Eastern Alps) from Rb/Sr mineral assemblage analysis. Contributions to Mineralogy and Petrology 149, 699-712.

Godard, G. & Van Roermund, H.L.M., 1995. Deformation-induced clinopyroxene from eclogites. Journal of Structural Geology 17, 1425-1443.

Griffin, W.L. & Brueckner, H.K., 1985. REE, Rb-Sr and Sm-Nd studies of Norwegian eclogites. Chemical Geology 52, 249-271.

Hacker, B.R., Andersen, T.B., Root, D.B., Mehl, L., Mattinson, J.M. & Wooden, J.L., 2003. Exhumation of high-pressure rocks beneath the Solund-Basin, Western Gneiss Region of Norway. Journal of Metamorphic Geology 21, 613-629.

Harland, W.B. & Gayer, R.A., 1972. The Arctic ocean and earlier oceans. Geological Magazine 109, 289-314.

Helmstaedt, H., Anderson, O.L. & Gavasci, A.T., 1972. Petrofabric studies of eclogite, spinel-websterite and spinel-lherzolite xenoliths from kimberlite-bearing breccia pipes in southeastern utah and northeastern arizona. Journal of Geophysical Research 77, 4350-4365.

Holland, T.J.B., 1977. Structural and metamorphic studies of eclogites and associated rocks in the central Tauern region of the eastern Alps. DPhil thesis, Oxford University.

Hoschek, G., 2001.Thermobarometry of metasediments and metabasites from the Eclogite Zone of the Tauern Window, Eastern Alps, Austria. Lithos 59, 127–150.

Hoschek, G., 2007. Metamorphic peak conditions of eclogites in the Tauern Window, Eastern Alps, Austria: Thermobarometry of the assemblage garnet+omphacite+phengite+quartz. Lithos 93, 1-16.

Jolivet, L., Raimbourg, H., Labrousse, L., Avigad, D., Leroy, L., Austrhein, H. & Andersen, T.B., 2005. Softening by eclogitization, the first step toward exhumation during continental subduction. Earth and Planetary Science Letters 237, 532-547.

Kikuchi, S., 1928. Diffraction of cathode rays by mica. Japanese Journal of Physics 5, 83-96

Krabbendam, M. & Wain, A., 1997. Late-orogenic structures, differential retrogression and structural position of HP and UHP rocks in the Nordfjord-Stadtlandet area, Western Gneiss Region. Norges Geologiske Undersøkelse Bulletin 432, 127-139.

Krabbendam, M. & Dewey, J.F., 1998. Exhumation of UHP rocks by transtension in the Western Gneiss Region, Scandinavian Caledonides. Geological Society London, Special Publications 135, 159-181.

Krogh, T., Kwok, Y., Robinson, P. & Terry, M.P., 2004. U-Pb constraints on the subduction-extension interval in the Averøya-Nordøyane area, Western Gneiss Region, Norway. Goldschmidt Conference Abstract.

Kurz, W., Neubauer F. & Dachs, E., 1998. Eclogite meso- and microfabriscs: Implications for the burial and exhumation history of eclogites in the Tauern Window (Eastern Alps) from p-T-d paths. Tectonophysics 285, 183-209.

Kurz, W. & Froitzheim, N., 2002. The exhumation of eclogite-facies metamorphic rocks – a review of models confronted with examples from the Alps. International Geology Review 44, 702-743.

Kurz, W., Fritz, H., Froitzheim, N., Tenzcer, V. & Unzog, W., 2003. Mechanics of the exhumation of eclogite-facies metamorphic rocks in convergent plate margins: models and examples from the Alps. Geophysical Research Abstracts, Vol. 5, European Geophysical Society 2003.

Kurz, W., Jansen, E., Hundenborn, R., Pleuger, J., Schäfer, W. & Unzog, W., 2004. Microstructures and crystallographic preferred orientations of omphacite in alpine eclogites: implications fort he exhumation of (ultra-) high-pressure units. Journal of Geodynamics 37, 1-55.

Labrousse, L., Jolivet, L., Andersen, T.B., Agard, P., Maluski, H. & Schärer, U., 2004. Pressure-temperature-time-deformation history of the exhumation of ultra-high-pressure rocks in the Western Gneiss Region, Norway. In: Whitney, D.L., Teyssier, C. & Siddoway, C.S. (eds.), Gneiss Domes in Orogeny. Geological Society of America, Special Paper 380, 155-185.

Lloyd, G.E., 1985. Review of instrumentation, techniques and applications of SEM in mineralogy. In: White, J.C. (ed.), Applications of Electron Microscopy in the Earth Science. Mineralogical Association of Canada, Shourt Course 11, 151-188

Lloyd, G.E., 1987. Atomic number and crystallographic contrast images with the SEM. A review of backscatterred electron techniques. Mineralogical Magazine 51, 3-19.

Mauler, A., 2000. Texture and microstructures in eclogites. Electron backscattered diffraction applied on samples from nature and experiment. Ph.D. Thesis, Eidgenössische Technische Hochschule, Zürich.

Mauler, A., Bystricky, M., Kunze, K. & Mackwell, S., 2000. Microstructures and lattice preferred orientations in experimentally deformed clinopyroxene. Journal of Structural Geology 22, 1633-1648.

Mauler, A., Godard, G. & Kunze, K., 2001. Crystallographic fabrics of omphacite, rutile and quartz in Vendee eclogites (Armorican Massif, France). Consequences for deformation mechanism and regimes. Tectonophysics 342, 81-112.

Mearns, E.W., 1986. Sm-Nd ages for Norwegian garnet peridotite. Lithos 19, 269-278.

Molinari, A., Canarova, G.R. & Azhy, S., 1987. A self-consistent approach of the large deformation polycrystal viscoplasticity. Acta Metallurgica 35, 2983-2994.

Prior, D.J., Trimby, P.W., Weber, D.U. & Dingley, D., 1996. Orientation contrast imaging of microstructures in rocks using forescatter detectors in the scanning electron microscope. Mineralogical Magazine 60, 859-869.

Raith, M., Mehrens, Ch. & Thöle, W., 1980. Gliederung, tektonischer Bau und metamorphe Entwicklung der penninischen Serien im südlichen Venediger-Gebiet, Osttiroler Jahrbuch der Geologie, Bundesanstalt 123, 1-37.

Ravna, E.J.K & Terry, M.P., 2004. Geothermobarometry of UHP and HP eclogites and schists; an evolution of equilibria among garnet-clinopyroxene-kyanite-phengite-coesite/quartz. Journal of Metamorphic Geology 22, 579-592.

Ring, U., Brandon, M.T., Willett, S. & Lister, G.S., 1999. Exhumation processes. In: Exhumation Processes: Normal faulting, ductile flow and erosion, Ring, U., Brandon, M.T., Lister, G.S., Willett, S. (eds.). Special Publications Geological Society of London 154, 1-28.

Roberts, D.A. & Sturt, B.A., 1980. Caledonian deformation in Norway. Journal of the Geological Society of London 137, 241-250.

Root, D.B., Hacker, B.R., Mattinson, J.M. & Woode, J.L., 2004. Young age and rapid exhumation of Norwegian ultrahigh-pressure rocks: An ion microprobe and chemical abrasion study. Earth and Planetary Science Letters 228, 325-341.

Root, D.B., Hacker, B.R., Gans, P., Eide, E., Ducea, M. & Mosenfelder, J., 2005. High-pressure allochtons overlie the ultrahigh-pressure Western Gneiss Region, Norway. Journal of Metamorphic Geology 23, 45-61.

Schmid, S.M. & Kissling, E., 2000. The arc of the Western Alps in the light of geophysical data on deep crustal structure. Tectonics 19, 62-85.

Schmid, S.M., Pfiffner, O.A., Froitzheim, N., Schönborn, G. & Kissling. E., 1996. Geophysical-geological transect and tectonic evolution of the Swiss-Italian Alps. Tectonics 15, 1036-1064.

Schmid, S.M., Fügenschuh, B., Kissling, E. & Schuster, R., 2004. Tectonic map and overall architecture of the Alpine orogen. Eclogae geologicae Helvetiae 97, 93-117.

Schuster, R. & Kurz, W., 2005. Eclogites in the Eastern Alps: High-pressure metamorphism in the context of the Alpine orogeny. Mitt. Österr. Min. Ges. 150, 173-188.

Selverstone, J., 1993. Micro- to macro-scale interactions between deformation and metamorphism, Tauern Window, Eastern Alps. Schweizerische Mineralogische und Petrographische Miteilungen 73, 229-239.

Smith, D.C., 1984. Coesite in clinopyroxene in the Caledonides and its implications for geodynamics. Nature 310, 641-644.

Smith, D.C., 1988. A review of peculiar mineralogy of the `Norwegian coesite-eclogite province`, with crystal-chemical , petrological, geochemical and geodynamical notesand an intensive bibliography. Eclogites and Eclogite-Facies Rocks. (ed. Smith, D.C.), Elsevier, Amsterdam, 1-206.

Smith, D.C., 1995. Microcoesites and microdiamonds in Norway. In: Ultrahigh Pressure Metamorphism (eds. Coleman, R.G. & Wang, X.), Cambridge University Press, Cambridge, 299-355.

Stöckhert, B., Massonne, H.J. & Nowlan , E.U., 1997. Low differential stress during high-pressure metamorphism: The microstructural record of a metapelite from the Eclogite Zone, Tauern Window, Eastern Alps. Lithos 41, 103-118.

Terry, M.P., Robinson, P. & Ravna, E.J.K., 2000. Kyanite eclogite thermobarometry and evidence for thrusting of UHP over HP metamorphic rocks, Nordøyane, Western Gneiss Region, Norway. American Mineralogist 85, 1651-1664.

Tucker, R.D., Krogh, T.E. & Råheim,, A., 1992. Proterozoic evolution and age–province boundaries in the central part of the Western Gneiss Region, Norway: Results of U-Pb dating of accessory minerals from Trondheimsfjord to Geiranger. In: Mid-Proterozoic Lauretia – Baltica (edited by by Gower, C.F., Rivers, T. & Ryan, B.). Geological Association of Canada 38, 149-173.

Venables, J.A. & Harland, C.J., 1973. Electron back-scattering patterns – A new technique for obtaining crystallographic information in the scanning electron microscope. Philosophical Magazine 27, 1193-1200.

Wain, A., 1997. New evidence for coesite in eclogite and gneisses; defining an ultrahigh pressure province in the Western Gneiss Region of Norway. Geology 25, 927-930.

Wain, A.L., Waters, D.J. & Austrheim, H., 2001. Metastability of granulites and processes of eclogitisation in the UHP region of western Norway. Journal of Metamorphic Geology 19, 609-625.

Walsh, E.O. & Hacker, B.R., 2004. The fate of subducted continental margins: Two-stage exhumation of the high-pressure to ultrahigh-pressure Western Gneiss Complex, Norway. Journal of Metamorphic Geology 22, 671-689.

Walsh, E.O., Hacker, B.R., Gans, P.G., Grove, M. & Gehrels, G., 2007. Timing the exhumation of (ultra)high-pressure rocks across the Western Gneiss Region, Norway. Geological Society of America Bulletin 119, 289-301.

Wheeler, J. Foreman, R., Andersen, T.B., Reddy, S.M. Cliff, R.A., 2005. Eclogite evolution in the Alps and Norway. Mitteilungen der Österreichischen Minereralogischen Gesellschaft 150. 7th International Eclogite Conference (IEC-7).

Young, D.J., Hacker, B.R., Andersen, T.B. & Corfu, F., 2007. Prograde amphibolite facies to ultrahigh-pressure transition along Nordfjord, western Norway: Implications for exhumation tectonics. Tectonics 26.

Curriculum Vitae

Name: Kai Neufeld
Date of birth: 18.09.1970
Place of birth: Bremerhaven, Germany
Nationality: German

Private address:
Mombacher Strasse 85a
D-55122 Mainz, Germany

Scientific career:

1993 -2000 Study of Geology at "Christian-Albrechts-Universität" in Kiel, Germany
1999-2000 Diploma thesis at "Forschungszentrum für marine Geowissenschaften" (GEOMAR) in Kiel, Germany
2000-2001 Technical assistant for electron microprobe analysis at "Roentgen Analytik Service Lechtenberg" (RASL) in Itzehoe, Germany
2001-2003: Research employee at "Bayerisches Geoinstitut", University of Bayreuth, Germany.
2003-2007: PhD student at Graduate School "Composition and evolution of crust and mantle", University of Mainz, Germany.